



## **Development of guidelines allowing to predict the contribution of the superstructure to the hull girder strength**

**Student: Farhad Ahmed**

**Supervisors:**

**Professor Dr. Maciej Taczala at ZUT  
Ing. Wa Nzengu Nzengu at Bureau Veritas**

**“EMSHIP”  
Erasmus Mundus Master Course  
in “Integrated Advanced Ship Design”**





## **ABSTRACT**

Longitudinal vertical bending of a ship consists of stress and strength transfer between hull and superstructure. This sharing of stress and strength is a very complex phenomenon, namely in the case of multiple deck vessels, which is being studied by naval architects for a long time.

On passenger vessels for architectural reasons, structural connections between decks are reduced to the minimum in passenger and public area. In addition, due to design specificity such as recesses in way of life boat, openings in side shell (windows), openings in longitudinal bulkheads, all superstructure tiers are not contributing similarly to the vessel hull girder strength. To take account of this phenomenon, one can introduce bending efficiencies of superstructure tiers. Bending efficiencies are percentages given tier by tier and used as follows:

- When calculating hull girder transverse section characteristics, contribution of one given superstructure tier is weighted by its bending efficiency.
- When evaluating the hull girder stress in way of a given tier, the stress is reduced by multiplying it by the tier bending efficiency.

It is to be noted that bending efficiencies have no real physical meaning but are very useful to take into account the specific global behavior of a vessel but still using usual beam theory to assess vessel strength. Bending efficiency of each superstructure tier is linked with global behavior of vessel. Hence, they cannot be evaluated without a complete finite element model (FEM) of the vessel. But, FEM is very time consuming and thus, very prohibitive namely for small ships. The main purpose of this research is to propose guidelines allowing prediction of the contribution of the superstructure to the hull girder strength.

A standard investigation finite element model is made of two superimposed box girders. The effect of different parameters in hull-superstructure interaction were investigated on this standard model. The investigated parameters are: ratio of superstructure length to hull length ( $r_L$ ), ratio of superstructure side openings to total lateral area ( $r_S$ ), location of superstructure side openings and ratio of deck openings to total deck area ( $r_D$ ). Based on these investigations, a new expression for bending efficiency ( $\nu$ ) is developed. This new formula is more accurate for finding hull girder normal stresses. Besides, guidelines were developed for implementation of bending efficiency in order to find the hull girder normal stresses of a passenger vessel.



## **Acknowledgments**

First of all, I would like to thank and express my gratitude to Mr. Nzengu Wa Nzengu, my supervisor in Bureau Veritas Inland Navigation Management who created the environment for my research. He guided me in my research in every step from beginning to the end. We spent a lot of time together investigating different parameters. Then, I came in touch with Prof. Maciej Taczala, my supervisor at ZUT. He also gave me much time and suggestions to conclude my research smoothly.

I would also like to thank Prof. Philippe Rigo, who is the coordinator of EMSHIP program. He helped me from the selection process of EMSHIP to the end of this program. He always stepped forward to help me, whenever I was asking for his suggestion about my research. He is also reviewer my thesis.

I would also like to thank all my colleagues in Bureau Veritas Office for their friendly behavior and supports, specially Mr. Hoang Tri Tran for his training and guidance. He trained me in different tools and also shared his previous experiences and knowledge.

Finally, my deepest gratitude goes to my beloved family for their endless support and encouragement.

This thesis was developed in the frame of the European Master Course in "Integrated Advanced Ship Design" named "EMSHIP" for "European Education in Advanced Ship Design", Ref.: 159652-1-2009-1-BE-ERA MUNDUS-EMMC.



## **Declaration of Authorship**

I declare that this thesis and the work presented in it are my own and has been generated by me as the result of my own original research.

Where I have consulted the published work of others, this is always clearly attributed.

Where I have quoted from the work of others, the source is always given. With the exception of such quotations, this thesis is entirely my own work.

I have acknowledged all main sources of help.

Where the thesis is based on work done by myself jointly with others, I have made clear exactly what was done by others and what I have contributed myself.

This thesis contains no material that has been submitted previously, in whole or in part, for the award of any other academic degree or diploma.

I cede copyright of the thesis in favour of the West Pomeranian University of Technology.

Date:

Signature



## **Contents**

<b>ABSTRACT</b>	<b>1</b>
<b>Acknowledgments</b>	<b>3</b>
<b>Declaration of Authorship</b>	<b>5</b>
<b>1 Introduction</b>	<b>18</b>
1.1 General . . . . .	18
1.2 Challenges . . . . .	19
1.3 Previous works . . . . .	20
1.4 Research objectives and methods . . . . .	21
1.5 Symbols and definitions . . . . .	21
<b>2 Hull-superstructure interaction</b>	<b>23</b>
2.1 General . . . . .	23
2.2 Kirchhoff's method . . . . .	24
2.3 Coupled beam method . . . . .	25
2.4 Plane stress theory . . . . .	26
2.5 Conclusion . . . . .	26
<b>3 Bending efficiency</b>	<b>27</b>
3.1 General . . . . .	27

3.2	Two beam deckhouse theory with shear effects . . . . .	28
3.2.1	Introduction . . . . .	28
3.2.2	Fundamental assumptions . . . . .	29
3.2.3	Equilibrium equations . . . . .	30
3.2.4	Navier bending . . . . .	31
3.2.5	Differential equations and solutions . . . . .	32
3.2.6	Design chart . . . . .	34
3.3	BV Inland Rules (NR 217) . . . . .	35
3.4	Scope of improvement . . . . .	37
<b>4</b>	<b>Study methodology</b>	<b>38</b>
4.1	Investigation . . . . .	38
4.2	Integration of new parameters . . . . .	39
<b>5</b>	<b>Tools</b>	<b>41</b>
5.1	Marsinland . . . . .	41
5.1.1	General . . . . .	41
5.1.2	SHELL . . . . .	42
5.1.3	Basic ship data . . . . .	42
5.1.4	Definition of a section . . . . .	43
5.1.5	Calculation of a section . . . . .	44
5.2	Femap . . . . .	46

5.2.1	Femap tool . . . . .	46
5.2.2	Simplified study models . . . . .	47
5.2.3	Complete ship model . . . . .	49
5.2.4	Features of FE modeling . . . . .	49
5.2.4.1	Coordinate system . . . . .	49
5.2.4.2	Net scantling approach . . . . .	50
5.2.4.3	Boundary conditions and bending moments . . . . .	51
5.2.4.4	Mesh characteristics . . . . .	53
5.2.4.5	Location of stress calculation . . . . .	55
<b>6</b>	<b>Influence of different parameters on bending efficiency</b>	<b>56</b>
6.1	General . . . . .	56
6.2	Ratio of superstructure length to hull length ( $r_L$ ) . . . . .	56
6.3	Ratio of superstructure side openings to total lateral area ( $r_S$ ) . . . . .	62
6.4	Location of superstructure side openings . . . . .	66
6.5	Ratio of superstructure deck openings to total deck area ( $r_D$ ) . . . . .	68
<b>7</b>	<b>Proposal of new formula</b>	<b>73</b>
7.1	General . . . . .	73
7.2	Integration of $r_S$ . . . . .	73
7.3	Proposal of new formula . . . . .	76
7.4	Validation . . . . .	76

7.4.1	Bending efficiency . . . . .	76
7.4.2	Normal Stress Distribution . . . . .	78
<b>8</b>	<b>Application</b>	<b>82</b>
8.1	General . . . . .	82
8.2	Determination of hull girder normal stresses . . . . .	84
8.2.1	General . . . . .	84
8.2.2	Determination guidelines . . . . .	85
8.3	Local shear force in way of window stiles . . . . .	87
8.3.1	General . . . . .	87
8.3.2	Determination guidelines . . . . .	88
<b>9</b>	<b>CONCLUSIONS AND RECOMMENDATIONS</b>	<b>89</b>
	<b>REFERENCES</b>	<b>91</b>
<b>A</b>	<b>APPENDIX: Visual Basic Code</b>	<b>92</b>
<b>B</b>	<b>APPENDIX: API Code</b>	<b>97</b>
<b>C</b>	<b>APPENDIX: Data</b>	<b>101</b>

## List of Figures

Figure 1	Different types of vessels and their structures ( <i>Vedran Zanic, 2016</i> ) . . . . .	18
Figure 2	Hull-superstructure behavior for different superstructure lengths in longitudinal bending . . . . .	23
Figure 3	Modeling in LBR5 . . . . .	24
Figure 4	Beam elements and springs of CB method ( <i>H. Naar, 2004</i> ) . . . . .	25
Figure 5	Example design demonstrated by Joseph T. Kammerer (1966) . . . . .	26
Figure 6	Different tiers in midship cross-Section . . . . .	27
Figure 7	Identification Sketches of Hull and Superstructure . . . . .	30
Figure 8	Trends of bending efficiency ( <i>Schade, 1965</i> ) . . . . .	34
Figure 9	General arrangement of the passenger vessel . . . . .	40
Figure 10	MARS Inland main interface . . . . .	41
Figure 11	Basic ship data input . . . . .	42
Figure 12	Defining a section in Marsinland . . . . .	43
Figure 13	Scantling check and normal bending stress calculation with Marsinland . . . . .	44
Figure 14	Introduction of bending efficiency in different tiers . . . . .	45
Figure 15	Shear stress at window stiles . . . . .	45
Figure 16	Standard investigation model . . . . .	47
Figure 17	Midship section of standard model for investigation . . . . .	48
Figure 18	Full FE model . . . . .	49
Figure 19	Coordinate system for modeling . . . . .	50

Figure 20	Cantilever beam (left) and bending moment diagram (right) . . . . .	51
Figure 21	Rigid element . . . . .	51
Figure 22	Boundary condition for investigation models (location marked by yellow line) . . . .	52
Figure 23	Boundary conditions for complete ship model (location marked by yellow lines) . . .	52
Figure 24	Selection of proper boundary condition . . . . .	52
Figure 25	Harmonized first edge (left) and normal vectors (right) . . . . .	54
Figure 26	Good aspect ratio (left) and bad aspect ratio (right) of mesh . . . . .	54
Figure 27	Mesh shapes . . . . .	54
Figure 28	Midship elements for stress calculation at deck (left) and midship sideplate nodes for stress calculation at N.A. of superstructure (right) . . . . .	55
Figure 29	FE model for $r_L = 1.0$ , $L_S = 63m$ , , $L = 63m$ . . . . .	57
Figure 30	FE model for $r_L = 0.90$ , $L_S = 63m$ , , $L = 70m$ . . . . .	57
Figure 31	FE model for $r_L = 0.82$ , $L_S = 63m$ , , $L = 77m$ . . . . .	57
Figure 32	FE model for $r_L = 0.75$ , $L_S = 63m$ , , $L = 84m$ . . . . .	57
Figure 33	FE model for $r_L = 0.69$ , $L_S = 63m$ , , $L = 91m$ . . . . .	57
Figure 34	FE model for $r_L = 0.64$ , $L_S = 63m$ , , $L = 98m$ . . . . .	57
Figure 35	FE model for $r_L = 0.60$ , $L_S = 63m$ , , $L = 105m$ . . . . .	58
Figure 36	FE model for $r_L = 0.56$ , $L_S = 63m$ , , $L = 112m$ . . . . .	58
Figure 37	FE model for $r_L = 0.53$ , $L_S = 63m$ , , $L = 119m$ . . . . .	58
Figure 38	FE model for $r_L = 0.50$ , $L_S = 63m$ , , $L = 126m$ . . . . .	58
Figure 39	FE model for $r_L = 0.47$ , $L_S = 63m$ , , $L = 133m$ . . . . .	58

Figure 40	Influence of $r_L$ . . . . .	59
Figure 41	Influence of $r_L$ . . . . .	60
Figure 42	Influence of $r_L$ . . . . .	60
Figure 43	Influence of $r_L$ on bending efficiency . . . . .	61
Figure 44	FE model for $r_S = 0.0$ (no window in superstructure) . . . . .	62
Figure 45	FE model for $r_S = 0.14$ (six windows in superstructure) . . . . .	62
Figure 46	FE model for $r_S = 0.19$ (eight windows in superstructure) . . . . .	62
Figure 47	FE model for $r_S = 0.24$ (ten windows in superstructure) . . . . .	63
Figure 48	FE model for $r_S = 0.43$ (eighteen windows in superstructure) . . . . .	63
Figure 49	Influence of $r_S$ . . . . .	64
Figure 50	Influence of $r_S$ . . . . .	64
Figure 51	Influence of $r_S$ . . . . .	65
Figure 52	Influence of $r_S$ on bending efficiency . . . . .	66
Figure 53	FE model for windows at midship . . . . .	66
Figure 54	FE model for windows at fore and aft end . . . . .	67
Figure 55	Influence of side opening location on longitudinal normal stress . . . . .	67
Figure 56	FE model for $r_D = 0.065$ . . . . .	68
Figure 57	FE model for $r_D = 0.41$ . . . . .	68
Figure 58	FE model for $r_D = 0.24$ . . . . .	68
Figure 59	FE model for $r_D = 0.003$ . . . . .	69
Figure 60	FE model for $r_D = 0.00$ . . . . .	69

Figure 61	Influence of $r_D$ . . . . .	70
Figure 62	Influence of $r_D$ . . . . .	70
Figure 63	Influence of $r_D$ . . . . .	71
Figure 64	Influence of $r_D$ on bending efficiency . . . . .	72
Figure 65	Influence of $r_S$ on $K_{r_S}$ . . . . .	74
Figure 66	Influence of $r_S$ on bending efficiency . . . . .	75
Figure 67	Calculation of bending efficiency . . . . .	78
Figure 68	Comparison of Normal Stress Distribution at $X = 31.5\text{m}$ . . . . .	79
Figure 69	Comparison of normal stress distribution at $X = 42\text{m}$ . . . . .	79
Figure 70	Comparison of normal stress distribution at $X = 49\text{m}$ . . . . .	80
Figure 71	Comparison of normal stress distribution at $X = 70\text{m}$ . . . . .	80
Figure 72	Comparison of normal stress distribution at $X = 80.5\text{m}$ . . . . .	81
Figure 73	Bending efficiency of tier 1 (left - hull and erection together; middle - hull; right - erection) . . . . .	82
Figure 74	Bending efficiency of tier 2 (left - hull and erection together; middle - hull; right - erection) . . . . .	82
Figure 75	Bending efficiency of tier 3 (left - hull and erection together; middle - hull; right - erection) . . . . .	83
Figure 76	Bending efficiency of tier 4 (left - hull and erection together; middle - hull; right - erection) . . . . .	83
Figure 77	Modeling for stress calculation at 'hull'(left) and recommended stress distribution (right) . . . . .	85

Figure 78 Modeling for stress calculation at 'tier 1'(left) and recommended stress distribution  
(right) . . . . . 85

Figure 79 Modeling for stress calculation at 'tier 2'(left) and recommended stress distribution  
(right) . . . . . 86

Figure 80 Modeling for stress calculation at 'tier 3'(left) and recommended stress distribution  
(right) . . . . . 86

Figure 81 Modeling for stress calculation at 'tier 4'(left) and recommended stress distribution  
(right) . . . . . 87

Figure 82 Deformation of window stiles . . . . . 87

## List of Tables

Table 1	Influence of $r_L$ on stress . . . . .	59
Table 2	Influence of $r_L$ on bending efficiency . . . . .	61
Table 3	Influence of $r_S$ on longitudinal stress . . . . .	63
Table 4	Influence of $r_S$ on bending efficiency . . . . .	65
Table 5	Influence of side opening location on longitudinal stress . . . . .	67
Table 6	Influence of $r_D$ on longitudinal stress . . . . .	69
Table 7	Influence of $r_D$ on bending efficiency . . . . .	71
Table 8	Influence of $r_S$ on $K_{r_S}$ . . . . .	74
Table 9	Calculation of $\nu_{new}$ according to $r_S$ . . . . .	75
Table 10	Calculation of Bending Efficiency according to existing formula . . . . .	77
Table 11	Calculation of Bending Efficiency according to proposed formula . . . . .	77
Table 12	Longitudinal Normal Stress Distribution at X = 31.5m . . . . .	102
Table 13	Longitudinal Normal Stress Distribution at X = 42m . . . . .	103
Table 14	Longitudinal Normal Stress Distribution at X = 49m . . . . .	104
Table 15	Longitudinal Normal Stress Distribution at X = 70m . . . . .	105
Table 16	Longitudinal Normal Stress Distribution at X = 80.5m . . . . .	106
Table 17	Recommended Normal Stress Distribution at X = 49m . . . . .	107

## **Nomenclature**

BV	: Bureau Veritas
NR 217	: Bureau Veritas Inland Navigation Rules
Pt B	: Part B
Sec	: Section
Ch	: Chapter
DNI	: Direction de la Navigation Intérieure (Inland Navigation Management)
FE	: Finite Element
FEA	: Finite Element Analysis
FEM	: Finite Element Method
DOF	: Degrees of Freedom
GUI	: Graphical User Interface
N.A.	: Neutral Axis

# 1 Introduction

## 1.1 General

Longitudinal vertical bending of a ship consists of stress and strength transfer between hull and superstructure. This sharing of stress and strength is a very complex phenomenon, namely in the case of multiple deck vessels, which is being studied by naval architects for a long time.

Different vessels have different types of structures. For example: car carriers have closed superstructure without openings, livestock carriers have open superstructure on pillar arrangements, cruise vessels have large openings in side superstructure, tank-car carriers have long deckhouse on very flexible upper deck, etc. In this research work we will mainly focus our study on cruise vessels. These examples of different structures are also illustrated in figure 1.

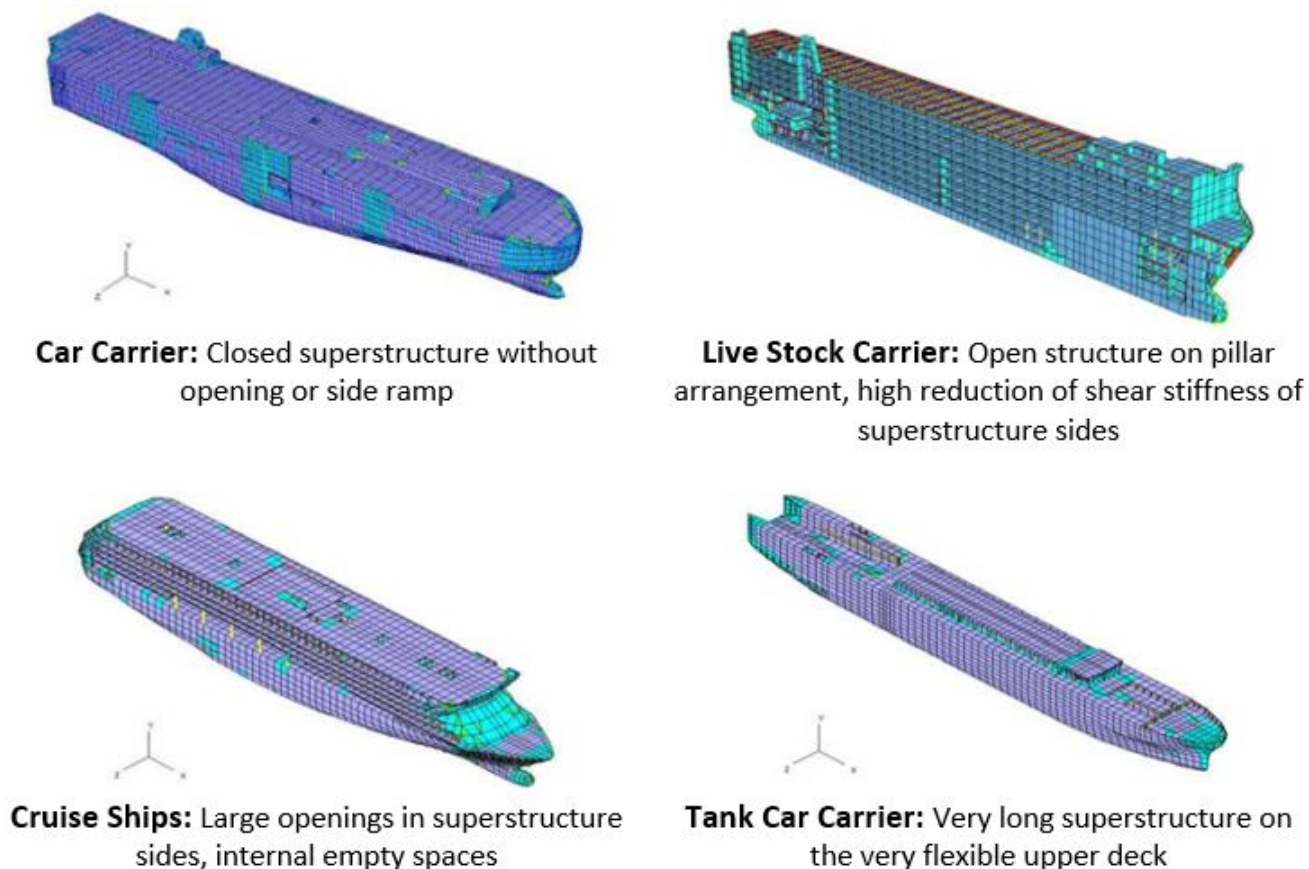


Figure 1: Different types of vessels and their structures (*Vedran Zanic, 2016*)

On passenger vessels for architectural reasons, structural connections between decks are reduced to the minimum in passenger and public area. In addition, due to design specificity such as recesses in way of life boat, openings in side shell (windows), openings in longitudinal bulkheads, all superstructure tiers are not contributing similarly to the vessel hull girder strength. To take account of this phenomenon, one can introduce bending efficiencies of superstructure tiers. Bending efficiencies are percentages given tier by tier and used as follows:

- When calculating hull girder transverse section characteristics, contribution of one given superstructure tier is weighted by its bending efficiency.
- When evaluating the hull girder stress in way of a given tier, the stress is reduced by multiplying it by the tier bending efficiency.

It is to be noted that bending efficiencies have no real physical meaning but are very useful to take into account the specific global behavior of a vessel but still using usual beam theory to assess vessel strength.

Bending efficiency of each superstructure tier is linked with global behavior of vessel. Hence, they cannot be evaluated without a complete finite element model (FEM) of the vessel. But, FEM is very time consuming and thus, very prohibitive namely for small ships. Hence, an analytical expression of bending efficiency is very helpful. The main purpose of this research is to propose guidelines allowing prediction of the contribution of the superstructure to the hull girder strength. These guideline should allow application of bending efficiency still using usual beam theory.

## **1.2 Challenges**

The stresses induced by the hull girder loads, assumed to be directly exerted on the main hull, are transferred to the superstructure, thus allowing sharing of strength between the main hull and the superstructure. The presence of superstructure can increase global hull girder strength as well as lead to failure in upper decks.

These stress transfer and strength sharing depends on a lot of design factors:

- Bending stiffness of hull and superstructure
- Foundation stiffness of deck
- Length and breadth of the superstructure compared to the length and breadth of hull girder

- Connections between hull and superstructure i.e. bulkheads, pillar lines, etc.
- Yield strength and thickness of the plates and other structural elements.
- Vertical and longitudinal continuity of the longitudinal bulkheads
- Use of pillars or large window bays, etc.

This is a big challenge to generalize all factors to form any simple analytical formula of bending efficiency due to wide range of structural diversity and complex interactions between all structural members.

### **1.3 Previous works**

A lot of research and studies have been performed regarding the hull-superstructure interaction in both analytical and numerical (mainly FE) approaches.

Crawford (1950), Terazava and Yagi (1964) worked on two beam theory for hull-superstructure interaction. Caldwell (1957) and Fransman (1988) worked on implementation of plane stress theory. However, an overview of two basic analytical approaches i.e. beam theory and plane stress theory were discussed by De Oliveira (1983). Later, a new approach called coupled beams (CB) theory was introduced by Naar (2004) for evaluating the global response of passenger ships. Naar studied the validity of this new approach on Dowlings Box Girder and also with FE model of post-panamax passenger ship. Bergstrm used ConStruct (a tool which utilizes coupled beam method) for structural analysis of a high and narrow superstructure on a cruise ship concept called xpTray. Besides, there is one software LBR5 - developed in University of Liege (Belgium) based on Kirchhoffs method of bending strip theory. Apart from these methods, an analytical formula is introduced in Bureau Veritas Inland Rules for calculating bending efficiency as discussed by Schade (1966).

Pauling and Payer (1968) carried out the first studies of 3D FEM approach for analyzing the hull-superstructure structural interaction. Different studies were carried out on 3D FE model of ships i.e. Zanic V. et al., 2004, Andric, et al., 2006, etc. Besides, some studies were also carried out on simplified 2D FE models by Mackney and Ross (1999), Heder and Ulfvarson (1991).

## **1.4 Research objectives and methods**

The main goal of this research is to develop guidelines to predict the superstructure contribution to the hull longitudinal strength. These guideline should allow application of bending efficiency to assess the global strength of the hull girder still using usual beam theory. Besides, different parameters affecting the bending efficiency, but not taken into account by Schade(1966) are investigated. The investigated parameters are as followed:

- a. Ratio of superstructure length to hull length ( $L_s/L$ )
- b. Ratio of total side opening area and lateral area of superstructure ( $A_{OS}/A_L$ )
- c. Side opening location
- d. Ratio of deck opening area to total deck area ( $A_{OD}/A_D$ )

The standard investigation model is made of two superimposed box girders. An improved expression of bending efficiency should be proposed based on the investigations. The new formula should be validated against values of bending efficiency derived by direct calculation.

## **1.5 Symbols and definitions**

$L$ : Overall length of the vessel

$B$ : Overall breadth of the vessel

$L_S$  : Overall length of the superstructure

$A_D$ : Total area of deck

$A_{OD}$ : Total opening area of deck

$A_L$ : Total lateral area of hull or superstructure

$A_{OL}$ : Total lateral opening area of hull or superstructure

$r$ : Lateral Shear Lag

$r_L$ : Ratio of superstructure length to hull length ( $L_S/L$ )

$r_D$ : Ratio of deck opening to total deck area ( $A_{OD}/A_D$ )

$r_S$ : Ratio of total side opening to total lateral area ( $A_{OD}/A_D$ )

$k$ : Foundation Modulus or Spring Constant of hull at bond

$M$ : Bending Moment generated by external forces

$m$ : Constant component of bending moment

$a$ : Amplitude of sinusoidal component of bending moment

$\sigma'_1$ : Actual stress at erection neutral axis

$\sigma_1$ : Hull girder stress at erection neutral axis according to beam theory

The primary member or hull is identified by subscript "1" and the erection is identified by subscript "e" for following parameters:

$p_1$  and  $p_e$ : Average longitudinal stress (x-direction)

$M_1$  and  $M_e$ : Stress Moment

$Z_1$  and  $Z_e$ : Section Modulus

$E_1$  and  $E_e$ : Material Modulus - normal

$G_1$  and  $G_e$ : Material Modulus - shear

$A_1$  and  $A_e$ : Effective Section Area of Deck (including webs and flanges)

$A_{SH1}$  and  $A_{SHe}$ : Shear Carrying Area (webs only)

$I_1$  and  $I_e$ : Section Moment of Inertia

$q_1$  and  $q_e$ : Vertical Load/Unit Length

$w_1$  and  $w_e$ : Vertical Deflection (+ down)

$Q_1$  and  $Q_e$ : Vertical Shear Force

$e_1$  and  $e_e$ : Distance from bond to individual neutral axis ( $e = e_1 + e_e$ )

## 2 Hull-superstructure interaction

### 2.1 General

As discussed earlier, hull-superstructure interaction is a very complex phenomenon, which depends on different parameters (section 1.2). For example, influence of superstructure length was addressed in M. Mano et al., 2009. M. Mano found that, hull and superstructure acts together as a single hull girder under longitudinal bending if the superstructure is long. On the other hand, superstructure bending deformation is opposite to the bending of hull if superstructure length is small i.e. the hull and superstructure act as separate beams.

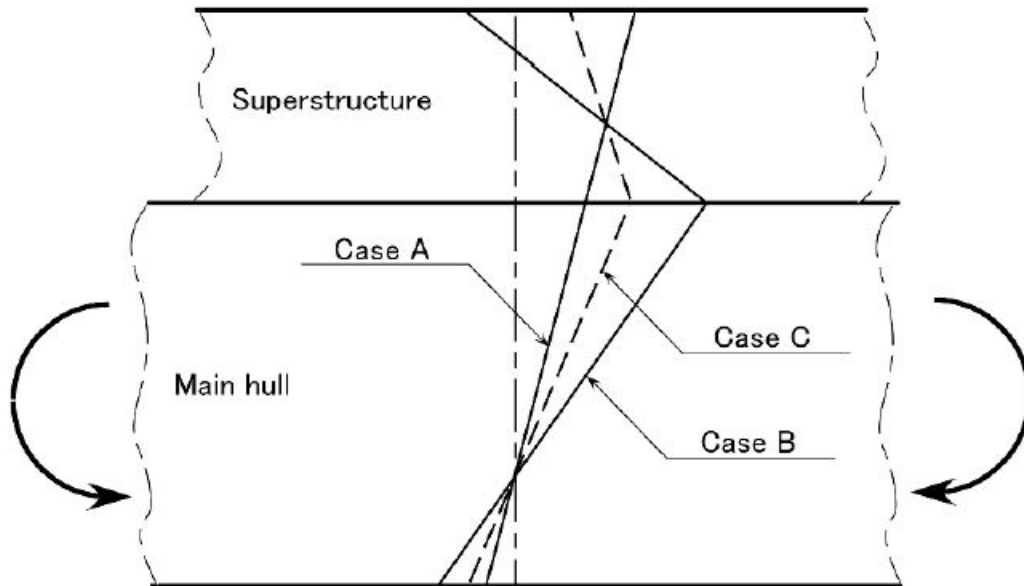


Figure 2: Hull-superstructure behavior for different superstructure lengths in longitudinal bending

We can see different situations for different superstructure lengths in figure 2. Here it is assumed that, a hogging bending moment is applied in the main hull. Case A represents a condition for long superstructure. So, the stress distribution is linear in Case A i.e. the hull and superstructure bends together as one single beam. Superstructure length is short compared to the main hull in Case B and there is a sharp change in stress distribution at the connection of main hull and superstructure i.e. the sign of the curvature is different. Case C is the intermediate case of Case A and Case B. A key finding from different investigations is that,

the superstructure can be defined as long if the superstructure length is more than 15% to 25% of the hull length.

Different analytical approaches or methods to deal with hull-superstructure phenomena will be highlighted in this section. The influence of different parameters on the hull-superstructure interaction is investigated and discussed in details in section 6.

## 2.2 Kirchhoff's method

Kirchoff developed the analytical approach of bending strip theory. Professor Dr. RIGO Philippe developed one software (LBR5) in University of Liege based on Kirchoff's method. LBR5 provides the opportunity to perform numerical modeling of a ship structure, which gives accurate values for longitudinal bending stresses. But, the main strength of this software is weight optimization at initial scantling phase.

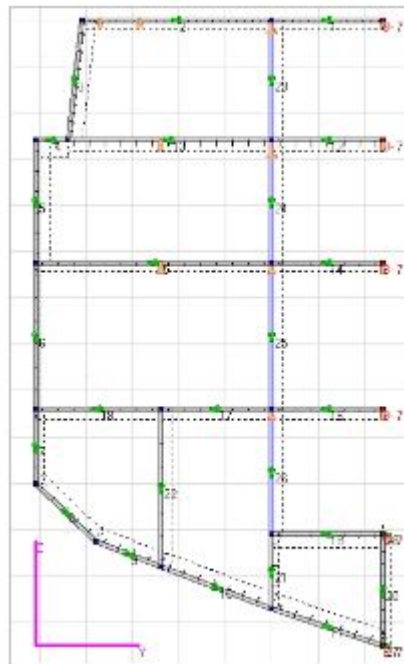


Figure 3: Modeling in LBR5

### 2.3 Coupled beam method

This method is focused on the global bending response of a long multi-deck ship, where superstructure and hull have same length. The whole hull girder is divided into longitudinal beams, where each beam consists of one deck structure with a connected side shell or side shells. Each beam has its own bending and axial stiffness. Longitudinally distributed load can be applied on each beam separately or as a resultant load on the hull beam. Besides, the beams are connected by distributed springs, which transfer vertical forces and longitudinal shear forces between the beams. The stiffness properties of the springs corresponds to the vertical elongation of the vertical structures as well as shear deformation of the structures connecting two decks. Coupling of the beams can be vertical as well as horizontal.

This method gives stress values close to the direct calculation(FEA). But, this method requires to solve a lot of equations in several steps, which makes it too much numerical. So, it does not provide any single analytical formula to determine the longitudinal bending stresses at the decks.

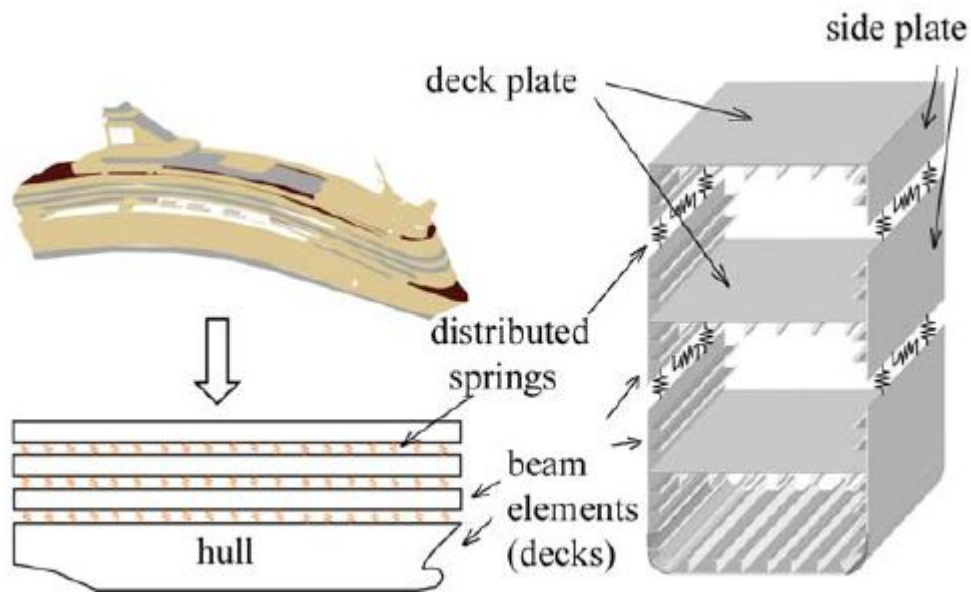


Figure 4: Beam elements and springs of CB method (H. Naar, 2004)

## 2.4 Plane stress theory

Joseph T. Kammerer (1966) developed an analytical design procedure for determining the stresses in superstructure. He used semi-empirical results of full scale experiments to evaluate the effect of differential deflections between superstructure and hull. These data were incorporated into the analytical approach based on the plane stress theory. He also demonstrated one example for finding the stresses in hull and superstructure decks. The design example ship consisted of an aluminum superstructure and steel hull. However, this method also consists of several steps including tabular calculations. So, this method also does not provide any single analytical formula to find the longitudinal bending stresses at the decks.

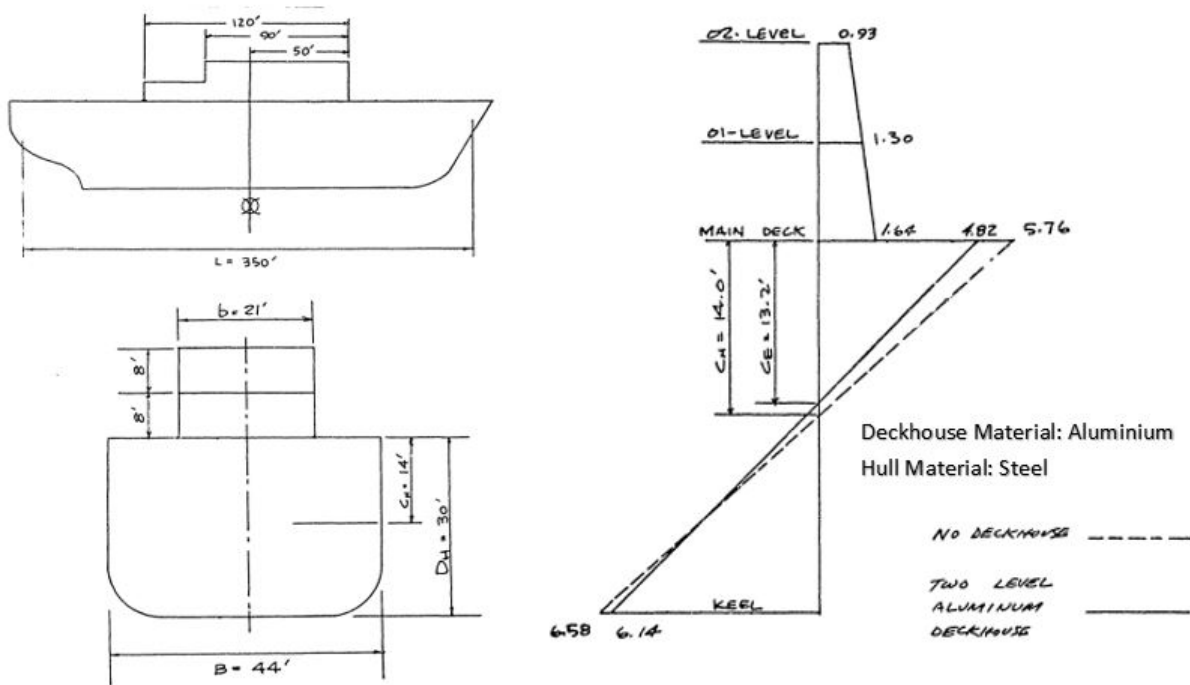


Figure 5: Example design demonstrated by Joseph T. Kammerer (1966)

## 2.5 Conclusion

None of the above methods provide any straight forward analytical formula to find longitudinal bending stresses at the superstructure. However, this problem can be quantified by taking into account the Bending Efficiency (Schade, 1965).

### 3 Bending efficiency

#### 3.1 General

The bending efficiency indicating the contribution degree of an erection to the hull girder strength may be defined as the ratio of actual stress at the erection neutral axis  $\sigma'_1$  to the hull girder stress at the same point  $\sigma_1$ , computed as if the hull and erection act as a single beam (NR 217, Pt B, Ch 4, Sec 1):

$$\nu = \frac{\sigma'_1}{\sigma_1} \quad (1)$$

According to definition, bending efficiency ( $\nu$ ) is calculated at erection neutral axis (or, neutral axis of the tier), separately for each tier. Thus, each tier have different bending efficiencies. But, the elements of same tier have same bending efficiency. Each tier consists of deck-plate elements as well as associated side-plate elements (figure 6).

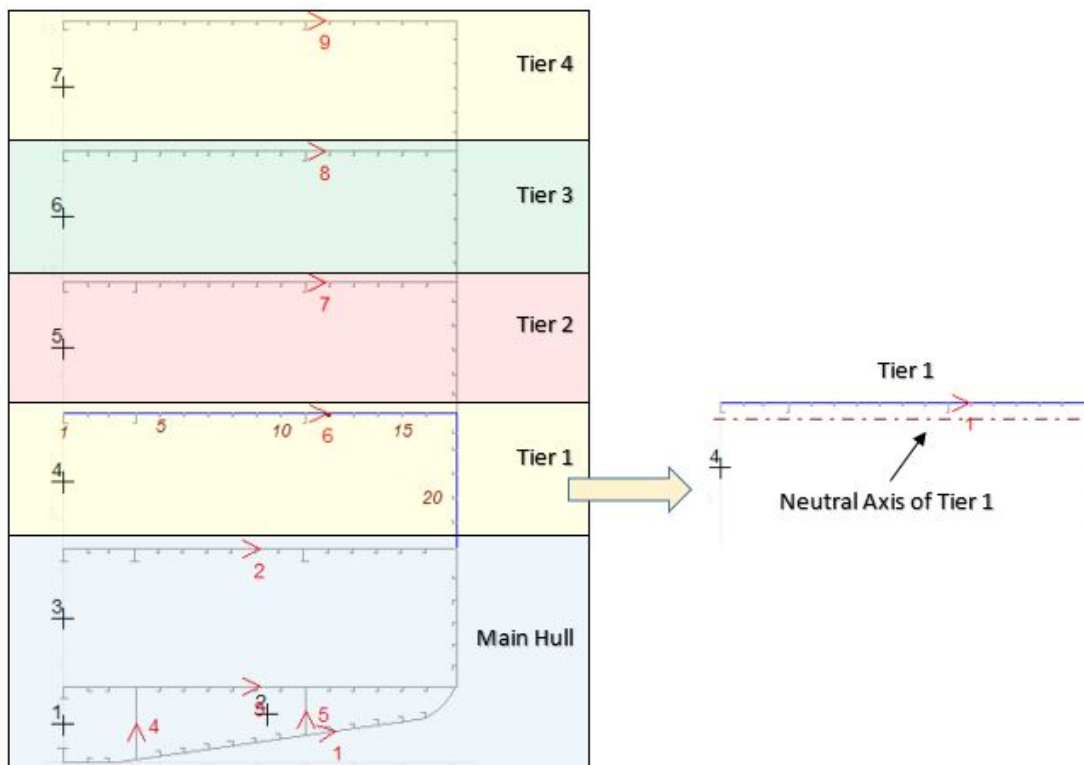


Figure 6: Different tiers in midship cross-Section

It is possible to find hull girder normal stresses at different locations of any erection, if the bending efficiency is known (section 8). Explanation of Bending Efficiency is obtained from 'Two Beam Deckhouse Theory With Shear Effects' (Schade, 1965).

## 3.2 Two beam deckhouse theory with shear effects

### 3.2.1 Introduction

The theory deals with structural response in vertical bending and shear, of the upright ship hull with an erection. The analysis is based on considering each component as thin-walled Navier beam and accounting for:

1. Vertical loading of the deckhouse by a foundation modulus  $k$  in the usual manner
2. Vertical shear deflection of each component in addition to bending deflection
3. Non-equality of longitudinal strain at deckedge and deckhouse connection of each component in addition to bending deflection

The superstructure is a special case, with only 2nd condition (above) being applicable.

However, above mentioned two terminologies 'deckhouse' and 'superstructure' are defined by Schade as:

- **Deckhouse** is an erection with side plates not being coplanar with the hull sides. Thus vertical deflections of hull and superstructure are not necessarily same.
- **Superstructure** is an erection with side plates being coplanar with main hull sides. Thus there is identical displacement between hull and superstructure as well as at the bond between them.

Respecting Schade, 'deckhouse' is used (in section 3.2) to describe both cases where the difference is immaterial. The 'superstructure' is considered as a special case of the deckhouse.

### 3.2.2 Fundamental assumptions

It is assumed that the longitudinal connection or bond between deckhouse side and deck is rigid (welded or equivalent), without slip and longitudinal stresses are related to longitudinal strains by  $\sigma = E\varepsilon$ . The longitudinal stress at the bond of deckhouse and hull can be different from the stress of hull edge. This can be corrected in simple beam theory by taking into account shear lag factor ( $r$ ):

$$p_1 - \frac{M_1}{Z_1} = \frac{1}{r} \left( p_e + \frac{M_e}{Z_e} \right) \quad (2)$$

Here,  $p_1$  and  $p_e$  are average longitudinal stresses (x-direction) in hull and erection respectively. To be noted, the longitudinal stresses at the joint of superstructure and hull are given by the sum of the average stress due to  $p$  and the bending stress due to the moment. The separate bending moments in hull and erection are  $M_1$  and  $M_e$ , and the section modulus in each are  $Z_1$  and  $Z_e$ , respectively. For simplification purpose,  $r$  is assumed to have the same value it would have without the deckhouse, determined by a box-girder analysis of the hull alone as in 'Thin-Walled Box Girder Theory' (Schade, 1965). According to this analysis, for a sinusoidal bending moment of length  $2\lambda$ :

$$r = \frac{1}{2} \frac{1}{\cosh \frac{\pi b}{2\lambda}} \left[ \frac{\pi y}{2\lambda} \sinh \frac{\pi y}{2\lambda} + 2 \cosh \frac{\pi y}{2\lambda} - \frac{\pi b}{2\lambda} \tanh \frac{\pi b}{2\lambda} \cosh \frac{\pi y}{2\lambda} \right] \quad (3)$$

But, obviously  $r$  should be taken as unity for a constant bending moment.

It is also assumed that the vertical unit load transmitted to the deckhouse through the bond may be represented by:

$$q_e = k(w_1 - w_e) \quad (4)$$

Here,  $w_1$  and  $w_e$  are vertical deflections of hull and erection respectively.  $k$  is foundation modulus and it has a dimension of stress. The formulation or method for determining  $k$  is illustrated in section 3.2.5 (equation 14 and 17). To be noted, the limit of foundation modulus is between zero and infinity for deckhouse ( $0 < k < \infty$ ), whereas it leads to infinity for superstructure ( $k \rightarrow \infty$ ).

### 3.2.3 Equilibrium equations

A vertical cut through the hull and superstructure at location  $x$ , measured from the end of the superstructure is assumed in figure 7. The superstructure and hull, when each bend as separate beams, will have individual neutral axis  $NA_1$  and  $NA_e$ , separated by the vertical distance  $e$ . The forces of interaction consists of a horizontal shear flow,  $N$ , and a vertical distributed loading,  $q_n$ , each having the dimensions of force per unit length. Other parameters related to this interaction between hull and erection are shown in figure 7.

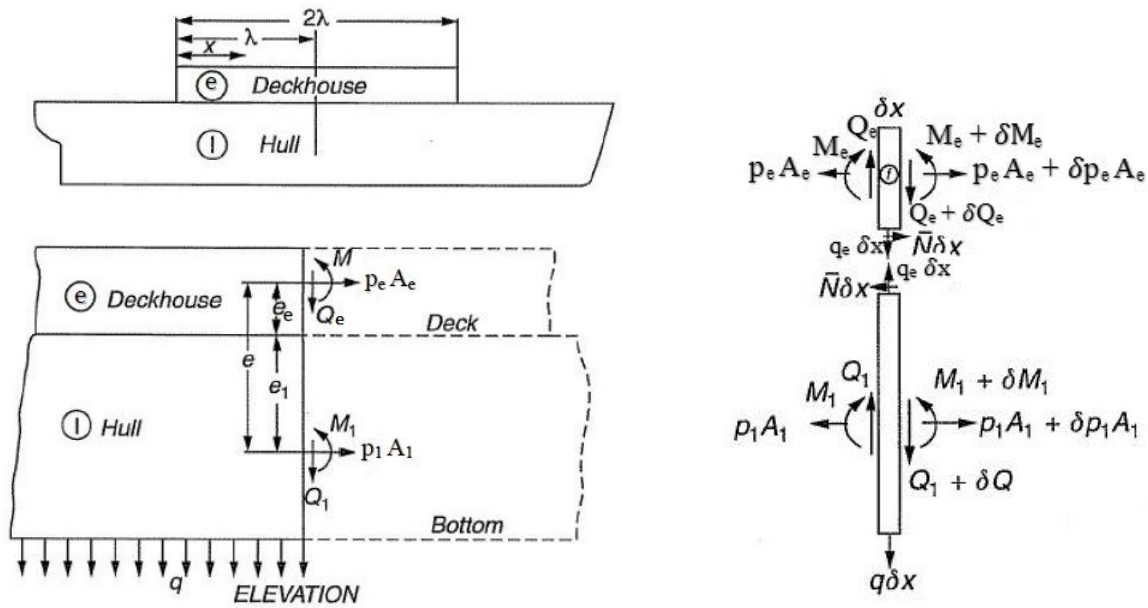


Figure 7: Identification Sketches of Hull and Superstructure

So, the equilibrium equations of longitudinal forces and equilibrium of moments about the respective neutral axis of hull and superstructure separately:

$$\begin{aligned} A_1 p_1 + A_1 p_1 &= 0 \\ M_1 + M_e - A_e e p_e &= M \end{aligned} \quad (5)$$

Here,  $A_1$  and  $A_e$  are effective section areas for hull and erection respectively. These effective section areas include webs and flanges. Combining Equations 5 and 2, and then solving for  $M_e$ :

$$M_e = \frac{r Z_e}{r Z_e - Z_1} \left\{ p_e \left[ A_e e + Z_1 \left( \frac{r A_e + A_1}{r A_1} \right) + M \right] \right\} \quad (6)$$

Vertical shear in erection,  $Q_e$  is obtained from Combining equation 6 with the equilibrium condition shown in figure 7:

$$Q_e = \frac{rZ_e}{Z_e - rZ_e} \left( \frac{p'_e}{C_1} + M' \right) \quad (7)$$

Combining equation 4 with the equilibrium condition shown in figure 7:

$$k(w_1 - w_e) = \frac{rZ_e}{Z_e - rZ_e} \left( \frac{p''_e}{C_1} + M'' \right) \quad (8)$$

### 3.2.4 Navier bending

Since both hull and erection are assumed to behave as Navier beams with shear deflection included:

$$\begin{aligned} M_1 &= -E_1 I_1 \left( \frac{d^2 w_1}{dx^2} + \frac{q_1}{A_{SH1} G_1} \right) \\ M_e &= -E_e I_e \left( \frac{d^2 w_e}{dx^2} + \frac{q_2}{A_{SHe} G_e} \right) \end{aligned} \quad (9)$$

Here,  $A_{SH1}$  and  $A_{SHe}$  are the vertical shear-carrying areas (i.e. section areas of webs only) of the hull and superstructure respectively.  $G_1$  and  $G_e$  are the shear modulus of elasticity of hull and superstructure respectively. Combining all these equations and equilibriums and eliminating  $M_1$ ,  $M_e$ ,  $Q_1$   $q_1$  and  $q_f$  gives:

$$\begin{aligned} \left( \frac{1}{A_{SH1} G_1} + \frac{1}{A_{SHe} G_e} \right) \frac{rZ_e}{C_1} p''_e - \frac{(A_1 + rA_e)(I_1 + I_e) + A_1 A_e e(re_1 + e_e)}{A_1 E_e e_1 e_e} p_e = \\ \frac{1}{E_1} \frac{(re_1 + e_e)}{e_1 e_e} M - \left( \frac{Z_1}{A_{SHe} G_1} + \frac{rZ_e}{A_{SHe} G_e} \right) M'' + (Z_1 - Z_{er})(w''_1 - w''_e) \end{aligned} \quad (10)$$

Here,  $C_1$  is a parameter defined as:

$$C_1 \equiv \frac{A_1 r Z_e}{(A_1 + rA_e) Z_1 Z_e + A_1 A_e (e_e S_1 + e_1 r Z_e)} \quad (11)$$

### 3.2.5 Differential equations and solutions

Equation 10 leads to two different differential equations for superstructure ( $k \rightarrow \infty$ ) and deckhouse ( $0 < k < \infty$ ). Here, the form of bending moment to be assumed:

$$M = m + a \left( \sin \frac{\pi x}{2\lambda} \right) \quad (12)$$

For a superstructure ( $k \rightarrow \infty$ ), equation 10 furnishes the differential equation in  $p_e$  directly (since  $w_1'' = w_e''$ ):

$$-\frac{1}{k^2} p_e'' + p_e = -C_2 \left[ m + \Theta a \left( \sin \frac{\pi x}{2\lambda} \right) \right] \quad (13)$$

Here for a superstructure ( $k \rightarrow \infty$ ),  $k$  is defined as:

$$k^2 = \frac{C_1 [(A_1 + A_e r)(I_1 + I_e) + A_1 A_e e(e_e + r e_1)]}{E_e + \left( \frac{1}{a_1 G_1} + \frac{1}{a_e G_e} \right) e_1 A_1 r I_e} \quad (14)$$

For a deckhouse ( $0 < k < \infty$ ), equation 10 leads to following fourth-order differential equation:

$$\frac{1}{4\omega^4} p_e^{IV} - \frac{\eta}{\omega^2} p_e'' + p_e = -C_2 \left[ m + \Theta a \left( \sin \frac{\pi x}{2\lambda} \right) \right] \quad (15)$$

In equation 15,  $\Theta$  is a parameter defined as:

$$\Theta \equiv 1 + \frac{E_1}{r e_1 + e_e} \left( \frac{I_1 e_e}{A_{SH1} G_1} + \frac{r I_e e_1}{A_{SHe} G_e} \right) \left( \frac{\pi}{2\lambda} \right)^2 + \frac{E_1}{r e_1 + e_e} \frac{r I_e e_e}{k} \left( \frac{\pi}{2\lambda} \right)^4 \quad (16)$$

Here, the value of  $k$ , without presence of transverse bulkheads, may be estimated by means of the simple beam theory. If the deck beam together with the effective deck plating as clamped at the hull sides and loaded with two identical line loads  $p$  at the deckhouse sides produce a unit deflection at the deckhouse sides, then

$$k = 2p \quad (17)$$

In equation 15,  $C_2$  is a parameter defined as:

$$C_2 = \frac{E_e}{E_1} \frac{A_1(re_1 + e_e)}{(A_1 + rA_e)(I_1 + I_e) + A_1A_ee(re_1 + e_e)} \quad (18)$$

Solution of the equation 15 formulates the equation for bending efficiency ( $\nu$ ) in three different forms depending on whether: a)  $\eta < 1$  b)  $\eta = 1$  c)  $\eta > 1$ . Where,  $\eta$  is defined as:

$$\eta = \frac{1}{2} \left( \frac{1}{A_{SH1}G_1} + \frac{1}{A_{SHe}G_e} \right) \sqrt{\frac{kE_1eI_ee_1 C_1}{(re_1 + e_e) C_2}} \quad (19)$$

So, the solutions of  $\nu$  are as followed:

a)  $\eta < 1$

$$\begin{aligned} \nu = 1 - \frac{1}{\sinh 2\lambda\alpha + \frac{\alpha}{\beta} \sin 2\lambda\beta} & \left[ \sinh \alpha (2\lambda - x) \cos \beta x + \frac{\alpha}{\beta} \cosh \alpha (2\lambda - x) \sin \beta x + \right. \\ & \left. + \sinh \alpha x \cos \beta (2\lambda - x) + \frac{\alpha}{\beta} \cosh \alpha x \sin \beta (2\lambda - x) \right] \end{aligned} \quad (20)$$

b)  $\eta = 1$

$$\begin{aligned} \nu = 1 - \frac{1}{\sinh 2\lambda\gamma + 2\lambda\gamma} & \left[ (\sinh 2\lambda\gamma + 2\lambda\gamma) \cosh \gamma x - \right. \\ & \left. - (1 - \cosh 2\lambda\gamma) \sinh \gamma x - \gamma x \sinh 2\lambda\gamma \sinh \gamma x \right] \end{aligned} \quad (21)$$

c)  $\eta > 1$

$$\begin{aligned} \nu = 1 - \frac{1}{\sinh 2\lambda\alpha + \frac{\alpha}{\beta} \sinh 2\lambda\beta} & \left[ \sinh \alpha (2\lambda - x) \cos \beta x + \frac{\alpha}{\beta} \cosh \alpha (2\lambda - x) \sinh \beta x + \right. \\ & \left. + \sinh \alpha x \cosh \beta (2\lambda - x) + \frac{\alpha}{\beta} \cosh \alpha x \sinh \beta (2\lambda - x) \right] \end{aligned} \quad (22)$$

The parameters  $\alpha$ ,  $\beta$  and  $\gamma$  used in equation 20, 21 and 22 are defined as:

$$\alpha^2 \equiv \omega^2(\eta + 1); \quad \beta^2 \equiv \omega^2(\eta - 1); \quad \gamma^2 \equiv 2\omega^2 \quad (23)$$

Where,

$$\omega = \sqrt[4]{\frac{k}{4rI_e} \frac{(re_1 + e_e)C_1}{E_1e_e C_2}} \quad (24)$$

The contribution of shear lag ( $r$ ) into bending efficiency ( $\nu$ ) is very evident from equation 20 to 24. Here,  $\omega$  is a parameter of unit  $in^{-4}$  or  $cm^{-4}$ , which is later expressed in more simplified form (equation 25) for using the design chart. However, the direct shear lag effect represented by  $r$  has importance only when the applied bending moment is not constant. In fact, different values of  $r$  applied in same model for sinusoidal bending moment will show considerable change in main deck edge stresses, but not in superstructure deck.

### 3.2.6 Design chart

The solutions for bending efficiency ( $\nu$ ) illustrated in section 3.2.5 were condensed into a single design chart suitable for most practical ship structural applications (figure 8).

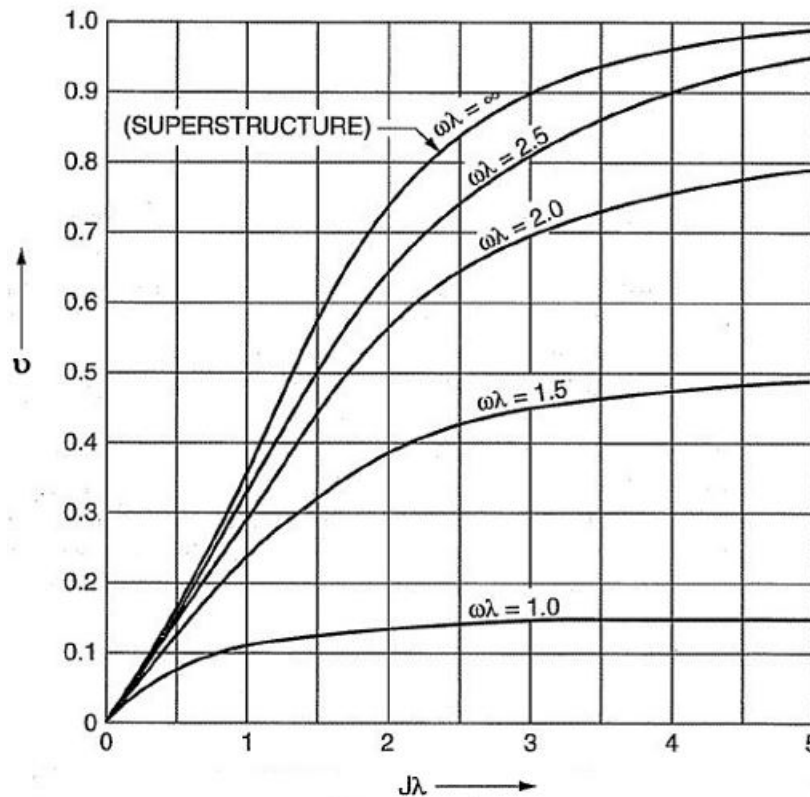


Figure 8: Trends of bending efficiency (Schade, 1965)

It is necessary to compute following three parameters to use the chart in figure8 :

$$\text{Section geometry parameter, } \Omega = \frac{(A_1 + A_e)(I_1 + I_e) + A_1 A_e (e_1 + e_e)^2}{(A_1 + A_e)I_1 I_e + A_1 A_e (I_1 e_e^2 + I_e e_1^2)} \quad (25)$$

$$\text{Foundation modulus parameter, } \omega^4 = \frac{k}{E_1} \frac{\Omega}{4} \quad (26)$$

$$\text{Shear stiffness parameter, } j = \sqrt{\frac{1}{\frac{1}{a_{SH1}} + \frac{1}{A_{SHe}}} \frac{\Omega}{2(1 + \mu)}} \quad (27)$$

Here,  $\mu$  is Poisson's ratio, usually taken as value 0.3;  $a_1$  and  $a_e$  are shear carrying areas in hull and erection respectively. This design chart was developed in imperial units. The solution from this chart can be used to obtain the loads in the middle portions of the erections, but not near the ends where large localize loads may occur.

### 3.3 BV Inland Rules (NR 217)

According to Pt B, Ch 4, Sec 1, the hull girder transverse sections are to be considered as being constituted by the members contributing to the hull girder longitudinal strength, i.e. all continuous longitudinal members below the strength deck, taking into account the following requirements:

*Strength deck:* In general the strength deck is the uppermost continuous deck.

*Longitudinal bulkheads with vertical corrugations:* Longitudinal bulkheads with vertical corrugations may not be included in the hull girder transverse sections.

*Members in materials other than steel:* Where a member made in material other than steel, its contribution to the longitudinal strength will be determined by the Society on case by case basis.

*Large openings and scallops:* Large openings are:

- in the side shell plating: openings having a diameter greater than or equal to 300 mm
- in the strength deck: openings having a diameter greater or equal to 350 mm

Large openings and scallops, where scallop welding is applied, are always to be deducted from the sectional areas included in the hull girder transverse sections.

*Lightening holes, draining holes and single scallops:* Lightening holes, draining holes and single scallops in longitudinals or girders need not be deducted if their height is less than  $0.25h_w$ , without being greater than  $75\text{mm}$ , where  $h_w$  is the web height, in  $\text{mm}$ . Otherwise, the excess is to be deducted from the sectional area or compensated.

According to NR 217 (Pt B, Ch 1, Sec 2), *superstructure* is a decked structure connected to the strength deck, extending from side to side of the vessel or with the side plating not being inboard of the shell plating more than  $0.04B$ , where  $B$  is breadth of the vessel. Any superstructure side plate outboard of  $0.04B$  is very near to the vicinity of hull side plate. Thus, any superstructure according to NR 217 can be considered as similar to the superstructure defined by Schade (section 3.2.1).

The design chart provided by Schade consists of several curves for several conditions based on the value of  $\omega\lambda$ . The formula provided by NR 217 for finding superstructure bending efficiency is based on the superstructure curve ( $k \rightarrow \infty \Rightarrow \omega\lambda = \infty$ ). The efficiency  $\nu_i$  of a superstructure  $i$ , rigidly constrained to act with the main hull girder, may be determined using the formula:

$$\nu_i = \nu_{i-1}(0.37\chi - 0.034\chi^2) \quad (28)$$

Here,  $\nu_{i-1}$  is bending efficiency of superstructure located below considered erection,  $\lambda$  is erection half length (in m) and  $\chi$  is a dimensionless coefficient defined as:

$$\chi = 100j\lambda \leq 5 \quad (29)$$

Here:

$\lambda$  : Erection half length, in  $m$

$j$  : Shear stiffness parameter, in  $\text{cm}^{-1}$ , defined in equation 27

$\Omega$  : Section geometry parameter, in  $\text{cm}^{-4}$ , defined in equation 25

$A_1, A_e$  : Independent sectional areas of hull, in  $\text{cm}^2$ , of hull and erection, respectively, determined separately for each tier as explained in section 3.1.

$A_{AH1}, A_{SHe}$  : Independent vertical shear areas, in  $\text{cm}^2$ , of hull and erection, respectively, determined

separately for each tier as explained in section 3.1.

$I_1, I_e$  : Independent section moment of inertia, in  $cm^4$ , of hull and erection, respectively, determined separately for each tier as explained in section 3.1.

$e_1, e_e$  : Vertical distances, in  $cm$ , from the main (upper) deck down to the neutral axis of erection respectively, as shown in figure 7.

### **3.4 Scope of improvement**

The formula of bending efficiency (equation 28) is applicable to superstructure according to BV inland Rules. It takes into account following parameters: superstructure length and breadth, shear stiffness parameter, section geometry, vertical shear lag and lateral shear lag, etc. But, it does not consider some parameters like ratio of superstructure length to hull length ( $r_L$ ), ratio of superstructure side openings to total lateral area ( $r_S$ ), ratio of superstructure deck openings to total deck area ( $r_D$ ), etc. Hence, there is a difference between the normal stress calculated analytically using bending efficiency and the normal stress from direct calculation (Zou Jiawei, 2013). It is possible to reduce this gap by incorporating the parameters which are not taken into account in the formula.

## 4 Study methodology

### 4.1 Investigation

A standard investigation model composed of two superimposed box girders (without any side opening or deck opening) was modeled in Finite Element. This model is considered as a standard study model or reference FE model. Affect of different parameters were studied in this standard investigation model. The parameters investigated in the standard study model are as followed:

1. *Ratio of superstructure length to hull length ( $r_L$ ):* Several investigation models of different  $r_L$  were created. Current formula of bending efficiency considers superstructure length. Hence, hull length was modified in these models. Nothing else was changed to avoid influence of other parameters.
2. *Ratio of superstructure side openings to total lateral area ( $r_S$ ):* Several investigation models of different  $r_S$  were created. Only side openings were modified in these models. Nothing else was changed to avoid influence of other parameters.
3. *Location of superstructure side openings:* Two investigation models of same  $r_S$  were created. Both of them have same number of windows of same size. But, locations of the windows are different. One model has all the windows at midship. The other model has windows at the fore and aft end of the ship. Nothing else was changed to avoid influence of other parameters.
4. *Ratio of deck openings to total deck area ( $r_D$ ):* Several investigation models of different  $r_D$  were created. Only deck openings were modified in these models. Nothing else was changed to avoid influence of other parameters.

Development of dedicated investigation models for above investigations are discussed in section 6 with corresponding data. Aim of these investigations are to develop a improved analytical expression allowing better/upgraded bending efficiency prediction.

It is to be noted that, the direct calculation of bending efficiency is performed according to the formula  $\nu = \sigma'_1/\sigma_1$  (equation 1). Where,  $\sigma'_1$  is the normal stress from direct calculation and  $\sigma_1$  is the normal stress from beam theory. Besides, the bending moment to be applied on investigation models should be very big in order to amplify the influence of investigated parameters.

## 4.2 Integration of new parameters

It is possible to integrate new parameter into the existing formula of bending efficiency based on the investigations. Hence, a new expression of bending efficiency should be obtained. This new expression of bending efficiency ( $\nu$ ) should fit the superstructure curve of design chart (figure 8). Hence, new parameters should be integrated in dimensionless coefficient -  $\chi$ , in order to affect the x-axis of the chart without changing the curve.

A real passenger vessel is modeled in finite element. This complete ship model will be used for validation of the new formula of bending efficiency. This ship complies with BV Inland Rules (NR 217, 2011) and has following specifications:

<b>Dimensions:</b>		<b>Machinery</b>	
Gross Tonnage:	2096 (Estimated)	Propelling Engine Type:	Diesel
Overall Length:	112m	Licence:	CATERPILLAR
LPP:	98m	<b>Power and rating</b>	
Breadth:	16.2m	Total Power (kW):	1710 kW
Depth:	4.4m	Total Power (HP):	2325 HP
Draught:	2.2m	<b>Propelling Machinery</b>	
		Internal Combustion Engine:	(3) 4T - 12 cyl - 13.72 cm x 15.24 cm at 2100 rpm
<b>Hull and Cargo:</b>		Electrical Installation	
Hull Material:	Steel	Frequency:	50 Hz
Machinery:	Aft	<b>Propellers and propellershafts</b>	
<b>Tanks</b>		Propelling system	2 Screw Propeller Solid Ord 10.00
LBC:	6985		1 Screw Propeller Solid Ord 10.00 at 719 rpm

General arrangement of the passenger vessel is shown in figure 9. There are total 4 decks (including sun deck) above main deck. There is a lower deck between main deck and double bottom. Total passenger capacity of this ship is 160 in spacious suits and staterooms. There are also some installations including a pool, Jacuzzi, gym and sauna with massage services. There are 80 comfortable staterooms including 12 suites, 68 veranda and 4 deluxe rooms. All of them are outside with river view. The category A (yellow color in figure 9) and category B (blue color in figure 9) rooms have veranda. The main entrance is located around midship with side openings of 2 decks height.

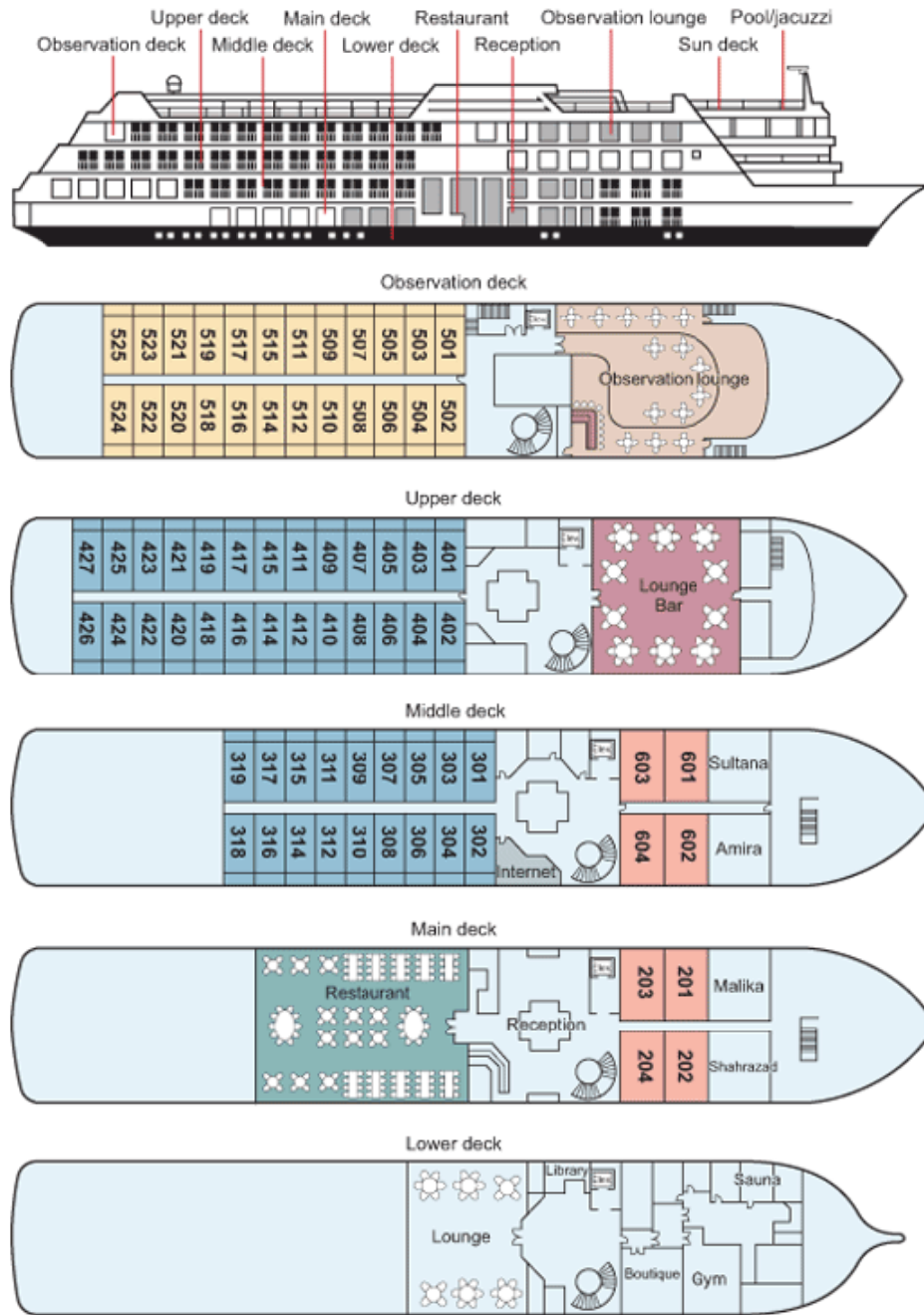


Figure 9: General arrangement of the passenger vessel

The lower deck is used mainly for leisure purposes such as lounge, gyms and library. There are restaurant, receptions and suits (red color in figure 9) in main deck. The restaurant is located new engine room, whereas living rooms are at fore part to avoid noise and vibration from engine rooms. The decks above main deck has suits, category A and B rooms. There are one swimming pool and two Jacuzzis in sun deck.

## 5 Tools

### 5.1 Marsinland

#### 5.1.1 General

Marsinland is a software developed by Bureau Veritas. It can be used to perform scantling check of plating and ordinary stiffeners of any transverse section located along the vessel central part according to BV rules for the Classification of Inland Navigation Vessels (NR 217). The software tool is organized around the following four modules:

- MARSSHELL (Shell)
- MIRE2000 (Basic Ship Data)
- MARSIN2000 (Section's Input)
- MARSRULE2000 (Section's Check)

The geometry and the scantling are defined using a user friendly process. Marsinland checks that the actual local scantlings (Hull girder strength, plating and ordinary stiffeners) are in accordance with NR 217.

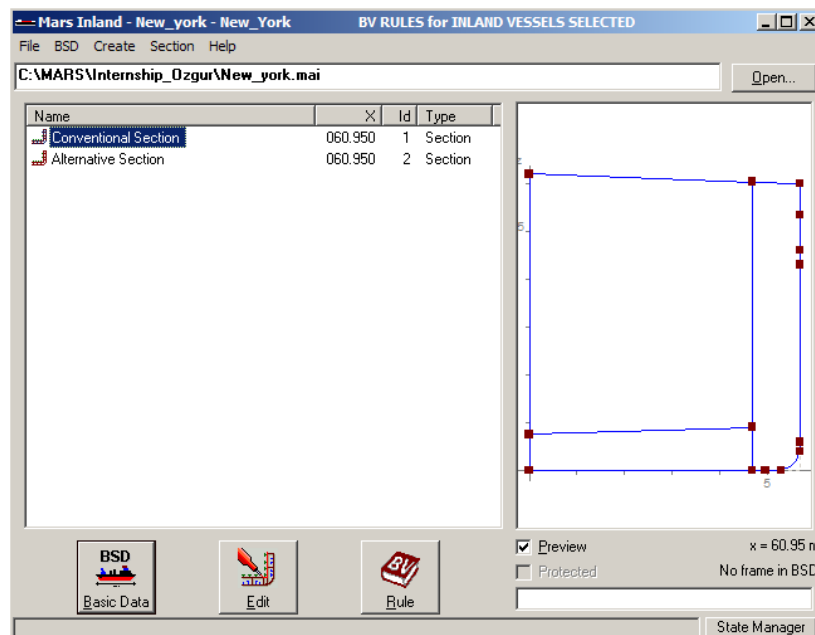


Figure 10: MARS Inland main interface

### 5.1.2 SHELL

The Marshell module allows creating a new database or choice of an existing database. The module is organized around the application in fig 10.

### 5.1.3 Basic ship data

Basic ship data module allows the input of general data common for all the transverse sections. It also performs calculations that may be done from those data. The basic ship data module is organized around the application shown in fig 11.

The screenshot shows the 'Basic Ship Data 2000' software interface. The window title is 'Basic Ship Data 2000 - New\_York - NEW\_YORK' and the subtitle is 'BY RULES FOR INLAND VESSELS SELECTED'. The interface is divided into several sections:

- General:** Contains a menu bar (File, About Mars...) and a toolbar with icons for file operations.
- Notations & Main Data:** This is the active section. It includes:
  - Service:** A dropdown menu set to 'Tanker'.
  - Navigation:** A dropdown menu set to 'IN(X)' and a text input field for '1.70 m'.
  - Loading:** A dropdown menu set to '2R (2 runs)'.
  - Self-propelled:** Radio buttons for 'Yes' (selected) and 'No'.
  - Main dimensions:**
    - Scantling length: 122.020 m
    - Breadth moulded: 11.400 m
    - Block coefficient: 0.900
    - Maximum service speed: 20.00 km/h
  - Fore, central and aft parts (from AE):**
    - After peak bulkhead: 2.000 m
    - Aftmost cargo bulkhead: 19.480 m
    - Foremost cargo bulkhead: 111.020 m
    - Collision bulkhead: 117.820 m
  - Depths:**
    - At strength deck: 6.000 m
    - At top of continuous member: 6.200 m
- Other sections:** Moments & Draughts, Bow Flare, Materials, Frame Locations, and Calculations & Print.

Figure 11: Basic ship data input

The BSD module is divided into seven main parts:

- General
- Notations and main data
- Moments and draught
- Materials
- Frame locations
- Hopper wells (Hopper dredgers and split dredgers only)
- Calculation and print

### 5.1.4 Definition of a section

MARSIN allows the input of any section along vessel length. The section is described by:

- Longitudinal elements contributing to the hull girder strength
- Transverse stiffeners
- Compartments

The module allowing to input the data of a section is organized around the application shown in figure 12. Besides, it is also possible to find out the normal bending stress at different locations. Warning box displays warning message when MARSIN detects incoherence in the section definition. The section is displayed in section view.

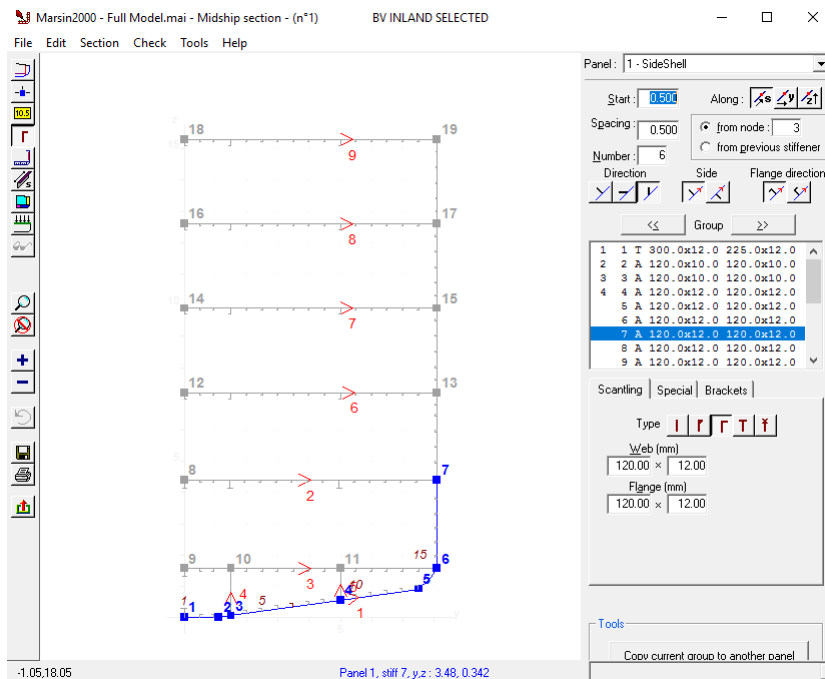


Figure 12: Defining a section in Marsinland

### 5.1.5 Calculation of a section

The MARSRULE module allows to check a section according to Bureau Veritas Rules for Classification of Inland Vessel. It checks:

- the strength characteristics of the hull girder
- the scantling of the continuous longitudinal members - strakes and longitudinal ordinary stiffeners
- the scantling of the transverse ordinary stiffeners

MARSRULE is able to perform calculations in any section all along the vessel length. The sections are to be defined as described in section 5.1.4. The module allowing to perform the calculations for a given section is organized around the application shown in figure 13.

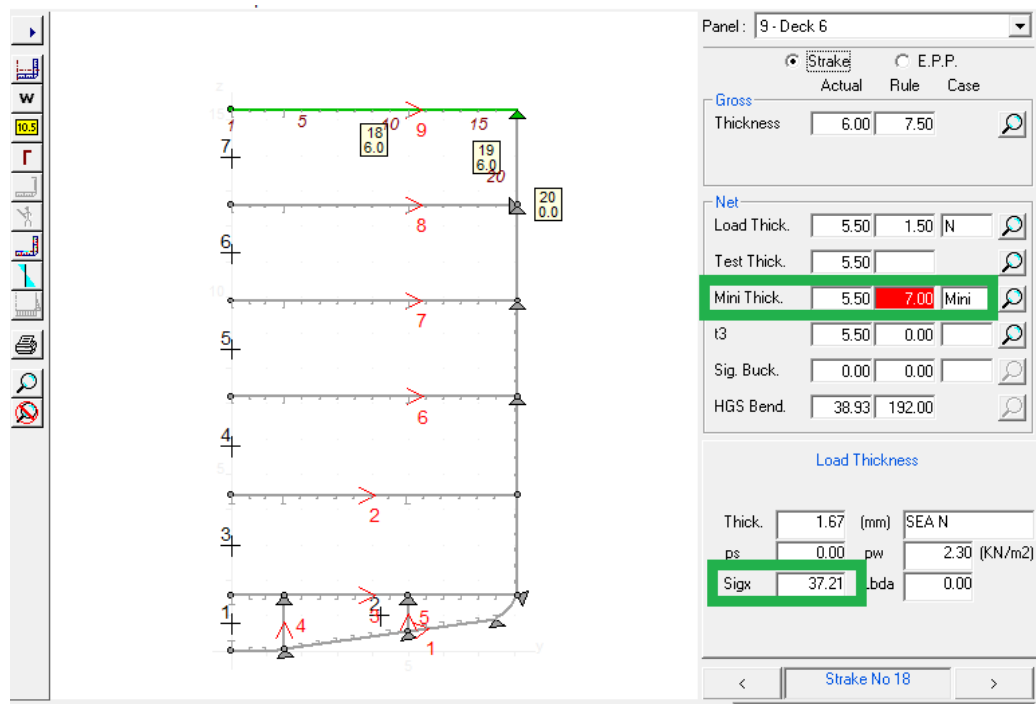


Figure 13: Scantling check and normal bending stress calculation with Marsinland

Figure 13 shows modeling of one transverse section of a vessel in Marsinland. In this model, the sun deck is selected. So, all values appearing in the panel at right is corresponding to sun deck. 'Mini' beside 'Mini Thick' is the minimum scantling thickness according to NR217. 'Sigx' shows the value of  $\sigma_1$ . Hence, the normal stress at sun deck,  $\sigma_1 = 37.21 N/mm^2$ . Similarly, it is also possible to check scantling and find normal stresses at other decks and different locations/heights of side plate.

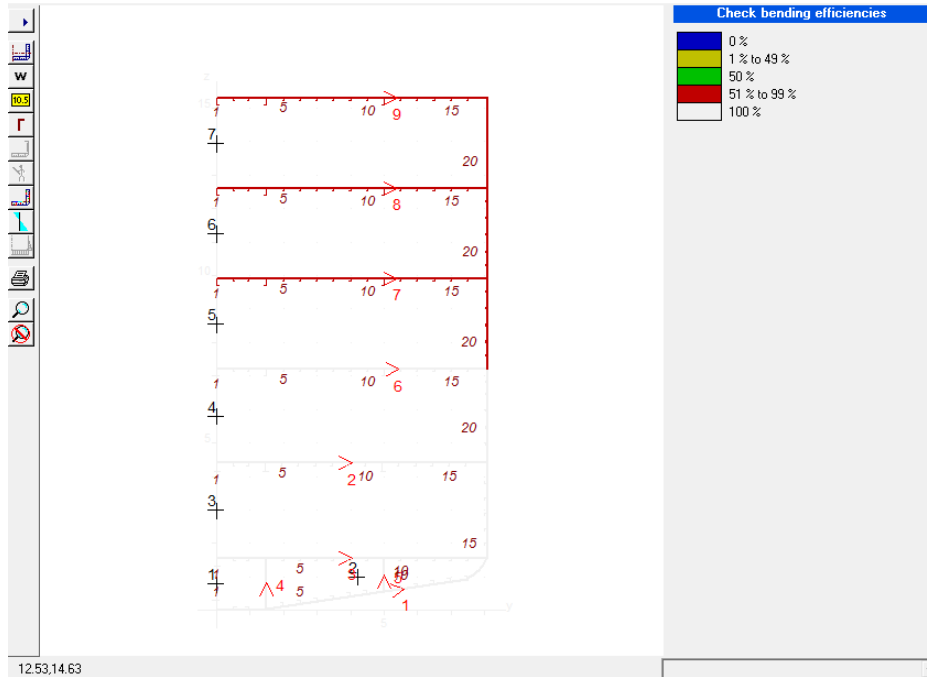


Figure 14: Introduction of bending efficiency in different tiers

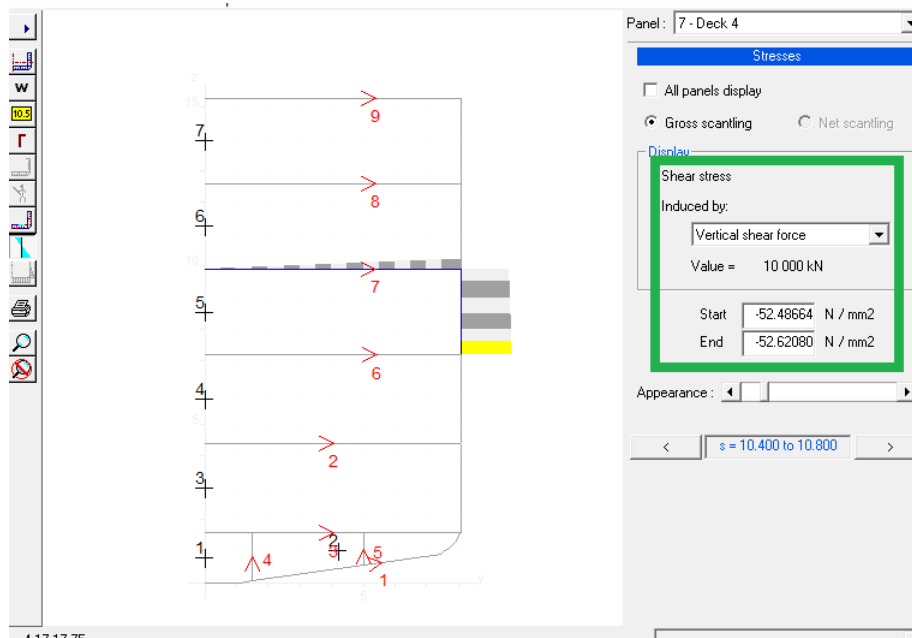


Figure 15: Shear stress at window stiles

Besides, bending efficiencies of different tiers can be introduced in Marsinland. Figure 14 shows different bending efficiencies in different tiers of a Marsinland model. Marsinland calculates the normal stress as per beam theory i.e. bending efficiency is 100% for all tiers. But, if different bending efficiencies are introduced in different tiers, the stress distribution is calculated according to following three steps:

1. Redistribution of moment of inertia in each tier according to corresponding bending efficiency
2. Calculation of  $\sigma_1$  according to redistributed moment of inertia
3. Calculation of  $\sigma'_1$  according to equation 1.

It is also possible to find shear stress at locations of window stiles using Marsinland, as shown in figure 15.

## 5.2 Femap

### 5.2.1 Femap tool

Femap is an advance engineering simulation software, which is used to create Finite Element Model. It is also possible to import CAD models from different softwares like CATIA, Solid Edge, SolidWorks, AutoCAD, etc. into Femap. Femap integrated with NX Nastran serves as a pre and post processing tool for Finite Element Analysis. Design decisions can be taken faster by integrating multiple analysis technologies and visualization environment to Femap. Femap not only supports Nastran series solver, but also Abaqus, LS-DYNA, SINDA, TMG, etc.

Femap also enables versatile visualization tools, which helps to understand the model behavior quickly and efficiently. Tools like contour plotting, deformed shape animations, dynamic cutting plane and iso-surfaces, time and frequency domain analysis, etc. are very useful for visualization and interpretation of output data. Besides, Femap is integrated with API programming and enables Macro program files.

### 5.2.2 Simplified study models

A standard investigation model composed of two superimposed box girders is modeled in FEMAP (a Finite Element tool) (figure 16). Characteristics of this investigation model are:

- Length of superstructure is equal to the length of hull,  $r_L = 1.0$
- Breadth of superstructure is equal to the length of hull,  $r_B = 1.0$
- It has only one superstructure deck above the main deck
- There is no deck opening in the superstructure deck,  $r_D = 0$
- There is no side opening in the superstructure side-plate,  $r_S = 0$
- Total length of the standard investigation model is 63 meter. Scantling and other information shown in figure 1
- Material: Normal Steel, Grade A
- Material Properties: Yield Strength =  $235MPa$ , Young's Modulus =  $206.0GPa$   
Shear Modulus =  $78.03GPa$ , Poisson's Ratio = 0.3

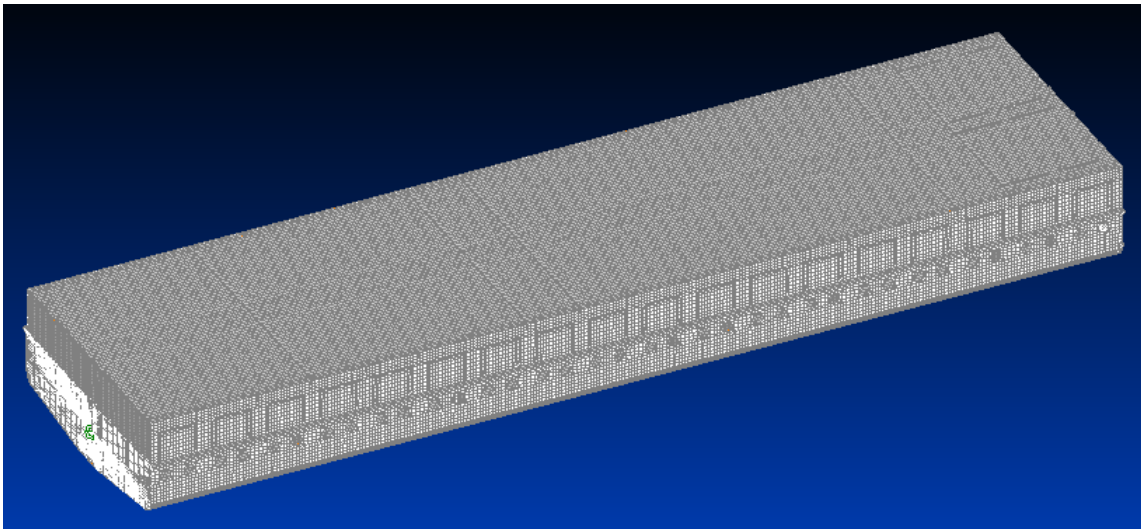


Figure 16: Standard investigation model

The transverse section details of this standard investigation model is shown in figure 17. As seen in figure, the superstructure sides are co-planar with hull sides. Besides, the superstructure and hull are connected by 4 pillars at frame. Different changes were made in this reference model in order to study different parameters. These changes in modeling and relevant investigations were described in details in section 6.



### 5.2.3 Complete ship model

Complete FE model of a passenger vessel was created for validation (figure 18). Some simplification was made in the FE model. For example, stairs, swimming pool, jacuzzi, manholes and storage tanks were not modeled. The bow was not modeled fully in fore part of the vessel as the concerned area for calculation is midship. Deck openings were also simplified in shape. However, all simplifications were considered in the analysis accordingly.

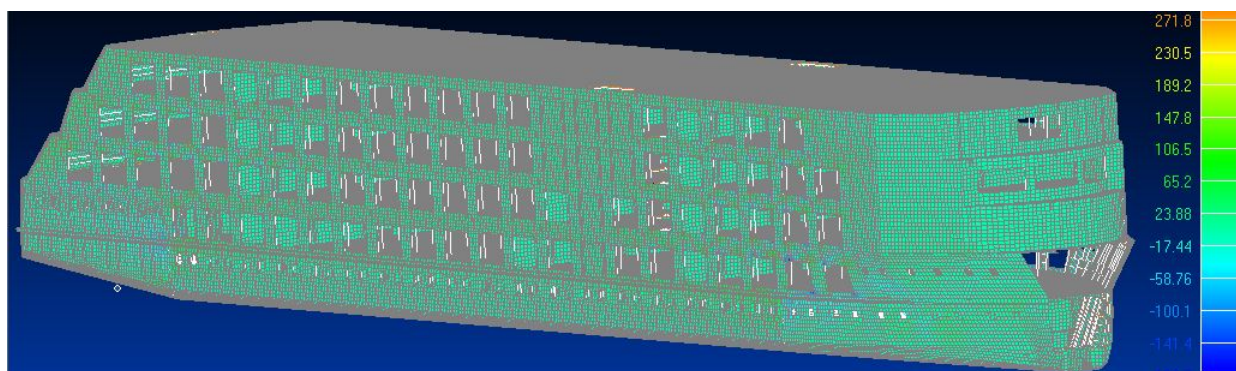


Figure 18: Full FE model

### 5.2.4 Features of FE modeling

#### 5.2.4.1 Coordinate system

The vessel's coordinate system is defined in NR 217 (Pt B, Ch 1, Sec 2) as right-hand coordinate system (figure 19):

- Origin: at the intersection among the longitudinal plane of symmetry of vessel, the aft end of  $L$  and the baseline
- X axis: longitudinal axis, positive forwards
- Y axis: transverse axis, positive towards portside
- Z axis: vertical axis, positive upwards

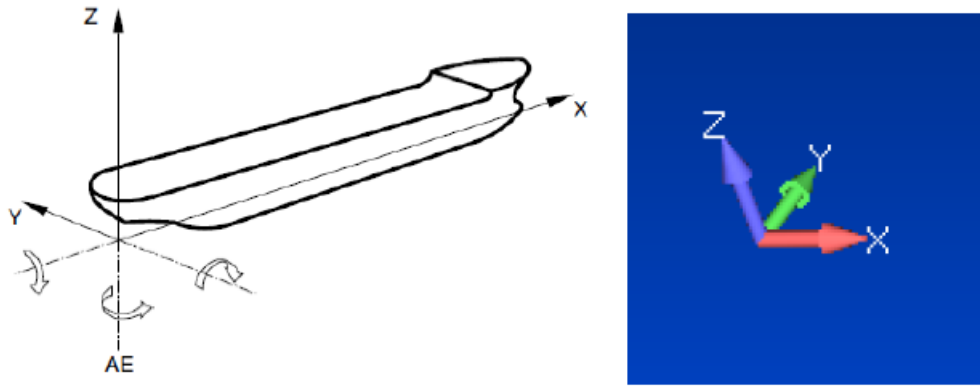


Figure 19: Coordinate system for modeling

The coordinate system according to NR 217 is shown in figure 19.

#### 5.2.4.2 Net scantling approach

All FE models were performed according to the net thickness. Thus corrosion thickness was deducted from gross thickness to achieve net thickness. The corrosion addition for each of the two sides,  $t_{C1}$  or  $t_{C2}$  are defined in NR 217 (Pt B, Ch 2, Sec 5). The total corrosion addition  $t_C$ , in *mm*, for both sides of a structural member, is equal to:

- for a plating with a gross thickness greater than *10mm*:  $t_C = t_{C1} + t_{C2}$
- for a plating with a gross thickness less than or equal to *10mm*:

$t_C = 20\%$  of the gross thickness, or

$$t_C = t_{C1} + t_{C2}$$

whichever is smaller.

For an internal member within a given compartment, the total corrosion addition  $t_C$  is to be determined as followed:

- for a plating a stiffener plating with a gross thickness greater than *10mm*:  $t_C = 2t_{C1}$
- for a plating or stiffener plating with a gross thickness less than or equal to *10mm*:

$t_C = 20\%$  of the gross thickness of the plating considered, or

$$t_C = 2t_{C1}$$

whichever is smaller.

### 5.2.4.3 Boundary conditions and bending moments

Cantilever bending moment (figure 20) was applied for all FE analysis. Bending moment was applied in the fore end of the model and aft end was clamped. Thus the bending moment was constant for full length of the models. Rigid elements were created under main deck, which allows transfer of load to various nodes. Rigid element connects free edge nodes and other nodes in the same plane, so that they act together as a single element. Thus, two rigid elements are required to create two boundary conditions:

1. Constraint: a rigid element at the aft of the model with zero DOF to clamp
2. Moment: Bending Moment is applied on a rigid element at the fore part of the model in positive y direction to create hogging condition.

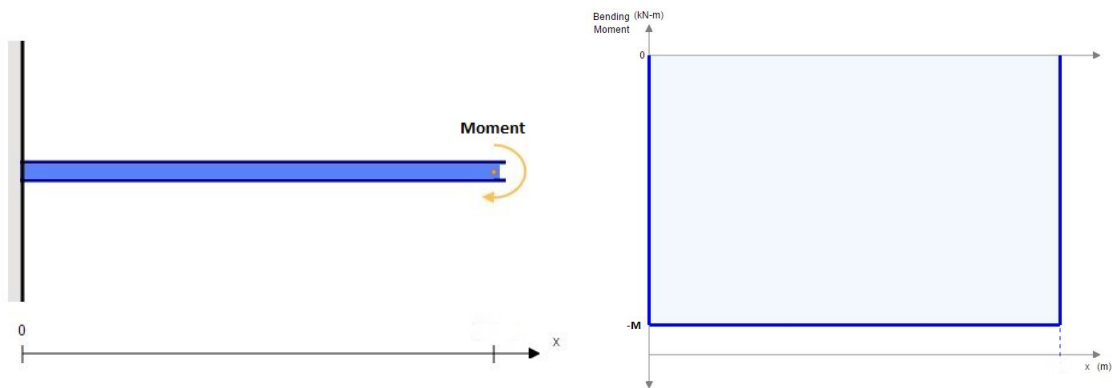


Figure 20: Cantilever beam (left) and bending moment diagram (right)

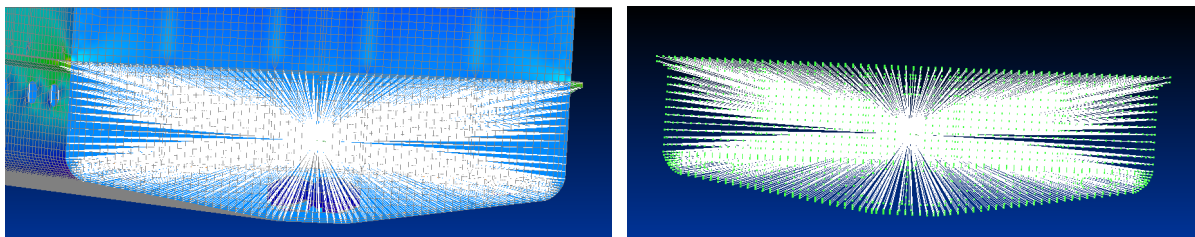


Figure 21: Rigid element

An imaginary big bending moment was applied for the simplified study models to exploit the influences of investigated parameters. The amount of the bending moment  $5E10^{10} MPa$ . For the investigation models, boundary condition was set on fore and aft peak of the hull (under the main deck).

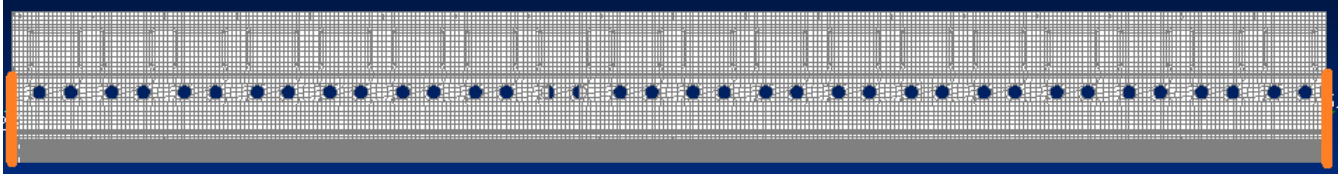


Figure 22: Boundary condition for investigation models (location marked by yellow line)

Since the real passenger vessel is very big, different boundary conditions were simulated to check the proper stress transfer throughout the whole model. Different locations of the boundary conditions are shown in figure 23. Among different boundary conditions, proper boundary condition was selected by maintaining the equilibrium of longitudinal forces (equation 5) as shown in the figure 24.

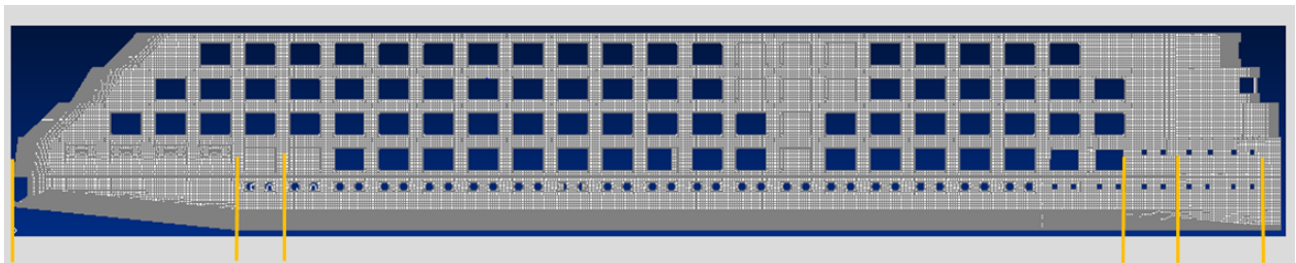


Figure 23: Boundary conditions for complete ship model (location marked by yellow lines)

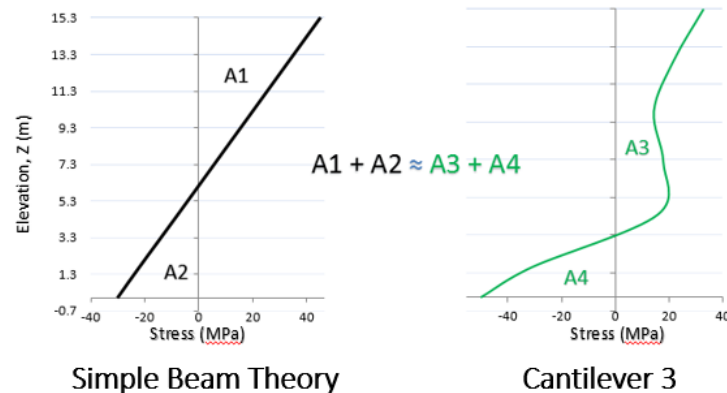


Figure 24: Selection of proper boundary condition

The formula to be used for bending moment calculation for a passenger vessel is given in NR 217 (Pt B, Ch 3, Sec 2). The still water bending moments (amidships), in KN.m, for passenger vessels with machinery aft are to be determined using following formula:

Still water hogging bending moment:

$$M_{HO} = 0.273L^2 B^{1.342} D^{0.172} (1.265 - C_B) = 126317kN.m \quad (30)$$

Still water sagging bending moment:

$$M_{SO} = 0 \quad (31)$$

The wave bending moment, in KN.m, for range of navigation IN ( $0.6 < x \leq 2$ ) :

Still water hogging bending moment:

$$M_W = 0.021nCL^2 B(C_B + 0.7) = 43629kN.m \quad (32)$$

Thus the total bending moment for calculation is  $170009KN.m$  or,  $1.7E10^{11}MPa$ .

The equilibrium of forces (as shown in figure 24) is obtained for following locations:

- Clamped at:  $X = 21m$
- Bending Moment applied at:  $X = 89.8m$

#### **5.2.4.4 Mesh characteristics**

Plate elements were used for modeling most of the structures. Beam elements were also used, but only for stiffener flanges. First Edge and normal vectors of all elements were harmonized as shown in figure 25. This is very important obtain correct result. Similarly the element size and shape were also taken care of. Most of the elements are quadrilateral. Triangular elements were used only in unavoidable cases. Besides, suitable aspect ratio was maintained for all element shapes. Two examples are shown in figure 26. Aspect ratio of the red elements shown in the figure at right are out of acceptable range, thus will lead to bad results. On the other hand, the figure at left represents the FE models used in this research, where all elements have nice aspect ratio. Besides, most of the mesh were quadrilateral (figure27). Triangular mesh was avoided as much as possible to obtain good accuracy in result.

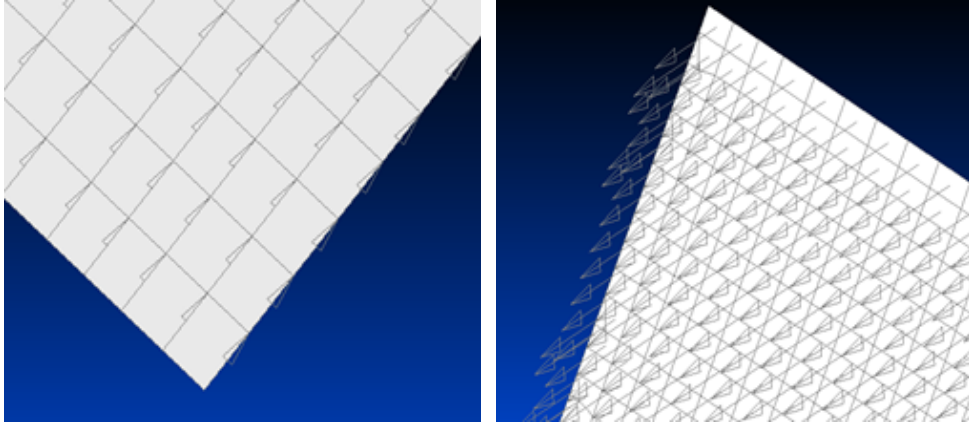


Figure 25: Harmonized first edge (left) and normal vectors (right)

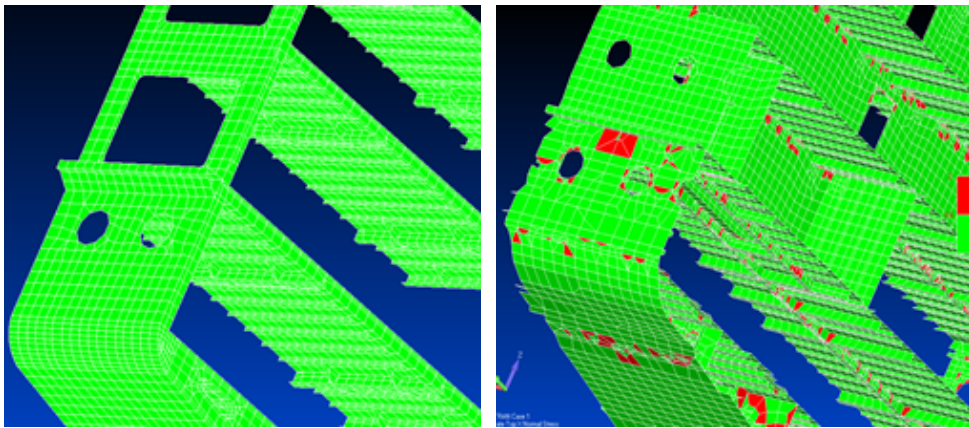


Figure 26: Good aspect ratio (left) and bad aspect ratio (right) of mesh

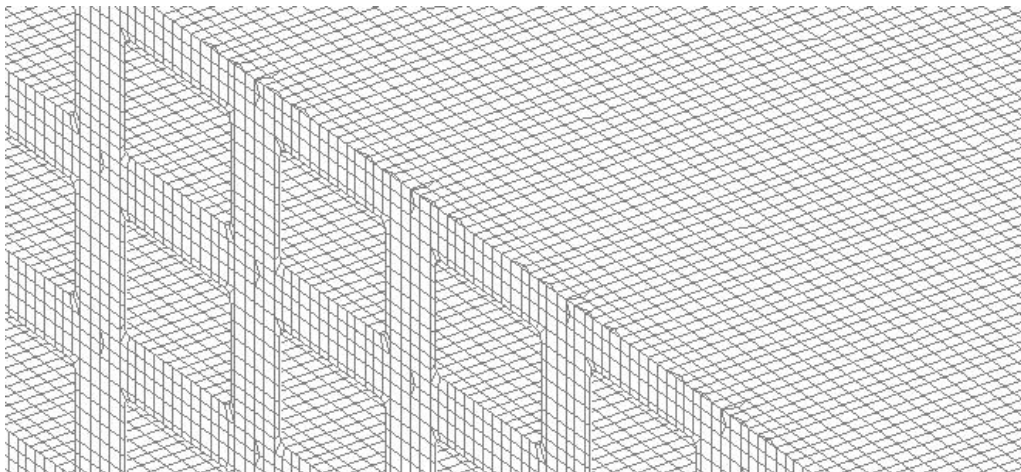


Figure 27: Mesh shapes

#### **5.2.4.5 Location of stress calculation**

All the stress calculation were done in midship of the models. Stress calculation was performed in locations other than midship in case the section of validation only.

In case of deck, average stress was taken from a elements near to side plate. This way, there is no loss of stress due to shear lag. But, the elements were not too near of the sideplate and deckplate connection in order to avoid any stress concentration (figure 28).

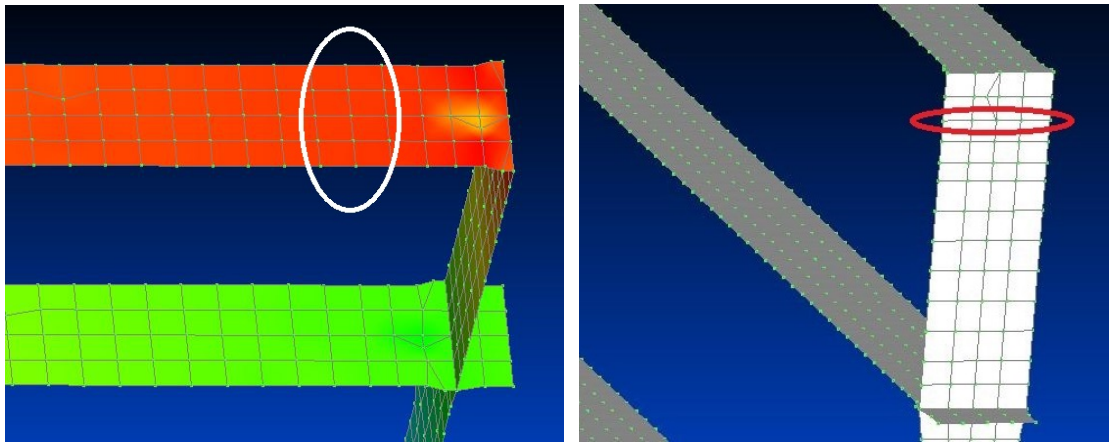


Figure 28: Midship elements for stress calculation at deck (left) and midship sideplate nodes for stress calculation at N.A. of superstructure (right)

In case of stress calculation in neutral axis of superstructure, average stress was calculated from 5 nodes at the height of neutral axis between two frames at midship. Since, there was no element or node in deck at this height, nodes from sideplate were used for this calculation (figure 28).

## 6 Influence of different parameters on bending efficiency

### 6.1 General

Influence of different parameters (deck opening, side opening, superstructure length, etc.) on superstructure bending efficiency will be discussed in this chapter. Normally several full scale experiment data or FE data is required for finding the influence of any single parameter. Thus, only one parameter will be changed, while other parameters will be kept constant in all experiments or tests to find out the influence of that parameter (as the reference FE models were created in section 5.2.2).

However, it is very costly for full scale ship experiments as well as time consuming for full FE model. So one simplified FE model is to be used for all these calculations. Rule formula is tier by tier, so a prismatic portion of a real passenger vessel was modeled from bottom to first deck (only one tier), as discussed in section 5.2.2. Then, the parameters were investigated one by one. We used the same simplified model for investigation of all parameters and used the same bending moment. However, the bending moment was very big and imaginary to exploit the influences of the parameters and differences. In the end, we will convert all the effects into equation of dimensionless coefficients, so that we can generalise the behaviour of superstructure. To be noted that, we will consider mid-ship section between two windows for all analysis.

### 6.2 Ratio of superstructure length to hull length ( $r_L$ )

The influence of ratio of superstructure length to hull length ( $r_L$ ) is investigated in this section. Superstructure length is taken into account in existing formula. Thus, the interest of this investigation lies in exploiting the influence of  $r_L$  in terms of hull length. So, different FE Models were created with various hull lengths. To be noted, only the hull lengths were different in these models, nothing else.

$r_L$  is 1.00 for the reference FE model, as superstructure length and hull length are equal. Length of the hull was modified in different FE models for studying different cases of  $r_L$ . But, the superstructure length was kept same for all cases ( $L_S = 63m$ ). All these FE models had same boundary conditions. All these models are shown in figure 29 to 39.

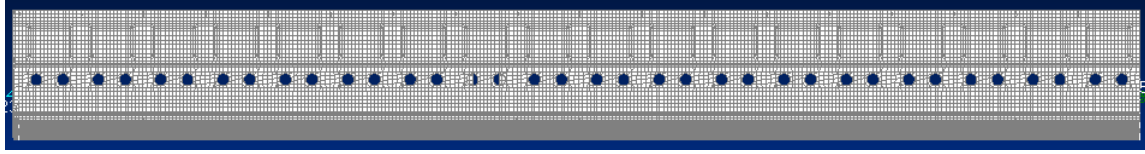


Figure 29: FE model for  $r_L = 1.0$ ,  $L_S = 63m$ ,  $L = 63m$

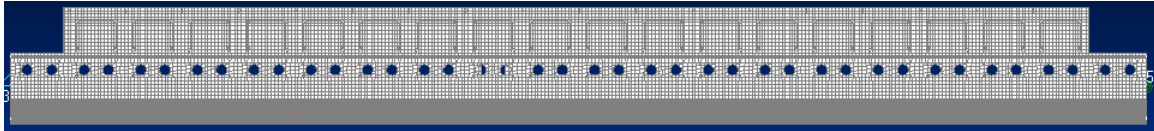


Figure 30: FE model for  $r_L = 0.90$ ,  $L_S = 63m$ ,  $L = 70m$

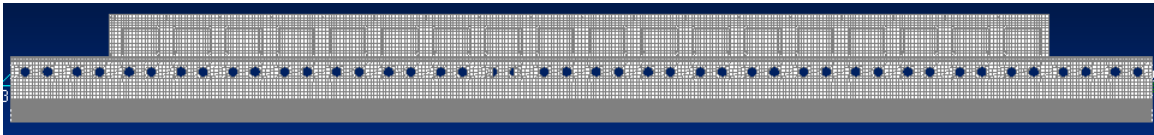


Figure 31: FE model for  $r_L = 0.82$ ,  $L_S = 63m$ ,  $L = 77m$

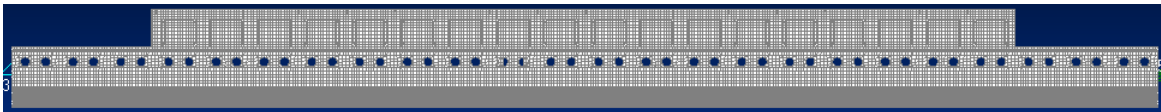


Figure 32: FE model for  $r_L = 0.75$ ,  $L_S = 63m$ ,  $L = 84m$

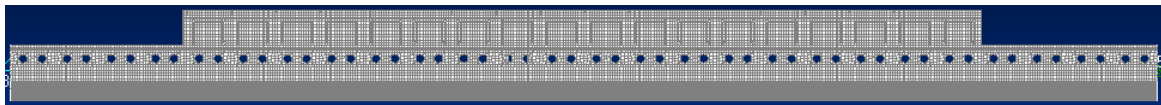


Figure 33: FE model for  $r_L = 0.69$ ,  $L_S = 63m$ ,  $L = 91m$

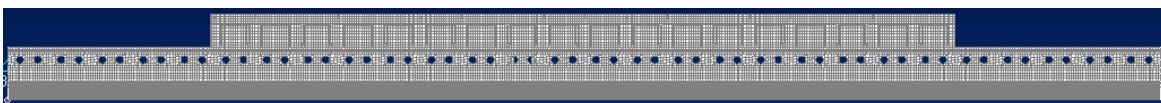


Figure 34: FE model for  $r_L = 0.64$ ,  $L_S = 63m$ ,  $L = 98m$

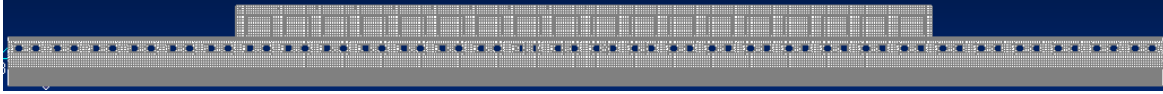


Figure 35: FE model for  $r_L = 0.60$ ,  $L_S = 63m$ ,  $L = 105m$



Figure 36: FE model for  $r_L = 0.56$ ,  $L_S = 63m$ ,  $L = 112m$

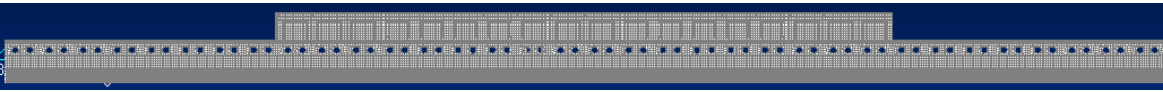


Figure 37: FE model for  $r_L = 0.53$ ,  $L_S = 63m$ ,  $L = 119m$

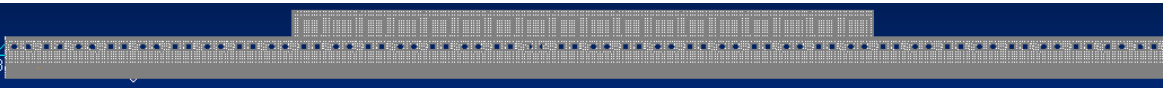


Figure 38: FE model for  $r_L = 0.50$ ,  $L_S = 63m$ ,  $L = 126m$

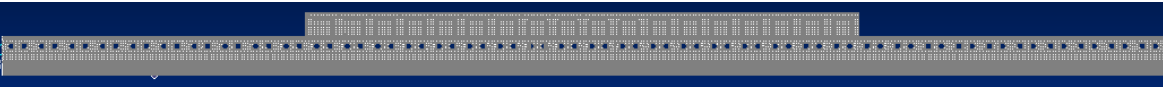


Figure 39: FE model for  $r_L = 0.47$ ,  $L_S = 63m$ ,  $L = 133m$

Stresses from FEA for all these different cases are illustrated in table 1. The influence of  $r_L$  on stresses can be exploited by visualization in graph (figure 40 to 42).

Table 1: Influence of  $r_L$  on stress

Case	$L_S(m)$	$L(m)$	$r_L$	Normal Stress (MPa)		
				N.A. of Superstructure	Superstructure Deck	Main Deck
1	63.00	63.00	1.00	30.03	30.75	12.14
2	63.00	70.00	0.90	29.92	30.60	12.58
3	63.00	77.00	0.82	29.90	30.54	12.66
4	63.00	84.00	0.75	29.90	30.53	12.54
5	63.00	91.00	0.69	29.90	30.54	12.54
6	63.00	98.00	0.64	29.90	30.54	12.54
7	63.00	105.00	0.60	29.90	30.54	12.53
8	63.00	112.00	0.56	29.90	30.54	12.53
9	63.00	119.00	0.53	29.90	30.55	12.53
10	63.00	126.00	0.50	29.90	30.55	12.53
11	63.00	133.00	0.47	29.90	30.55	12.53

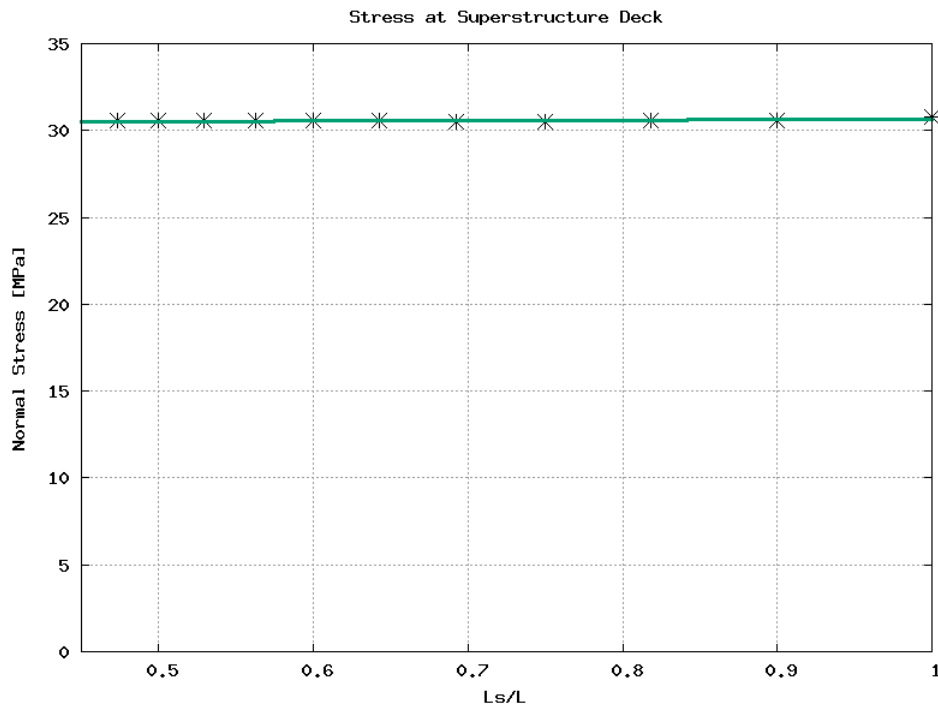
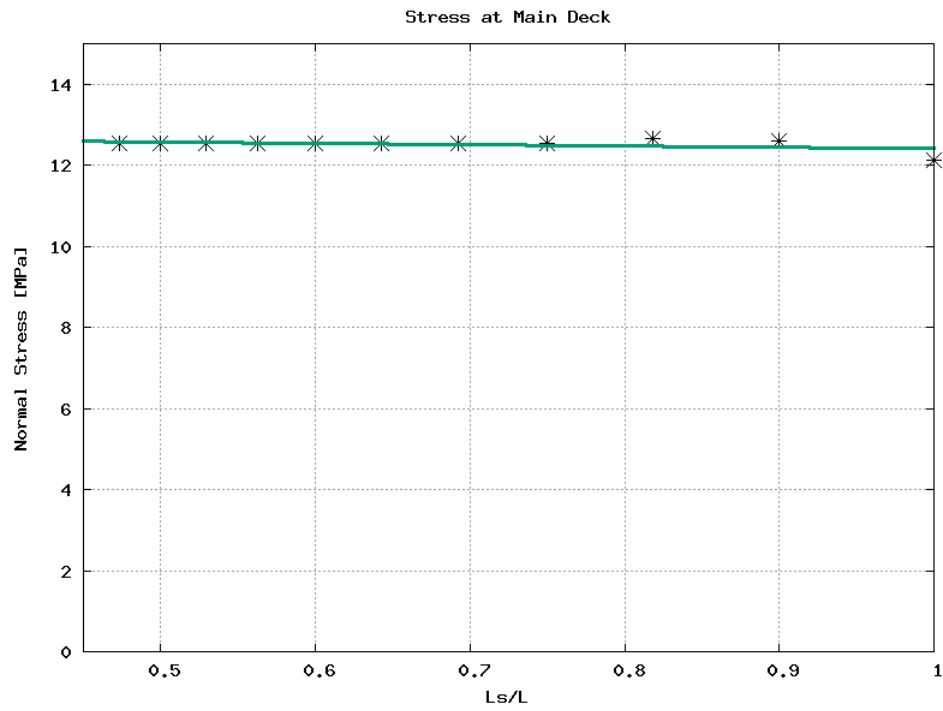
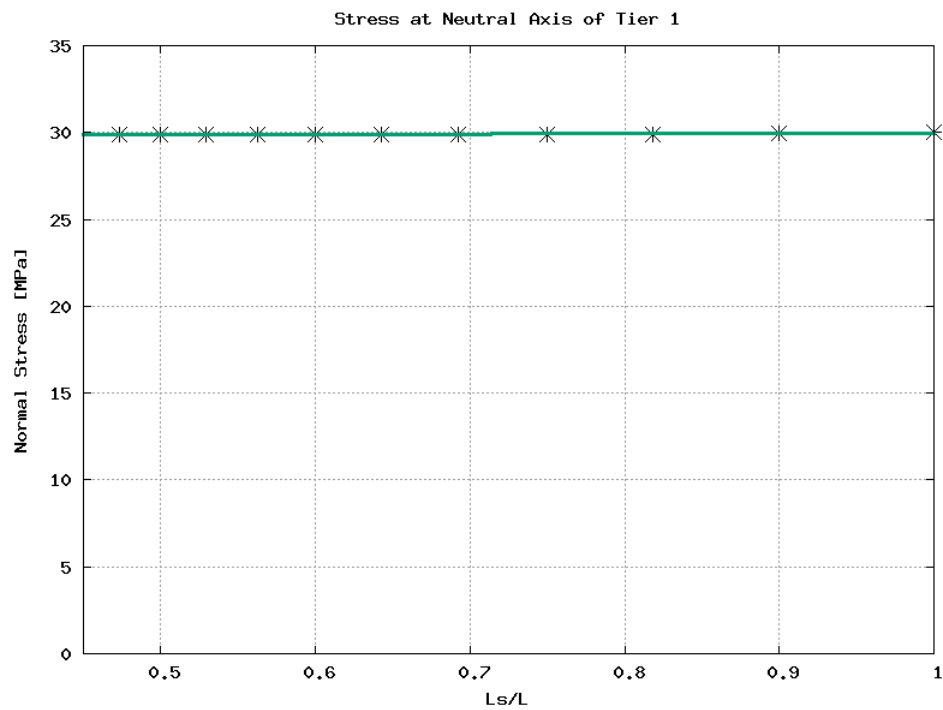


Figure 40: Influence of  $r_L$

Figure 41: Influence of  $r_L$ Figure 42: Influence of  $r_L$

As we can see from figures,  $r_L$  does not have much influence on stresses (figure 40 to 42). Let's look at the influence of  $r_L$  on bending efficiency (table 2 and figure 43).

Table 2: Influence of  $r_L$  on bending efficiency

Case	$L_S(m)$	$L(m)$	$r_L$	Normal Stress(MPa) at NA		Bending Efficiency
				FEA Data	Beam Theory	
1	63.00	63.00	1.00	30.00	31.54	0.95
2	63.00	70.00	0.90	29.92	31.54	0.95
3	63.00	77.00	0.82	29.90	31.54	0.95
4	63.00	84.00	0.75	29.90	31.54	0.95
5	63.00	91.00	0.69	29.90	31.54	0.95
6	63.00	98.00	0.64	29.90	31.54	0.95
7	63.00	105.00	0.60	29.90	31.54	0.95
8	63.00	112.00	0.56	29.90	31.54	0.95
9	63.00	119.00	0.53	29.90	31.54	0.95
10	63.00	126.00	0.50	29.90	31.54	0.95
11	63.00	133.00	0.47	29.90	31.54	0.95

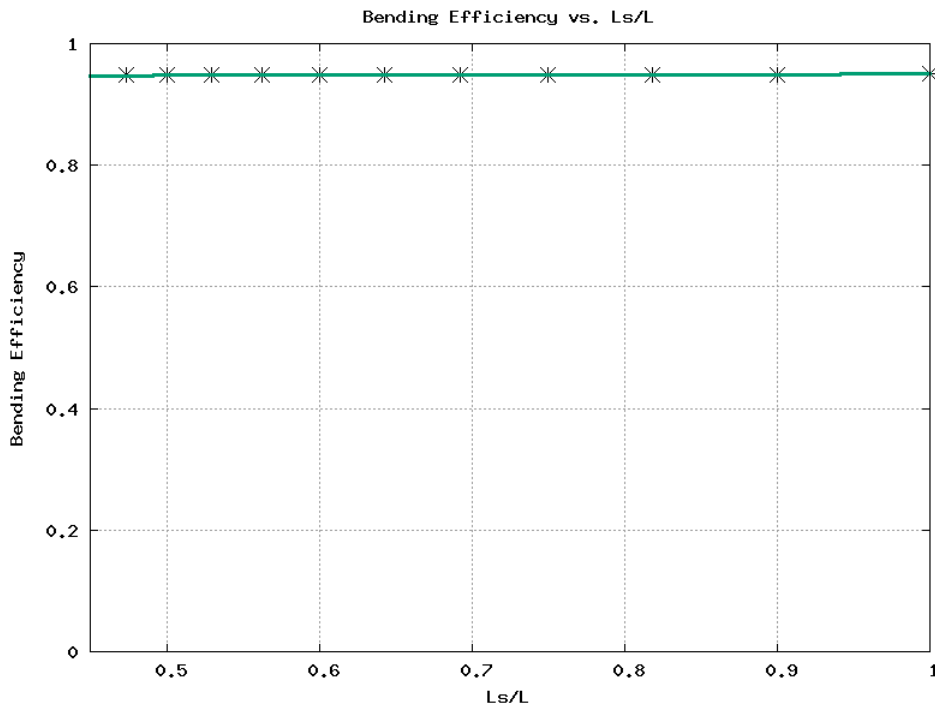


Figure 43: Influence of  $r_L$  on bending efficiency

It is clear from the tables (table 1 to 2) and graphs (figure 40 to 43) that,  $r_L$  does not have any significant influence on superstructure longitudinal stress or bending efficiency. The lowest value of  $r_L$  investigated was 0.47 (figure 39). According to M. Mano et al. (2009), all of these superstructures are long, as  $r_L > 0.25$  (section 2.1). So, the hull and superstructure bends together as a same beam for all these cases.

### 6.3 Ratio of superstructure side openings to total lateral area ( $r_S$ )

The influence of ratio of superstructure side openings to total lateral area ( $r_S$ ) is investigated in this section.  $r_S$  is 0.00 for the reference FE model, as there is no side opening in the superstructure. Different number of windows were created in different FE models for studying different cases of  $r_S$ . To be noted, only the superstructure side opening was modified in these models, nothing else. All these FE models had same boundary conditions. All these models were shown in figure 44 to 48. All FE data is given in table 3.

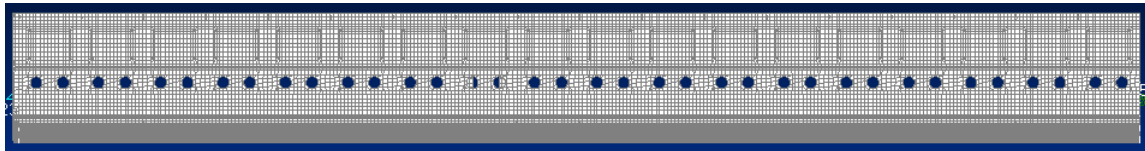


Figure 44: FE model for  $r_S = 0.0$  (no window in superstructure)

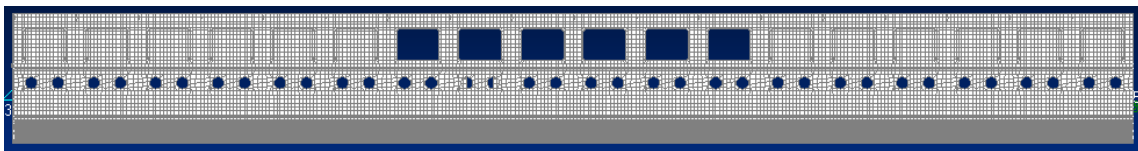


Figure 45: FE model for  $r_S = 0.14$  (six windows in superstructure)

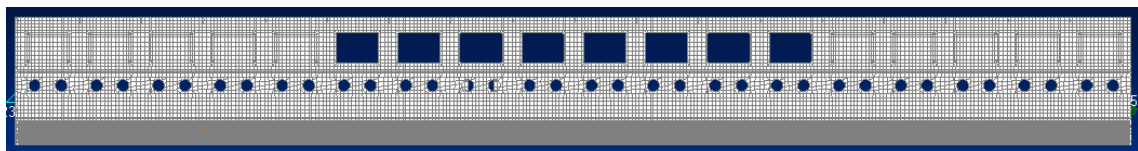


Figure 46: FE model for  $r_S = 0.19$  (eight windows in superstructure)

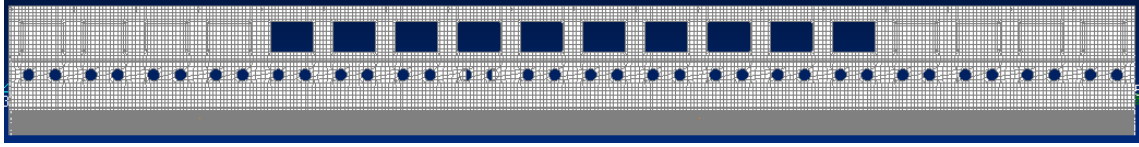


Figure 47: FE model for  $r_S = 0.24$  (ten windows in superstructure)

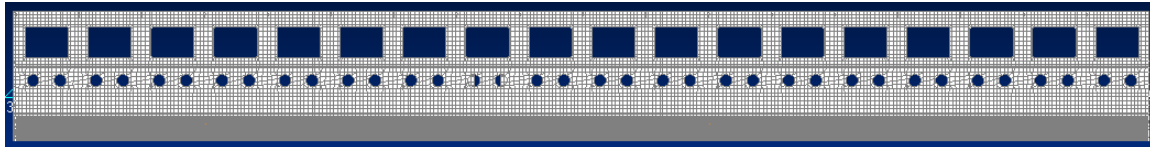


Figure 48: FE model for  $r_S = 0.43$  (eighteen windows in superstructure)

Table 3: Influence of  $r_S$  on longitudinal stress

Case	$A_{OL}(m^2)$	$A_L(m^2)$	$r_S$	Normal Stress (MPa)		
				N.A. of Superstructure	Superstructure Deck	Main Deck
1	0	176.40	0.00	30.03	30.75	12.14
2	25.20	176.40	0.14	29.26	32.11	14.44
3	33.60	176.40	0.19	28.57	31.47	14.85
4	42.00	176.40	0.24	28.04	31.10	15.39
5	75.60	176.40	0.43	22.93	26.01	22.24

The data of table 3 regarding influence of  $r_S$  on longitudinal stresses is represented in figures 49 to 51.

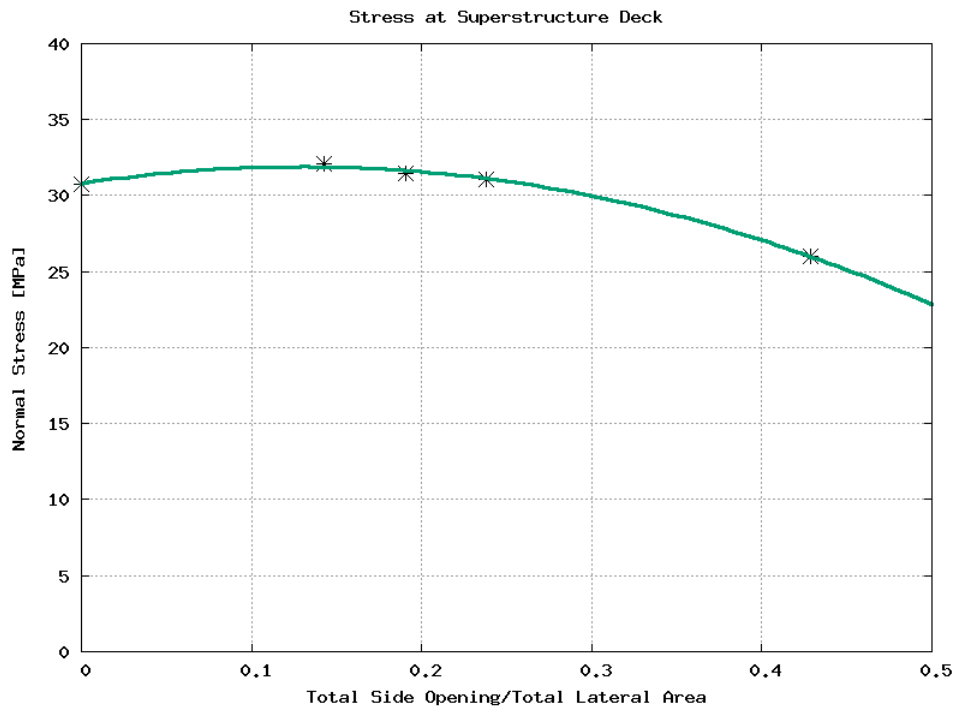


Figure 49: Influence of  $r_S$

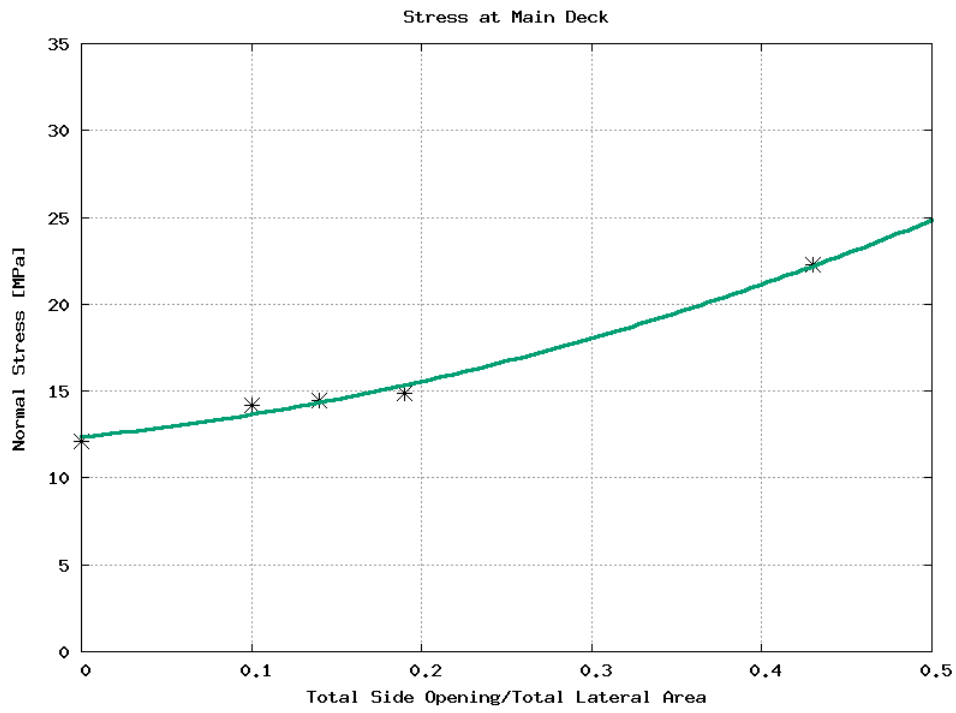


Figure 50: Influence of  $r_S$

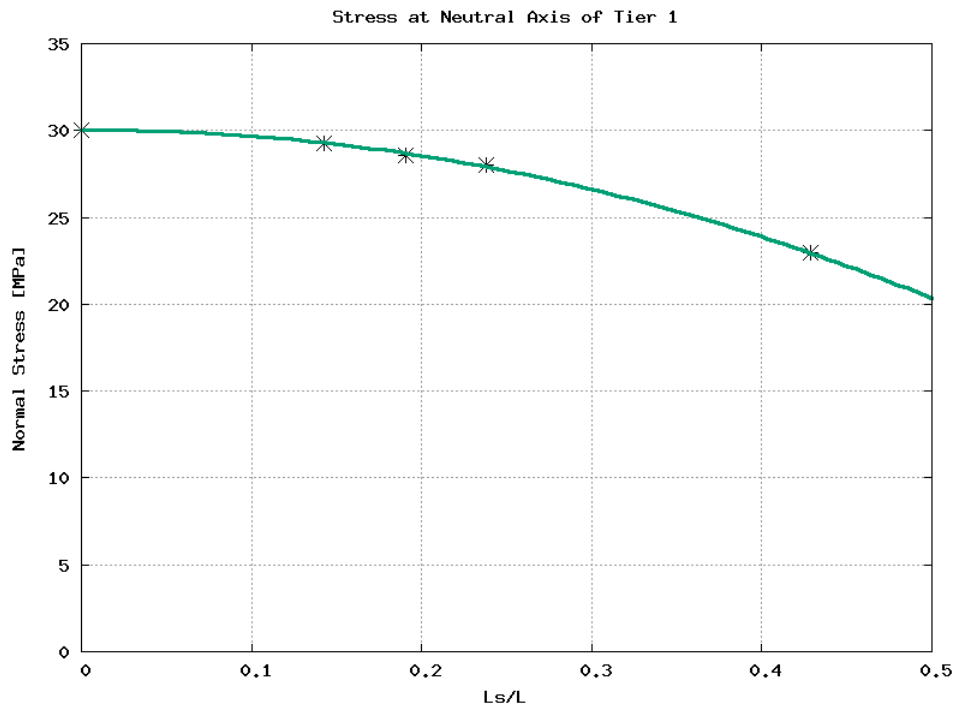


Figure 51: Influence of  $r_S$

Table 3 and figures 49 to 51 show that, the longitudinal stress reduces in superstructure as the side opening (or  $r_S$ ) increases. On the other hand, longitudinal stress increases in main deck as the superstructure side opening (or  $r_S$ ) increases. This increase or decrease of stress is nonlinear. The influence of  $r_S$  on bending efficiency can be seen from table 4 and figure 52.

Table 4: Influence of  $r_S$  on bending efficiency

Case	$A_{OL}(m^2)$	$A_L(m^2)$	$r_S$	Normal Stress (MPa) at NA		Bending Efficiency
				FEA Data	Beam Theory	
1	0	176.40	0.00	30.03	31.54	0.95
2	25.20	176.40	0.14	29.26	31.54	0.93
3	33.60	176.40	0.19	28.57	31.54	0.91
4	42.00	176.40	0.24	28.04	31.54	0.89
5	75.60	176.40	0.43	22.93	31.54	0.73

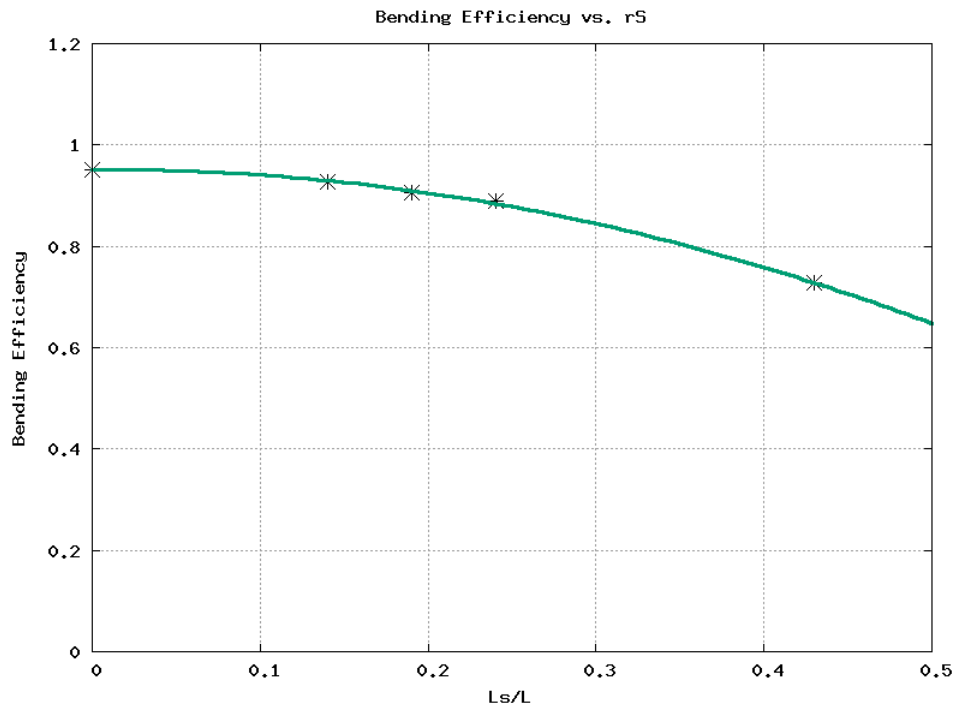


Figure 52: Influence of  $r_S$  on bending efficiency

From table 4 and graph figure 52, it is clear that the bending efficiency decreases non-linearly as  $r_S$  increases.

#### 6.4 Location of superstructure side openings

Two different FE models were considered with same number of windows but at different locations, to observe the influence of the location of side opening. For first model, all the windows were located in midship. For the second model, the windows were located in fore and aft end equally. So, the value of  $r_S$  is same for both cases. To be noted, only the locations of superstructure side opening were different in these models, nothing else. These models are shown in figure 53 and 54.

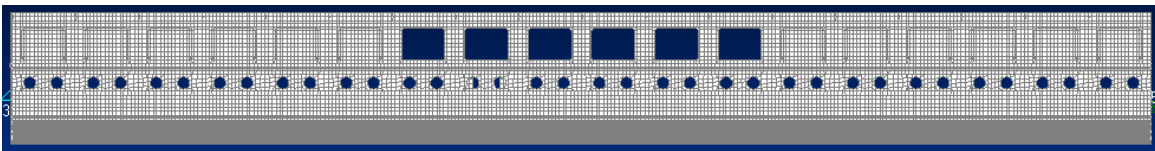


Figure 53: FE model for windows at midship

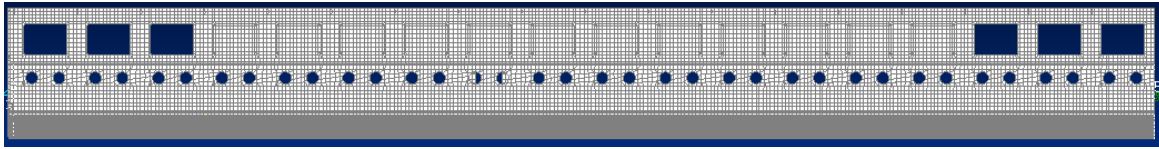


Figure 54: FE model for windows at fore and aft end

FEA data is illustrated in table 5 and figure 55:

Table 5: Influence of side opening location on longitudinal stress

Deck	Z (m)	Normal Stress (MPa)	
		Opening at Midship	Opening at End
Upper Deck	7.20	32.11	28.90
Main Deck	4.40	14.44	14.89
Bottom	0.00	-28.65	-29.16

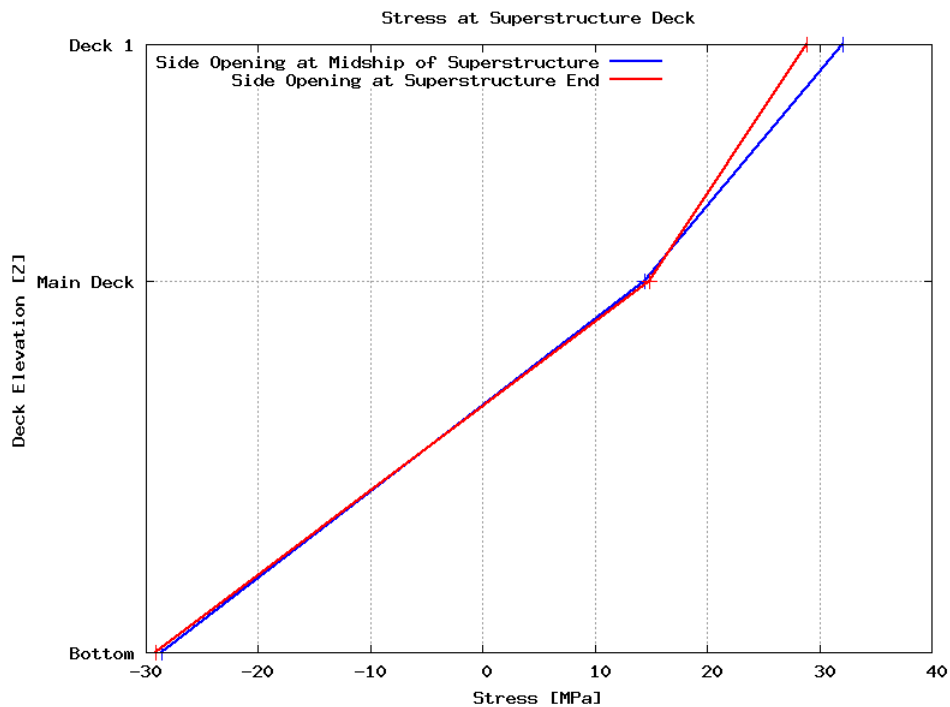


Figure 55: Influence of side opening location on longitudinal normal stress

From above data and figure it is obvious that the longitudinal stress of superstructure increases in midship if the side openings are located at midship. In this case, the difference in stress for two cases is almost 10%.

## 6.5 Ratio of superstructure deck openings to total deck area ( $r_D$ )

Different FE models were created to study the influence of deck opening in longitudinal stress and bending efficiency. For the reference FE model,  $r_D = 0$ , as there is no deck opening in the superstructure. Different sizes of deck openings were created in different FE models for studying different cases of  $r_D$ . To be noted, only the superstructure deck opening was modified in these models, nothing else. The first FE model has three big openings in superstructure deck. These openings were reduced both transverse and horizontal direction gradually until all the openings were closed (figure 56 to 60).

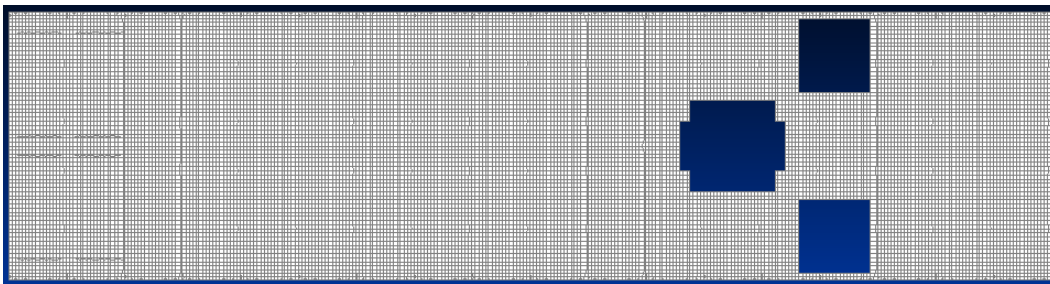


Figure 56: FE model for  $r_D = 0.065$

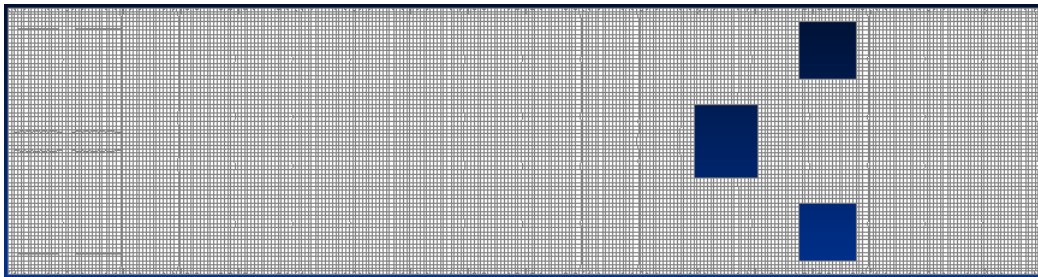


Figure 57: FE model for  $r_D = 0.41$

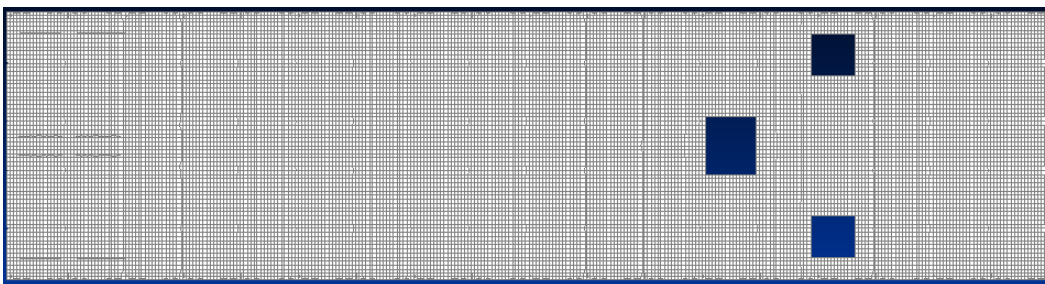


Figure 58: FE model for  $r_D = 0.24$

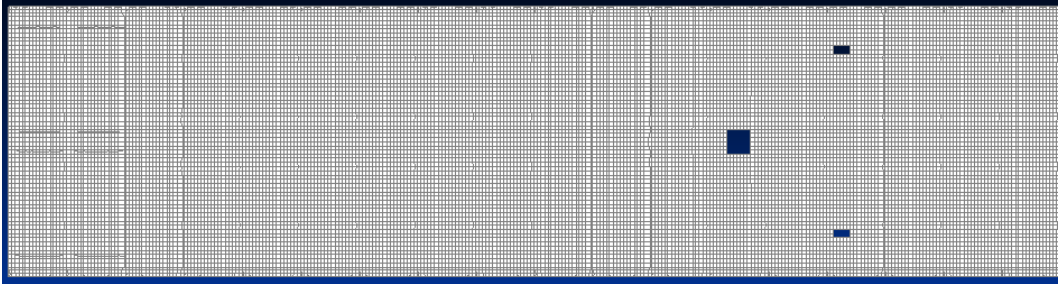


Figure 59: FE model for  $r_D = 0.003$

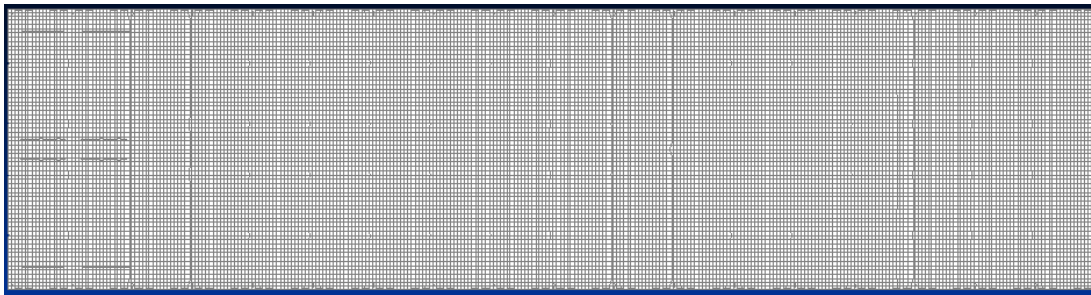


Figure 60: FE model for  $r_D = 0.00$

FEA data is illustrated in table 6 and figure 61 to 63.

Table 6: Influence of  $r_D$  on longitudinal stress

Case	$A_{OD}(m^2)$	$A_D(m^2)$	$r_D$	Normal Stress (MPa)		
				NA	Superstructure Deck	Main Deck
1	66.80	1020.60	0.065	32.89	31.71	14.46
2	42.10	1020.60	0.041	32.50	31.56	13.92
3	24.19	1020.60	0.024	31.02	31.17	12.88
4	3.12	1020.60	0.003	30.17	30.86	12.27
5	0.00	1020.60	0.000	30.00	30.75	12.14

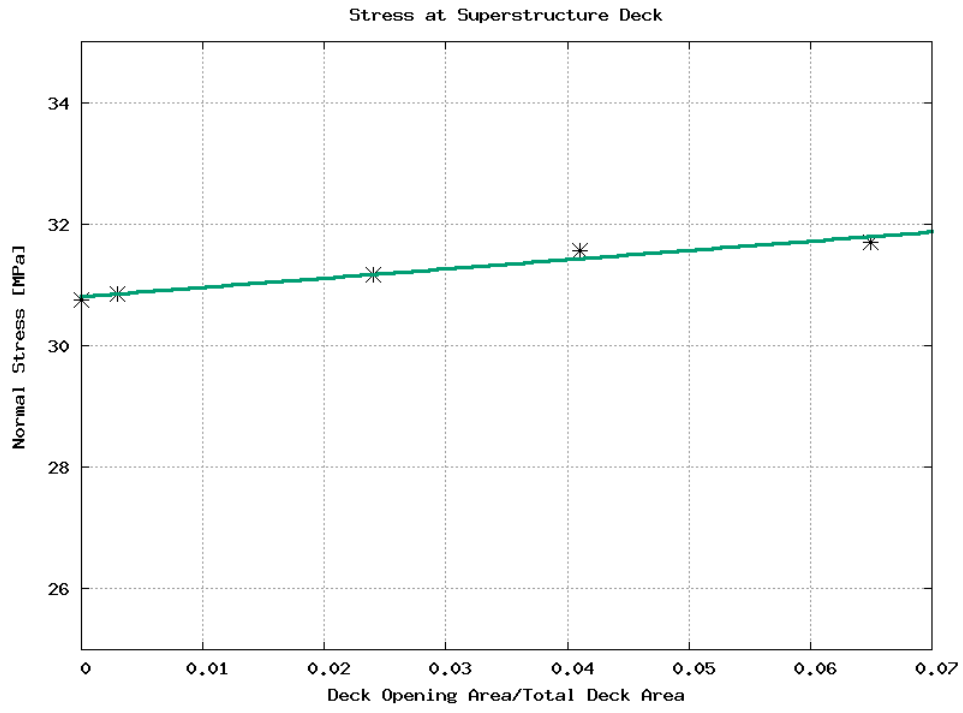


Figure 61: Influence of  $r_D$

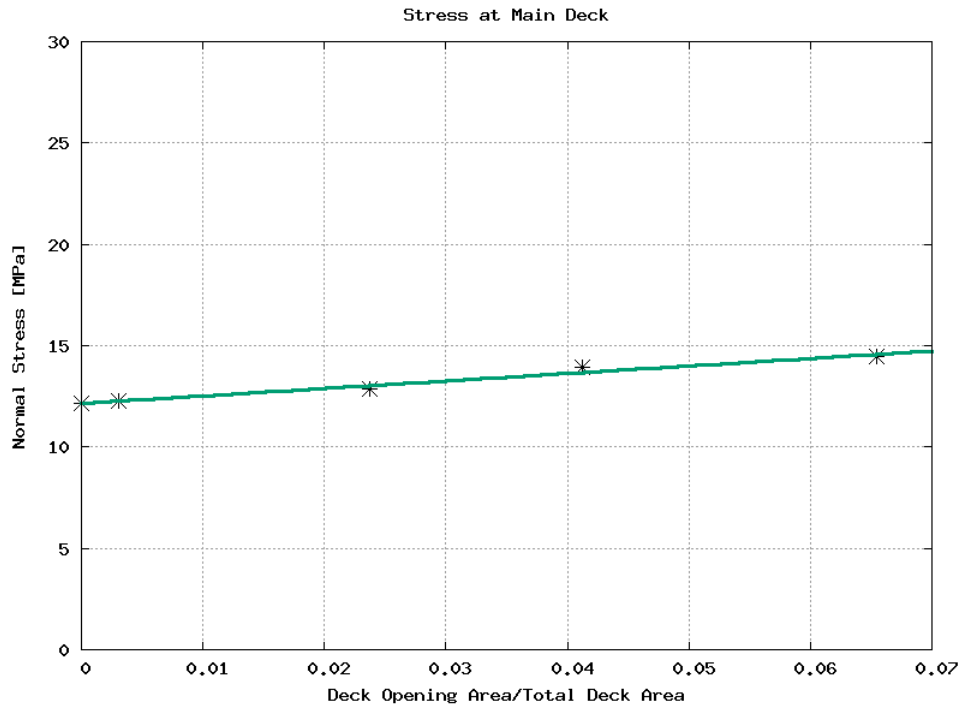


Figure 62: Influence of  $r_D$

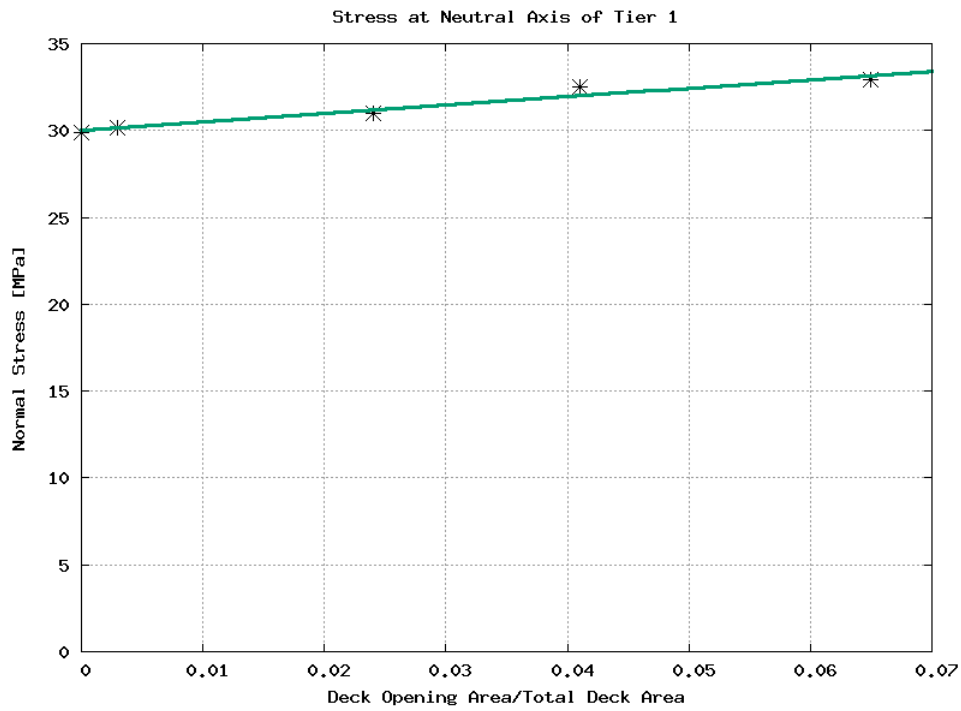


Figure 63: Influence of  $r_D$

It is clear from figure 61 to 63 that the stress increases in superstructure, neutral axis and main deck as the deck opening area or  $r_D$  increases. The influence of  $r_D$  on bending efficiency can be seen from table 7 and figure 64.

Table 7: Influence of  $r_D$  on bending efficiency

Case	$A_{OD}(m^2)$	$A_D(m^2)$	$r_D$	Normal Stress (MPa)		Bending Efficiency
				FEA Data	Beam Theory	
1	66.80	1020.60	0.065	32.89	31.54	1.04
2	42.10	1020.60	0.041	32.50	31.54	1.03
3	24.19	1020.60	0.024	31.02	31.54	0.98
4	3.12	1020.60	0.003	30.17	31.54	0.96
5	0.00	1020.60	0.000	30.00	31.54	0.95

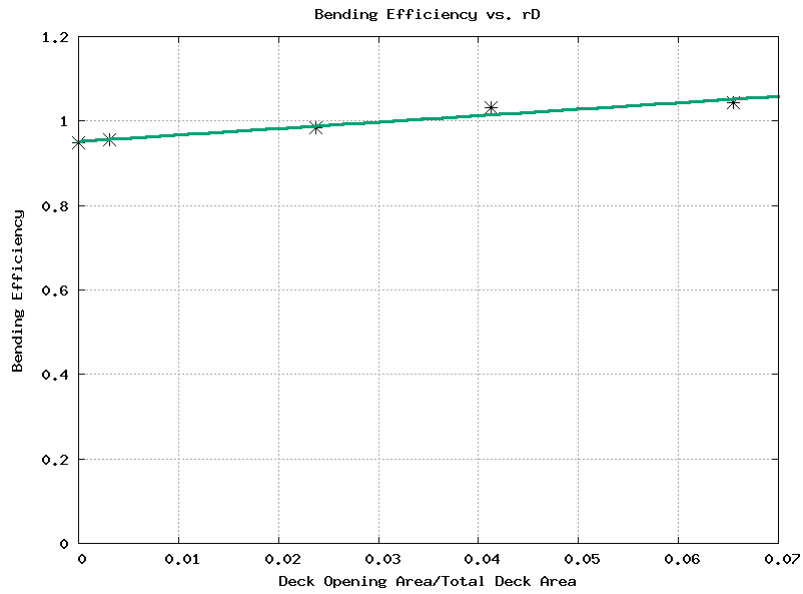


Figure 64: Influence of  $r_D$  on bending efficiency

From above data and figure, it is clear that bending efficiency increases linearly as the deck opening area or  $r_D$  increases. It rises very high (above 1.00) for even small value of  $r_D$ . This behavior of obtaining bending efficiency more than 1.00 may be the result of stress concentration or diffusion in the region of calculation. This behavior may be further investigated in future.

## 7 Proposal of new formula

### 7.1 General

It is clear from the investigation that  $r_S$  has an influence on bending efficiency. So,  $r_S$  can be inserted in existing formula. Calculation of bending efficiency involves multiple equations and steps. The influence of  $r_S$  will be inserted in  $\chi$ . Thus,  $\chi_{new}$  will be used for finding bending efficiency instead of  $\chi$  in equation 28. So, the new parameter is assumed as:

$$\chi_{new} = \chi K_{r_S} \quad (33)$$

Where:

$$K_{r_S} = f(r_S) \quad (34)$$

### 7.2 Integration of $r_S$

As discussed before, rule formula does not consider side opening. Thus, there is no effect of  $r_S$  in the bending efficiency calculated by rule formula. The rule value of  $\chi$  as well as bending efficiency is same for different cases of side opening. On contrary, FEA considers all structural details. Hence, the influence of  $r_S$  on bending efficiency can be observed from direct calculation. So, different values of  $\chi_{new}$  can be obtained for different FE models (or different  $r_S$ ) through equation 28:  $\nu_i = \nu_{i-1}(0.37\chi_{new} - 0.034\chi_{new}^2)$ , where  $\nu_i$  is FE bending efficiency.

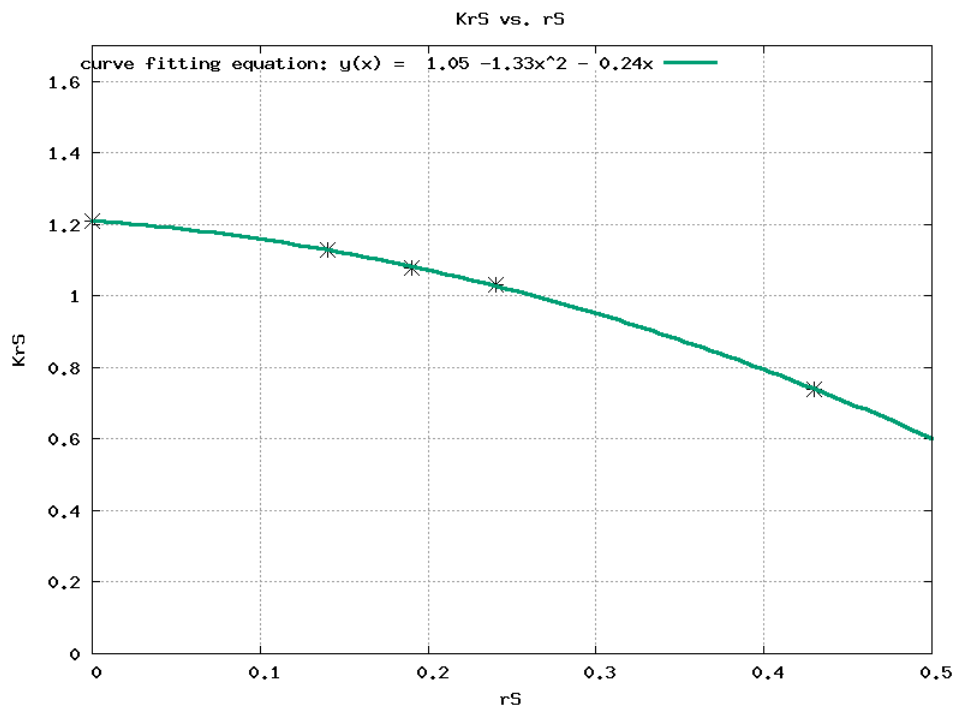
Then, it is possible to find  $K_{r_S}$  for different FE models (or different  $r_S$ ), as equation 33 gives:

$$K_{r_S} = \frac{\chi_{new}}{\chi} \quad (35)$$

This, in fact, gives different values of  $K_{r_S}$  for different values of  $r_S$ . Hence a relation can be obtained between  $K_{r_S}$  and  $r_S$ . FE data from investigation of  $r_S$  (section 6.3) are used to perform these analysis. All these calculations are shown in table 8. The influence of  $r_S$  on  $K_{r_S}$  is shown in figure 65.

Table 8: Influence of  $r_S$  on  $K_{r_S}$ 

	Hull	Model 1	Model 2	Model 3	Model 4	Model 5
$A$	7398.80	2128.30	2128.30	2128.30	2128.30	2128.30
$I$	1.90E+08	1.03E+07	1.03E+07	1.03E+07	1.03E+07	1.03E+07
$e$	235.00	245.80	245.80	245.80	245.80	245.80
$A_{SH}$	268.85	210.00	210.00	210.00	210.00	210.00
$L$	63.00	63.00	63.00	63.00	63.00	63.00
$\lambda$		31.50	31.50	31.50	31.50	31.50
$\Omega$		2.66E-08	2.66E-08	2.66E-08	2.66E-08	2.66E-08
$j$		1.10E-03	1.10E-03	1.10E-03	1.10E-03	1.10E-03
$\chi$		3.46	3.46	3.46	3.46	3.46
$r_S$		0.00	0.14	0.19	0.24	0.43
$\nu$	1.00	0.87	0.87	0.87	0.87	0.87
$\sigma_{FEA}/\sigma_{BEAM}$		0.9521	0.9279	0.9061	0.8892	0.7272
$\chi_{new}$		4.180	3.920	3.720	3.580	2.575
$K_{r_S}$		1.21	1.13	1.08	1.03	0.74

Figure 65: Influence of  $r_S$  on  $K_{r_S}$

So, the influence of  $r_S$  on  $K_{r_S}$  can be expressed into a function from the trendline of figure 65:

$$K_{r_S} = 1.05 - 1.33(r_S)^2 - 0.24r_S \quad (36)$$

The equation for finding  $K_{r_S}$  is formed and  $\chi$  is already calculated in table 8. So, equations 33 and 28 give the new bending efficiency, which is expressed as  $\nu_{proposal}$  in table 9:

Table 9: Calculation of  $\nu_{new}$  according to  $r_S$

$r_S$	0.00	0.14	0.19	0.24	0.43
$K_{r_S}$	1.05	0.99	0.95	0.91	0.70
$\chi_{new}$	4.18	3.92	3.72	3.58	2.58
$\nu_{proposal}$	0.953	0.928	0.906	0.889	0.727

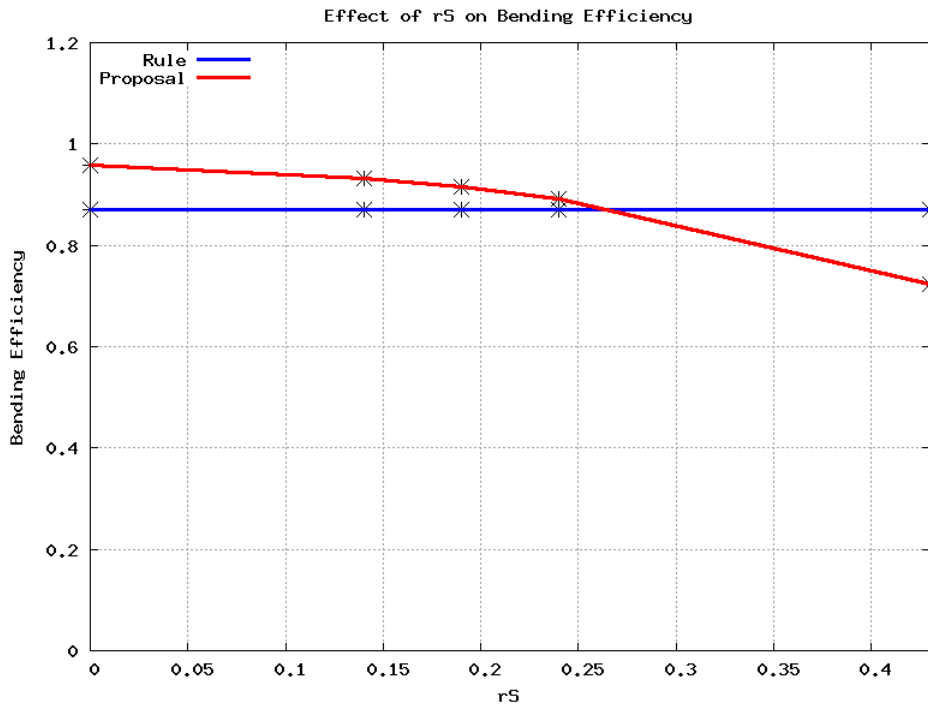


Figure 66: Influence of  $r_S$  on bending efficiency

Figure 66 shows the influence of  $r_S$  on bending efficiency. Rule bending efficiency ( $\nu$ ) is constant over different values of  $r_S$  in this figure. But, the influence of  $r_S$  on bending efficiency according to new proposal ( $\nu_{proposale}$ ) is clear in this figure.

The value of  $\nu_{proposal}$  is higher compared to  $\nu$  for the reference investigation model, which does not have any side opening ( $r_S = 0$ ). This is due to the fact that, the standard FE models used for investigation is identical to a real passenger ship with pillars, frames, brackets, bilge and other structural details compared to the model of Schade. Thus, FEM calculated all the details. Specially 4 pillars in each frame made sure that the superstructure is connected with the hull, which allowed much stress transfer from hull to the superstructure. Whereas, Schade's formula is analytical and the superstructure is connected with hull via only the shear carrying area (sideplates of superstructure). This difference at  $r_S = 0$  indicates that,  $\nu_{proposal}$  is more conservative. Besides, it corresponds to the direct calculation of a real passenger vessel.

### 7.3 Proposal of new formula

So, the equations to find bending efficiency can be re-written as:

$$\nu_i = \nu_{i-1}(0.37\chi_{new} - 0.034\chi^2) \quad (37)$$

$$\chi_{new} = 100(K_{r_S})(j\lambda) \leq 5 \quad (38)$$

$$K_{r_S} = 1.05 - 1.33(r_S)^2 - 0.24r_S \quad (39)$$

$$j = \sqrt{\frac{1}{\frac{1}{a_{SH1}} + \frac{1}{A_{SHe}}} \frac{\Omega}{2.6}} \quad (40)$$

$$\Omega = \frac{(A_1 + A_e)(I_1 + I_e) + A_1 A_e (e_1 + e_e)^2}{(A_1 + A_e)I_1 I_e + A_1 A_e (I_1 e_e^2 + I_e e_1^2)} \quad (41)$$

## 7.4 Validation

### 7.4.1 Bending efficiency

Since, the new formula is formulated, it is possible to calculate bending efficiency according to the new proposal and compare with the existing formula. Table 10 and 11 shows the calculation of bending efficiency on a real passenger vessel.

Table 10: Calculation of Bending Efficiency according to existing formula

	Deck 1		Deck 2		Deck 3		Sun Deck	
	l	e	l	e	l	e	l	e
$A$	7398.80	2128.30	9651.20	1843.50	11698.90	1600.90	13502.10	1524.10
$I$	1.90E+08	1.03E+07	5.88E+08	9.13E+06	1.21E+09	7.68E+06	2.25E+09	6.46E+06
$e$	235.00	245.80	413.60	232.80	565.20	234.00	730.00	239.00
$A_{SH}$	268.85	210.00	478.85	202.50	681.35	175.50	856.85	148.50
$\Omega$		2.66E-08		2.18E-08		2.00E-08		1.81E-08
$j$		1.10E-03		1.09E-03		1.04E-03		9.40E-04
$\lambda$		49.43		47.74		45.72		43.19
$\chi$		5.00		5.00		4.73		4.06
$\nu$	1.00	1.00	1.00	1.00	1.00	0.99	0.99	0.93

Table 11: Calculation of Bending Efficiency according to proposed formula

	Deck 1		Deck 2		Deck 3		Sun Deck	
	l	e	l	e	l	e	l	e
$A$	7398.80	2128.30	9651.20	1843.50	11698.90	1600.90	13502.10	1524.10
$I$	1.90E+08	1.03E+07	5.88E+08	9.13E+06	1.21E+09	7.68E+06	2.25E+09	6.46E+06
$e$	235.00	245.80	413.60	232.80	565.20	234.00	730.00	239.00
$A_{SH}$	268.85	210.00	478.85	202.50	681.35	175.50	856.85	148.50
$L$	99.20	98.85	98.85	94.50	94.50	91.40	91.40	86.40
$A_{OL}$		84.03		92.40		79.80		71.40
$A_L$		276.78		243.00		246.62		235.03
$r_S$		0.30		0.38		0.32		0.30
$K_{r_S}$		0.96		0.83		0.93		0.96
$\Omega$		2.66E-08		2.18E-08		2.00E-08		1.81E-08
$j$		1.10E-03		1.09E-03		1.04E-03		9.40E-04
$\lambda$		49.43		47.74		45.72		43.19
$\chi$		5.20		4.34		4.39		3.88
$\nu$	1.00	1.00	1.00	0.97	0.97	0.94	0.94	0.87

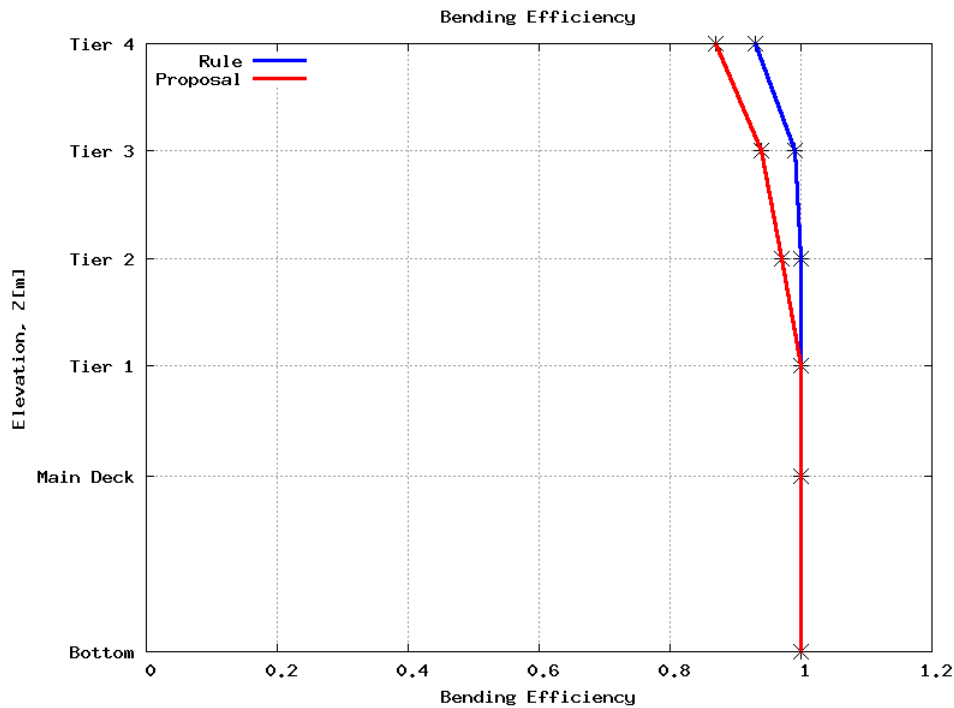


Figure 67: Calculation of bending efficiency

The difference in bending efficiency according to existing formula and proposed formula can be seen from figure 67. Clearly the new parameter inserted in the formula reduces the bending efficiency.

#### 7.4.2 Normal Stress Distribution

For cruise vessels, only the full ship 3D FE analysis is considered to be sufficient for assessment of global structural response (ISSC, 1997). So, the reference for comparison of analytical hull girder normal stress calculation should be FEA. The analytical approach of calculating hull girder normal stresses using bending efficiency considers mainly section geometry, superstructure length, vertical and lateral shear lag, etc. It cannot consider all the structural details like FEA. Analytical approach gives only one normal stress distribution which is mostly suitable for midship section. On the contrary, FEA gives different normal stress distribution at different cross-sections of vessel. FEA normal stress distributions are complicated, irregular and noncontinuous. The comparison of normal stress distributions between analytical method and FEA are shown in figure 68 to 72. All relevant data for these stress distribution are given in Appendix C.

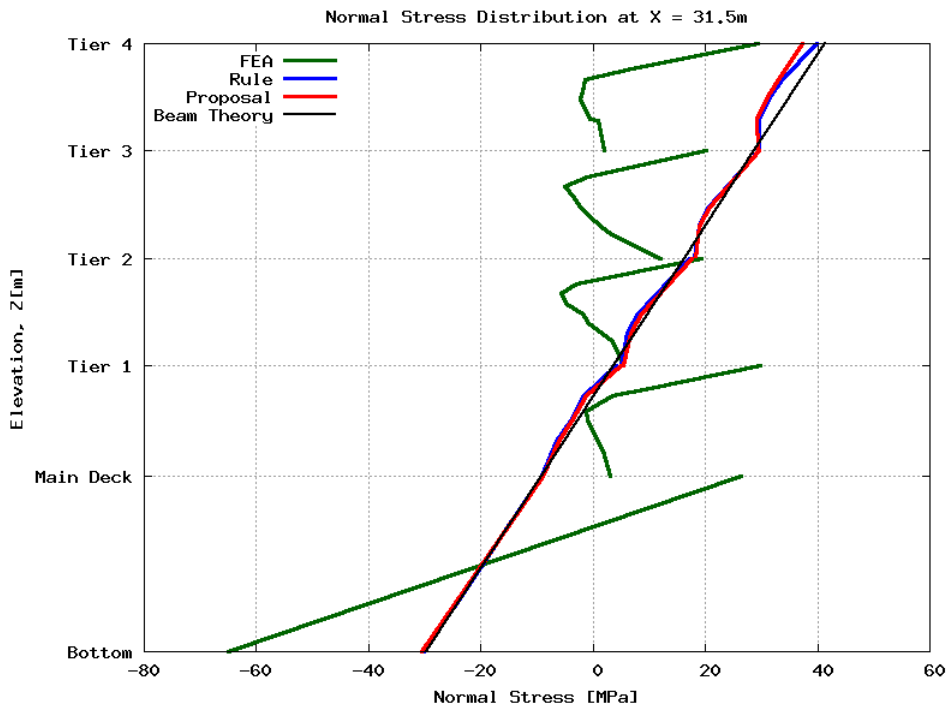


Figure 68: Comparison of Normal Stress Distribution at X = 31.5m

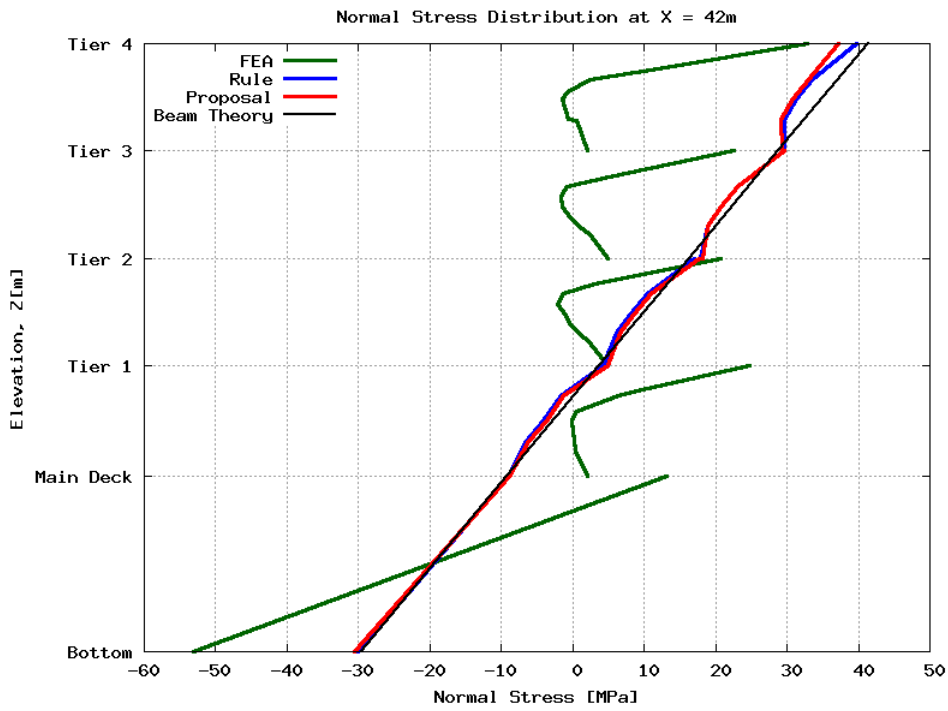


Figure 69: Comparison of normal stress distribution at X = 42m

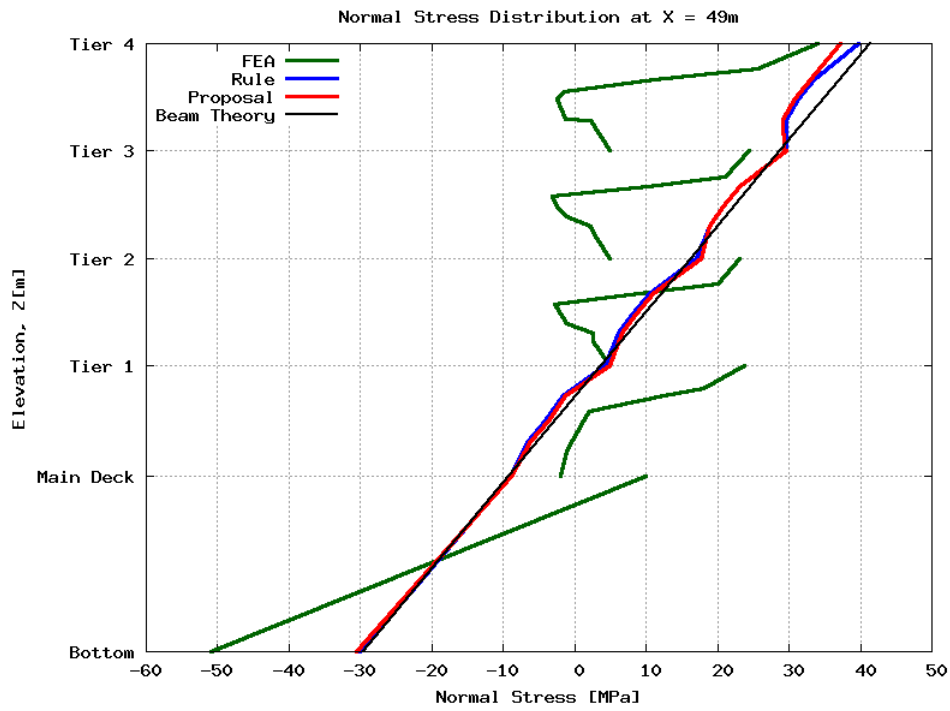


Figure 70: Comparison of normal stress distribution at X = 49m

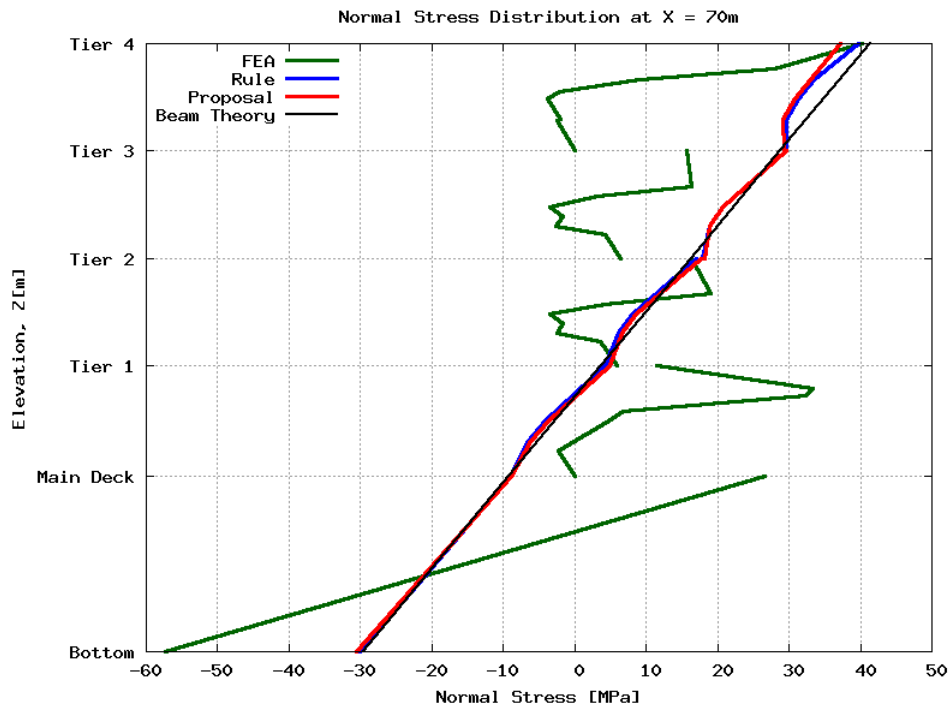


Figure 71: Comparison of normal stress distribution at X = 70m

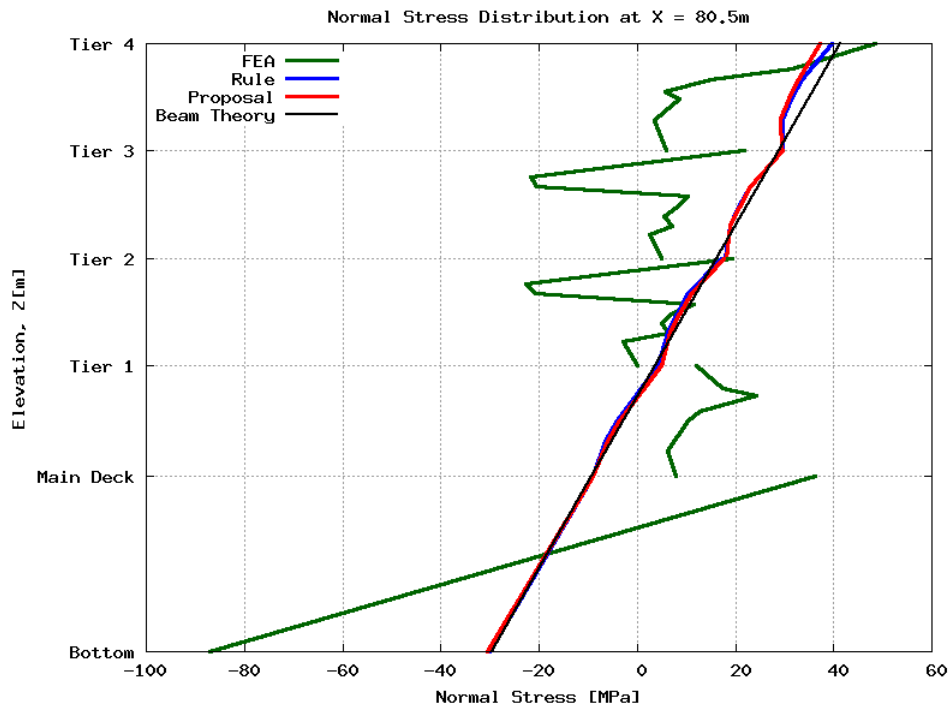


Figure 72: Comparison of normal stress distribution at  $X = 80.5m$

As discussed previously, a cantilever bending moment condition was applied on the FE model. The bending moment is applied at fore part ( $X = 89.8m$ ) of the vessel. Besides, there are big openings in decks of tier 1, 2 and 3 between  $X = 58m$  and  $X = 69.5m$ . Hence, these deck openings are located towards fore end of the ship. Besides, there is transition of vessel cross-section from prismatic shape to non-prismatic shape in the fore part.

Due to above reasons, the normal stress from FEA is more than the analytical normal stress at superstructure top ( $Z = 15.3m$ ) of fore part (figure 72). Whereas, the normal stress from FEA is much less than the analytical bending stress at superstructure top ( $Z = 15.3m$ ) of aft part (figure 68). Besides, the normal stress distribution in fore part ( $X = 70m$  or  $X = 80.5m$ ) is more irregular compared to aft part ( $X = 31.5m$ ).

However, the area of interest is midship ( $X = 49m$ ). The normal stress at top of superstructure (sun deck or  $Z = 15.3m$ ) according to existing formula has a difference of 17% from direct calculation, whereas the new proposal has a difference of 9.3%. Thus, the proposed formula is 7.7% more accurate compared to existing formula for finding the normal stress at sun deck of midship in this case.

## 8 Application

### 8.1 General

The formula and parameters for calculating bending efficiency are discussed in details in previous sections. The bending efficiency is to be determined tier by tier according to the following process:

#### 1) *Bending efficiency of main hull*

Bending efficiency is always 1.00 for main hull.

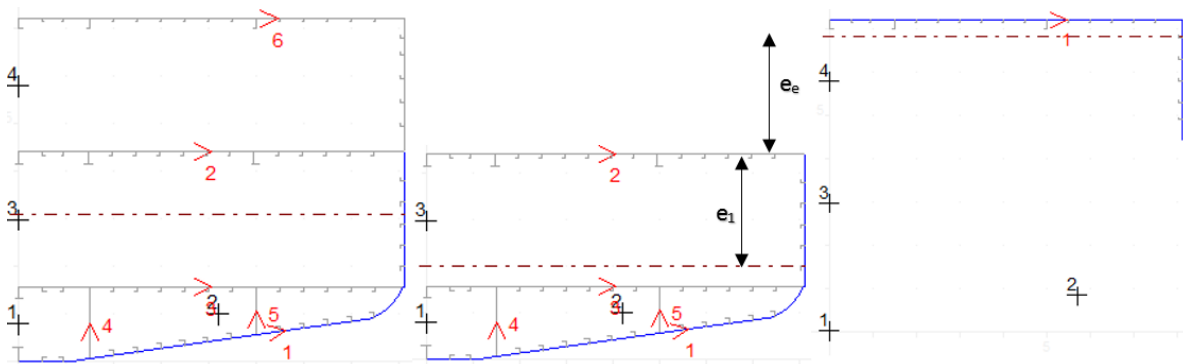


Figure 73: Bending efficiency of tier 1 (left - hull and erection together; middle - hull; right - erection)

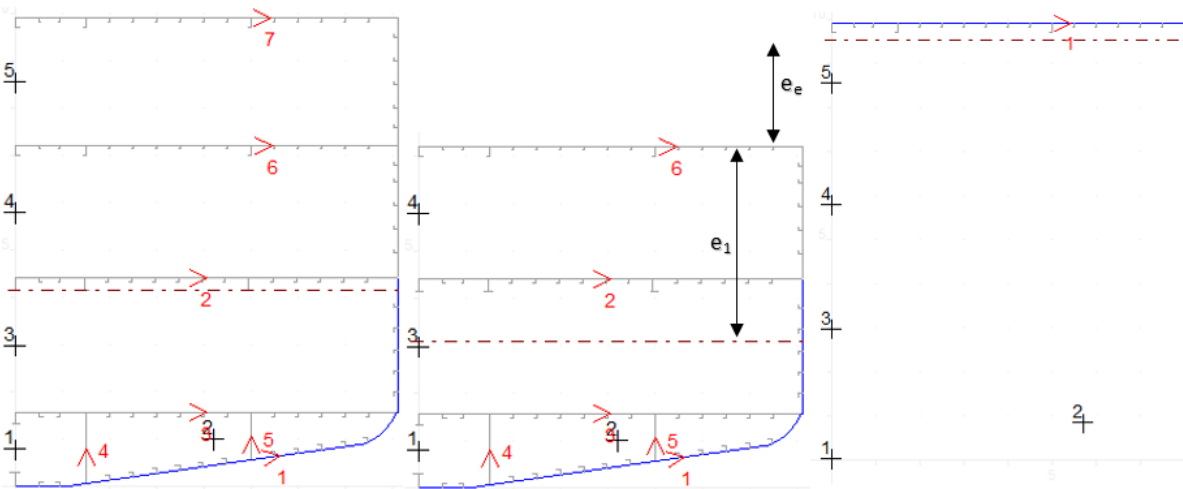


Figure 74: Bending efficiency of tier 2 (left - hull and erection together; middle - hull; right - erection)

#### 2) *Bending efficiency of tier 1*

The main hull is considered as 'hull' for calculation of  $A_1$ ,  $I_1$  and  $e_1$ . Tier 1 is considered as 'erection' for calculation of  $A_e$ ,  $I_e$  and  $e_e$ . The hull and erection for calculation of  $\nu$  for tier 1 is shown in figure 73.

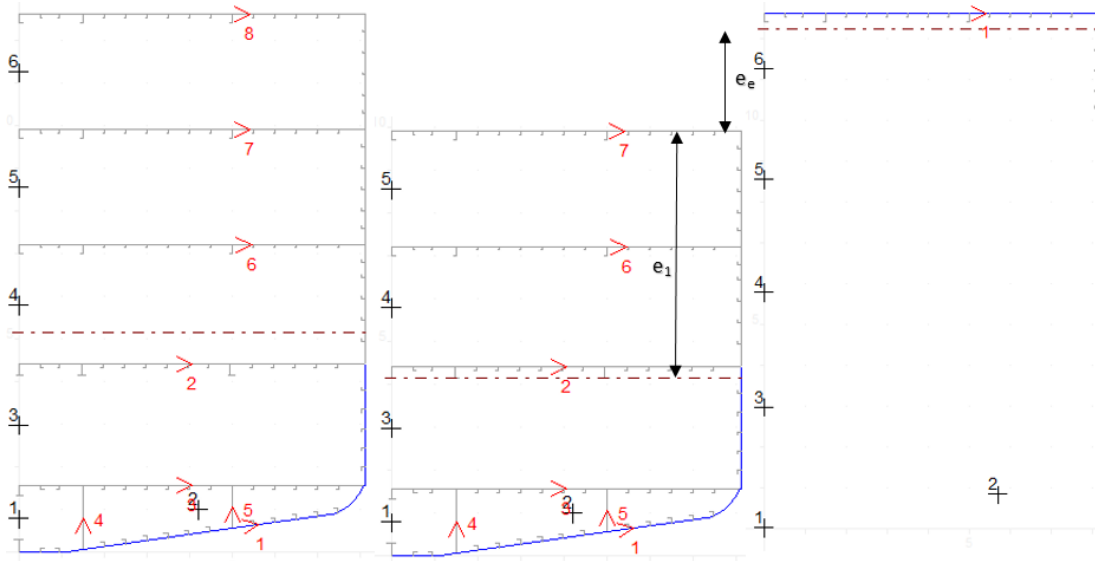


Figure 75: Bending efficiency of tier 3 (left - hull and erection together; middle - hull; right - erection)

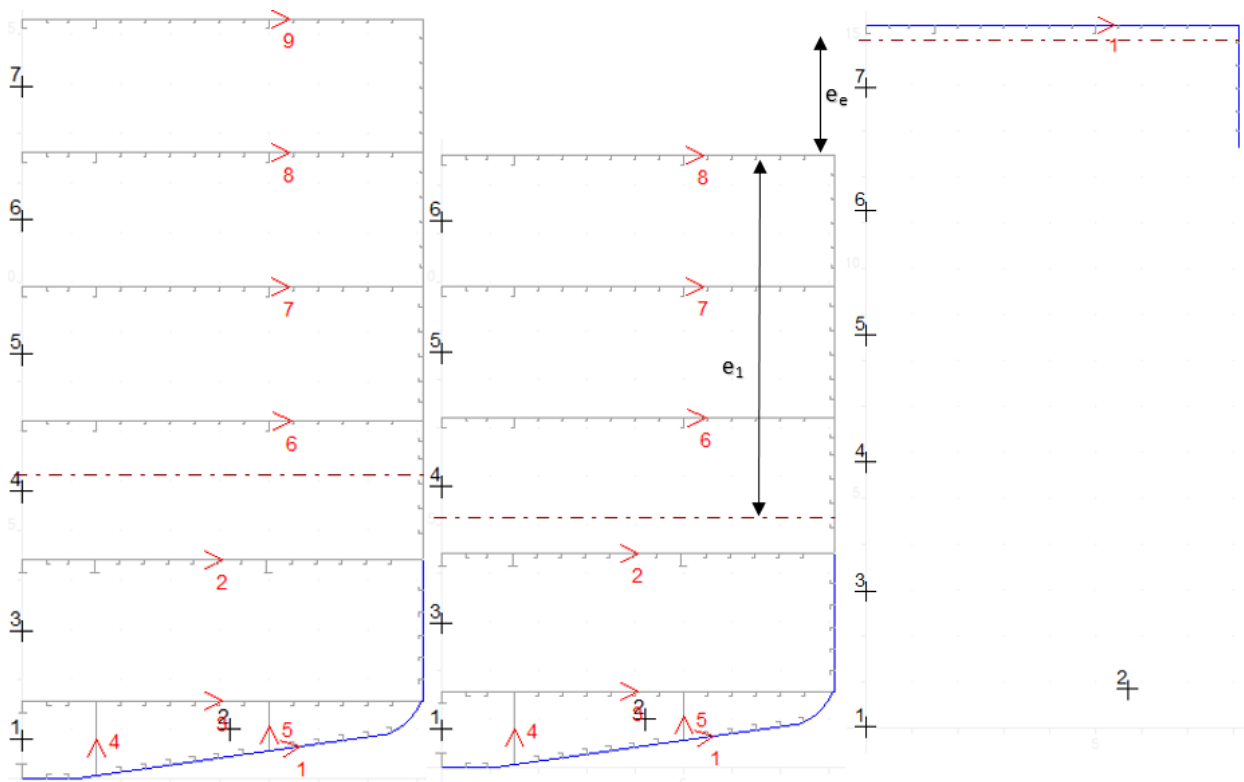


Figure 76: Bending efficiency of tier 4 (left - hull and erection together; middle - hull; right - erection)

### 3) *Bending efficiency of tier 2*

The main hull and tier 1 together are considered as 'hull' for calculation of  $A_1$ ,  $I_1$  and  $e_1$ . Tier 2 is considered as 'erection' for calculation of  $A_e$ ,  $I_e$  and  $e_e$ . The hull and erection for calculation of  $\nu$  for tier 2 is shown in figure 74.

### 4) *Bending efficiency of tier 3*

The main hull, tier 1 and tier 2 together are considered as 'hull' for calculation of  $A_1$ ,  $I_1$  and  $e_1$ . Tier 3 is considered as 'erection' for calculation of  $A_e$ ,  $I_e$  and  $e_e$ . The hull and erection for calculation of  $\nu$  for tier 3 is shown in figure 75.

### 5) *Bending efficiency of tier 4*

The main hull, tier 1, tier 2 and tier 3 together are considered as 'hull' for calculation of  $A_1$ ,  $I_1$  and  $e_1$ . Tier 4 is considered as 'erection' for calculation of  $A_e$ ,  $I_e$  and  $e_e$ . The hull and erection for calculation of  $\nu$  for tier 4 is shown in figure 76.

## 8.2 Determination of hull girder normal stresses

### 8.2.1 General

Determination of hull girder normal stresses is very important for hull scantling and hull girder yielding check of any vessel. According to NR 217 (Pt B, Ch 4, Sec 2), the hull girder normal stresses induced by vertical bending moments are obtained, in  $N/mm^2$ , from the following formula:

$$\sigma_1 = \frac{M_T}{Z} 10^3 \quad (42)$$

Here,  $M_T$  is total vertical bending moment in hogging condition, in  $kN.m$  and  $Z$  is net hull girder section modulus, in  $cm^3$ .

$\sigma_1$  is combined with local stress  $\sigma_l$  to determine the scantling of structural elements.  $\sigma_1$  should also comply with the hull girder yielding check criterion defined by classification societies Rules.

## 8.2.2 Determination guidelines

The hull girder normal stresses are to be determined tier by tier according to the following process:

### 1) Stress calculation in main hull

Cross-section of 'hull' is modeled in Marsinland, not the full vessel. The bending moment for full vessel (section 5.2.4.3) should be applied at this model to obtain the normal stresses at hull. The Marsinland model and normal stress distribution are shown in figure 77.

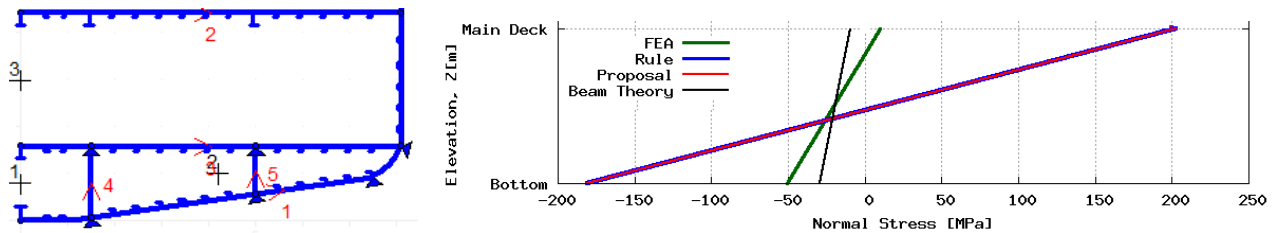


Figure 77: Modeling for stress calculation at 'hull'(left) and recommended stress distribution (right)

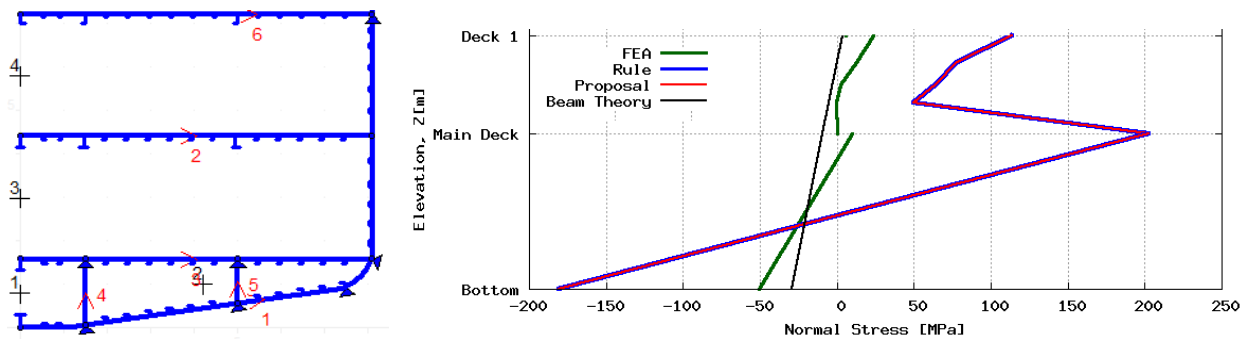


Figure 78: Modeling for stress calculation at 'tier 1'(left) and recommended stress distribution (right)

### 2) Stress calculation in tier 1

Cross-section of 'hull' and 'tier 1' are modeled in Marsinland, not the full vessel. The bending moment for full vessel (section 5.2.4.3) should be applied at this model to obtain the normal stresses at tier 1. The Marsinland model and normal stress distribution are shown in figure 78.

### 3) Stress calculation in tier 2

Cross-section of 'hull', 'tier 1' and 'tier 2' are modeled in Marsinland, not the full vessel. The bending moment for full vessel (section 5.2.4.3) should be applied at this model to obtain the normal stresses at tier 2. The Marsinland model and normal stress distribution are shown in figure 79.

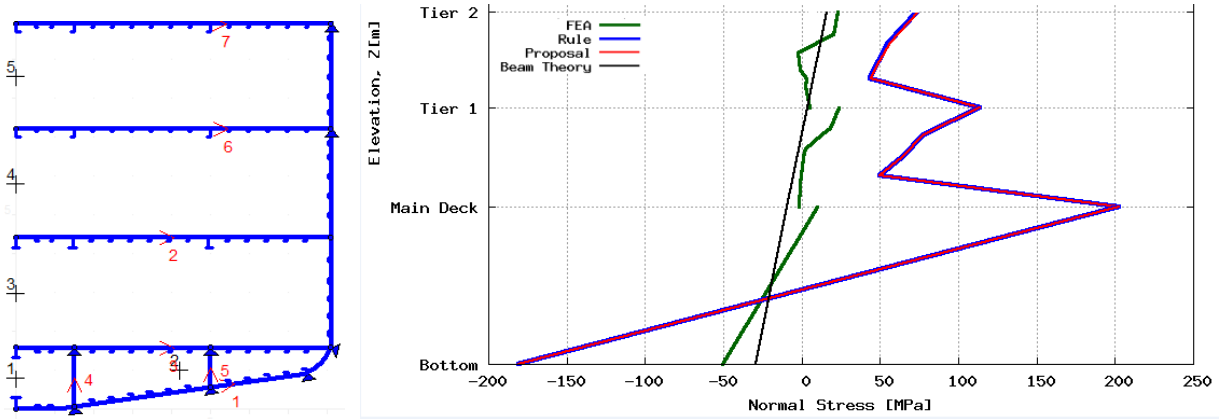


Figure 79: Modeling for stress calculation at 'tier 2' (left) and recommended stress distribution (right)

#### 4) Stress calculation in tier 3

Cross-section of 'hull', 'tier 1', 'tier 2' and 'tier 3' are modeled in Marsinland, not the full vessel. The bending moment for full vessel (section 5.2.4.3) should be applied at this model to obtain the normal stresses at tier 3. The Marsinland model and normal stress distribution are shown in figure 80.

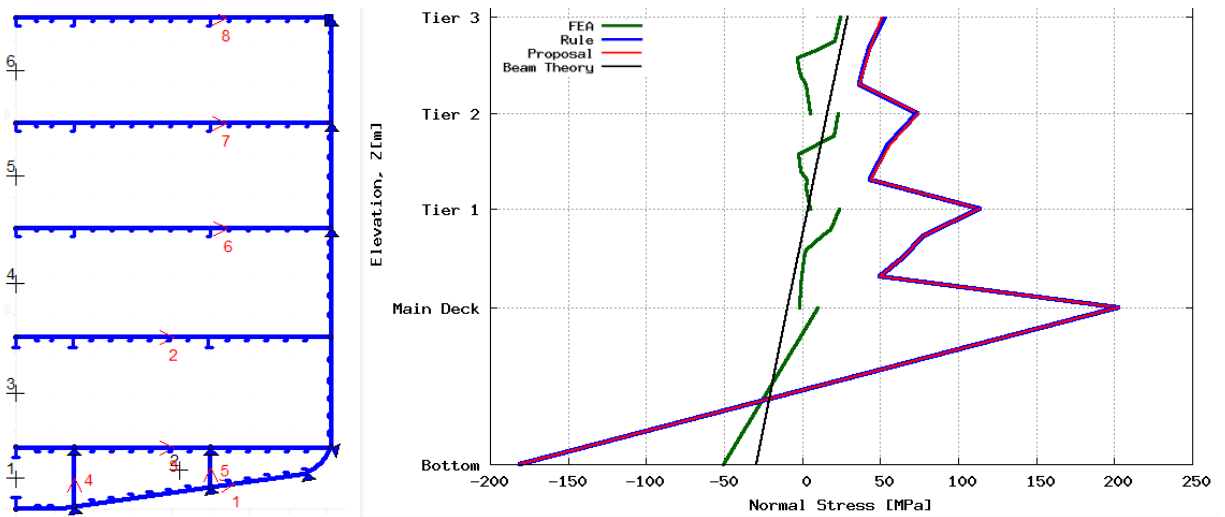


Figure 80: Modeling for stress calculation at 'tier 3' (left) and recommended stress distribution (right)

#### 5) Stress calculation in tier 4

Cross-section of 'hull', 'tier 1', 'tier 2', 'tier 3' and 'tier 4' are modeled in Marsinland. The bending moment for full vessel (section 5.2.4.3) should be applied at this model to obtain the normal stresses at tier 4. The Marsinland model and normal stress distribution are shown in figure 81.

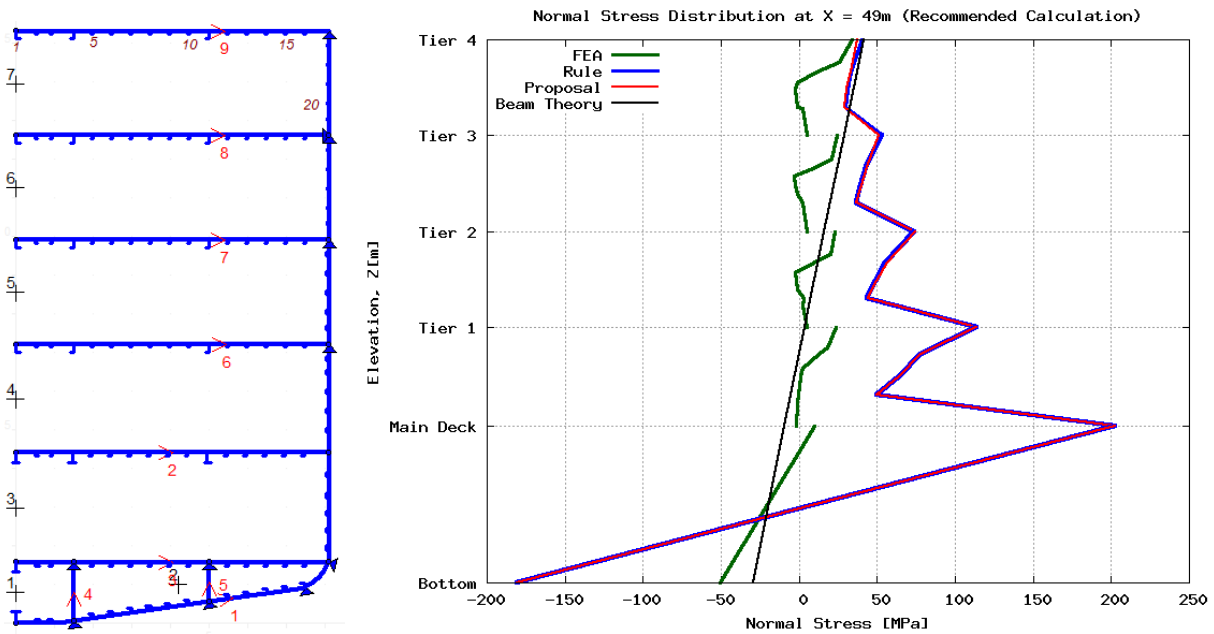


Figure 81: Modeling for stress calculation at 'tier 4' (left) and recommended stress distribution (right)

### 8.3 Local shear force in way of window stiles

#### 8.3.1 General

Usually passenger vessels have large windows or side openings. According to NR 217 (Pt D, Ch 1, Sec 6), the geometric characteristics of the hull girder used for the scantling of window stiles are to be determined in compliance with Pt B, Ch 4, Sec 1 (section 3.3), assuming that the hull girder extends up to the uppermost contributing superstructure/deckhouse deck. The hull girder loads induce a force  $F$  tending to deform the window stile as a girder clamped at the lower end, and whose upper end moves horizontally (figure 82).

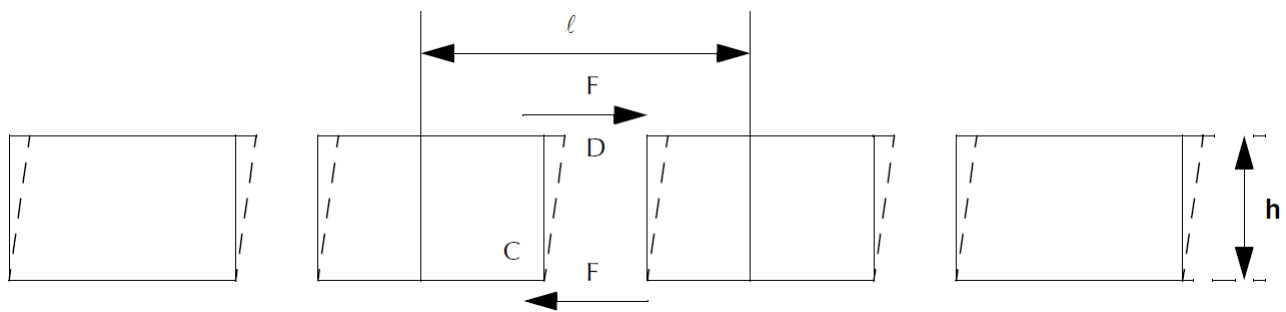


Figure 82: Deformation of window stiles

According to NR 217 (Pt D, Ch 1, Sec 6), local shear force acting on window stiles,  $F$ , in  $N/mm^2$  can be found through following formula:

$$F = \frac{\tau}{2} \cdot t \cdot l \quad (43)$$

Here,  $\tau$  is shear stress in way of window ( $N/mm^2$ );  $t$  is mean net thickness of the hull girder web in  $mm$ , in way of the window;  $l$  is distance between centers of two successive windows (in  $m$ ).

### 8.3.2 Determination guidelines

#### *Step 1: Calculation of vertical shear force*

According to NR 217 (Pt B, Ch 3, Sec 2), estimated total design vertical shear Force,  $T_S$  is found from following formula:

$$T_S = \frac{\pi M}{L} \quad (44)$$

Here,  $M$  is total vertical bending moment in  $kN.m$  and  $L$  is rule length as defined in NR 217 (Pt B, Ch 1, Sec 2).

#### *Step 2: Calculation of shear stress*

Local shear stress for any location can be obtained from Marsinland. Marsinland gives the shear stress per 10000N vertical shear force for any given location (figure 15). If Marsinland provides shear stress  $\tau'$   $N/mm^2$ , actual shear stress ( $\tau$ ) for actual vertical shear force ( $T_S$ ) is to be calculated as:

$$\tau = \frac{\tau'}{10000} * T_S$$

#### *Step 3: Calculation of horizontal shear force*

If web thickness ( $t$ ) and distance between centers of two successive windows ( $l$ ) is known, equation 43 gives the shear force ( $F$ ) as:

$$F = \frac{\tau}{2} \cdot t \cdot l$$

## **9 CONCLUSIONS AND RECOMMENDATIONS**

The purpose of this research was to investigate different parameters affecting hull-superstructure phenomenon to develop an improved analytical expression allowing better bending efficiency prediction. Effect of different parameters on hull-superstructure interaction were investigated using dedicated study model. These investigations led to an improved formula of bending efficiency, which is more accurate for normal stress calculation. Eventually, guidelines were established to implement bending efficiency ( $\nu$ ) for finding global stresses. Hence, the objectives of this research can be deemed as achieved.

The investigations suggest following conclusions about influence of different parameters affecting hull-superstructure interaction:

*Ratio of superstructure length to hull length ( $r_L$ ):* The longitudinal stress of a superstructure depends on superstructure length. But, it is independent of hull length. It depends on superstructure length only.

*Ratio of superstructure deck openings to total deck area ( $r_D$ ):* Stress increases in superstructure as well as in main deck as the deck opening increases. This increase of stress is linear.

*Ratio of superstructure side openings to total lateral area ( $r_S$ ):* Stress decreases in superstructure and increases in main deck as the side opening increases. This decrease or increase of stress is non-linear.

*Location of side openings:* According to the investigation it is clear that, more side opening at midship leads to more stress at superstructure.

Based on investigations, the parameter for side opening ( $r_S$ ) was integrated to the existing formula. This newly proposed formula is 7.7% more accurate compared to the existing formula for finding normal stress at midship sun deck (section 7.4.2). Then guidelines were developed to calculate longitudinal stresses in the superstructure and local shear force in window stiles. The guideline for calculation of longitudinal stresses in superstructure is very conservative.

There is always scope to improve any research work. Since this work is mainly focusing on midship, there could be some interesting research on fore and aft part of the ship. Besides, the stress concentration areas like side openings, deck openings or other discontinuities can be studied in detail. Other structural details like jacuzzi, swimming pool, manhole, etc. can also be studied. In this case, there is still scope remaining for more investigation regarding short superstructure ( $r_L < 0.25$ ). Besides, investigations can be performed in order to have a better understanding of the influence of  $r_D$  in order to include this parameter into the expression of bending efficiency ( $\nu$ ). Furthermore, Schade's design curves for  $\omega\lambda = 2.5, 2.0, 1.5$  and  $1.0$  (figure 8) are yet to be explored.

## **REFERENCES**

- Two-Beam Deckhouse Theory With Shear Effects, H.A. Schade, 1965
- The Effective Breadth Concept in Ship-Structure Design, H.A. Schade
- Thin-Walled Box Girder- Theory and Experiment, H.A. Schade, 1965
- Nonlinear Distribution of Bending Stresses Due to Distortion of the Cross Section, H.H. Bleich, 1952
- Principal of Naval Architecture, Volume 1, Chapter 4, Section 3
- Investigation of the Hull-Superstructure Interaction in order to Predict the Contribution of Superstructures to Hull Girder Strength, Zou Jiawei, 2013
- Ultimate strength of hull girder for passenger ships, Naar H., 2006
- Longitudinal strength analysis of a cruise ship with a narrow superstructure, Bergstrom M., 2010
- A theory of coupled beams for strength assessment of passenger ships, Naar H. et all, 2004
- Concept and preliminary structural design methods for the modern multi-deck ships, Zanic V.
- Hull Beam Behaviour of Passenger Ships, Heder M. et Ulfvarson A., 1990
- Hull-Superstructure structural interaction by finite element calculations, Zanic V. et all, 2004
- The global structural response model for multi-deck ships in concept design phase, Andric J. et Zanic V., 2009
- NTNU, n.d. TMR4190 Finite Element Method in Structural Analysis, s.l.: Norwegian University of Science and Technology.
- NR 217, 2014. Rules for the Classification of Inland Navigation Vessels
- M. Mano et al., Design of Ship Hull Structures, DOI 10.1007/978-3-540-88445-3 31
- A design procedure for determining the contribution of deckhouses to the longitudinal strength of ships, J. T. Kammerer

## **A APPENDIX: Visual Basic Code**

**Visual Basic Code for Creating Nodes:**

```
Private Sub CommandButton1_Click()  
Dim gfemap As Object  
Dim oNode As Object  
Dim iNID As Integer 'Will be used to count the node ID  
Dim dx As Double  
Dim dy As Double  
Dim dz As Double  
Dim WS As Worksheet  
Dim iRow As Integer  
'The following line sets the ws variable to the worksheet  
'This allows us to reference the cells without specifying  
'ThisWorkbook.Worksheets("Sheet1").cells(R,C) Sets:  
'WS = ThisWorkbook.Worksheets("Sheet1")  
'The following line will connect the gfemap variable to the open femap  
'session. Using gfemap we can access all the functionality of  
'femap from our VBA code.  
Set gfemap = GetObject(, "femap.model")  
'The next line connects oNode to the femap feNode object  
Set oNode = gfemap.fenode  
iRow = 2 ' The start row of our data in Excel  
Do While WS.Cells(iRow, 1) <> ""  
' loop until no data is in cells(iRow,1)  
iNID = WS.Cells(iRow, 1) ' The node id we specified on the worksheet  
dx = WS.Cells(iRow, 2)  
' the X,Y and Z ordinates specified on the worksheet  
dy = WS.Cells(iRow, 3)  
dz = WS.Cells(iRow, 4)  
'Set the femap node to our read values
```

```
oNode.ID = iNID
oNode.x = dx
oNode.y = dy
oNode.Z = dz
'Put it into femap
oNode.put (iNID)
iRow = iRow + 1 'increment the Excel row number
Loop 'Repeat until done
End Sub
```

**Visual Basic Code for Creating Points:**

```
Private Sub CommandButton1_Click()  
Dim gfemap As Object  
Dim oNode As Object  
Dim iNID As Integer 'Will be used to count the node ID  
Dim dx As Double  
Dim dy As Double  
Dim dz As Double  
Dim WS As Worksheet  
Dim iRow As Integer  
'The following line sets the ws variable to the worksheet  
'This allows us to reference the cells without specifying  
'ThisWorkbook.Worksheets("Sheet1").cells(R,C) Sets:  
'WS = ThisWorkbook.Worksheets("Sheet1")  
'The following line will connect the gfemap variable to the open femap  
'session. Using gfemap we can access all the functionality of  
'femap from our VBA code.  
Set gfemap = GetObject(, "femap.model")  
'The next line connects oNode to the femap feNode object  
Set oNode = gfemap.fepoint  
iRow = 2 ' The start row of our data in Excel  
Do While WS.Cells(iRow, 1) <> ""  
' loop until no data is in cells(iRow,1)  
iNID = WS.Cells(iRow, 1) ' The node id we specified on the worksheet  
dx = WS.Cells(iRow, 2)  
' the X,Y and Z ordinates specified on the worksheet  
dy = WS.Cells(iRow, 3)  
dz = WS.Cells(iRow, 4)  
'Set the femap node to our read values
```

```
oNode.ID = iNID
oNode.x = dx
oNode.y = dy
oNode.Z = dz
'Put it into femap
oNode.put (iNID)
iRow = iRow + 1 'increment the Excel row number
Loop 'Repeat until done
End Sub
```

## **B APPENDIX: API Code**

**API Code for Finite Element Post-Processing:**

```
Sub Main
'Attach To the model In a femap session that Is already running
Dim App As femap.model
Set App = feFemap()
'Dimension of Excel Application, Workbook and Worksheet.
Dim appExcel As Excel.Application
Set appExcel = New Excel.Application
Dim wbkReport As Excel.Workbook
Set wbkReport = appExcel.Workbooks.Add
Dim wksReport As Excel.Worksheet
Set wksReport = wbkReport.Worksheets(1)
Dim Row As Long
Dim Col As Long
'Dimension all other objects and variables
Dim s As Object
Dim v As Object
Dim e As Object
Set e = App.feSet
Dim ov As femap.Output
Set ov = App.feOutput
Dim minID As Long
Dim maxID As Long
Dim minVAL As Double
Dim maxVAL As Double
Dim Count As Long
im ID As Variant
Dim IDen As Long
Dim Title As Variant
Dim ouSetID As Long
```

```
Dim ouVec As femap.Output
Set ouVec = App.feOutput
Dim CurrentData As Double
'Ask the API to create the titles in the first row of the worksheet
wksReport.Cells( 1, 1 ) ="Output Set ID"
wksReport.Cells( 1, 2 ) ="Element ID"
i = 3
'Select Output Set and Output Vectors of interest
If App.feSelectOutput( "Select Output Vectors", 0, FOT_ANY, FOC_ANY,
FT_ELEM, False, s, v ) = FE_OK Then
'Select Elements of interest
If e.Select( FT_ELEM, True, "Select Elements" ) = FE_OK Then
'Cycle through all selected Output Sets and Output Vectors
While s.Next
v.Reset
Col=3
While v.Next
e.Reset
ov.GetFromSet( s.CurrentID, v.CurrentID )
'Get the Titles and IDs of the selected Output Vectors
ov.GetTitleIDList(False, v.CurrentID, v.CurrentID, Count, ID, Title)
Row = i
'Print the Output Set IDs and Element IDs and write into first two
columns of the Excel file
While e.Next()
wksReport.Cells( Row, 1 ).Value =s.CurrentID
wksReport.Cells( Row, 2 ).Value =e.CurrentID
'Print the Output Vector data into coresponding cells of the Excel file
'Note: The Get command requires an INT4 input so you must identify the
first value of the ID array with (0)
```

```
ouVec.setID = s.CurrentID
rc = ouVec.Get(v.CurrentID)
CurrentData = ouVec.Value( e.CurrentID )
wksReport.Cells( Row, Col ) =CurrentData
Row=Row+1
Wend
'Print the Titles and IDs of the selected Output Vectors into
'the first two rows of the Excel file
wksReport.Cells( 1, Col ).Value =Title
wksReport.Cells( 2, Col ).Value =ID
Col=Col+1
Wend
i = Row
Wend
End If
End If
'Make the Excel spreadsheet visible
appExcel.Visible = True
End Sub
```

## **C APPENDIX: Data**

Table 12: Longitudinal Normal Stress Distribution at X = 31.5m

Deck/Position	Elevation, Z (m)	Normal Stress (MPa)			
		FE Analysis	NR 217	Proposal	Beam Theory
Sun Deck	15.30	29.29	39.80	37.21	41.37
-	14.65	7.01	-	-	-
-	14.40	-1.47	33.60	32.93	-
-	14.10	-1.89	-	-	-
-	13.90	-2.29	31.38	30.79	-
-	13.40	-0.67	29.61	29.08	-
-	13.20	0.96	-	-	-
Deck 3	12.60	20.22	29.64	29.57	28.84
-	11.95	-1.00	-	-	-
-	11.70	-5.13	23.04	23.10	-
-	11.45	-3.61	-	-	-
-	11.20	-2.28	20.68	20.79	-
-	10.95	-0.60	-	-	-
-	10.70	1.40	18.80	18.94	-
-	10.50	3.28	-	-	-
Deck 2	9.90	19.42	17.08	17.63	16.32
-	9.25	-3.02	-	-	-
-	9.00	-5.77	10.42	10.95	-
-	8.75	-4.56	-	-	-
-	8.50	-1.96	8.04	8.57	-
-	8.25	-0.69	-	-	-
-	8.00	1.48	6.13	6.66	-
-	7.80	3.43	-	-	-
Deck 1	7.20	29.73	4.23	4.90	3.79
-	6.63	10.21	-	-	-
-	6.45	3.55	-1.72	-1.25	-
-	6.05	-1.12	-	-	-
-	5.80	-0.94	-4.10	-3.71	-
-	5.05	1.75	-	-	-
Main Deck	4.4	26.3	-9.10	-8.88	-9.21
Bottom	0	-65	-30.04	-30.5	-29.62

Table 13: Longitudinal Normal Stress Distribution at X = 42m

Deck/Position	Elevation, Z (m)	Normal Stress (MPa)			
		FE Analysis	NR 217	Proposal	Beam Theory
Sun Deck	15.30	32.82	39.80	37.21	41.37
	14.65	12.01	-	-	-
-	14.40	2.35	33.60	32.93	-
	14.10	-0.65	-	-	-
-	13.90	-1.49	31.38	30.79	-
-	13.40	-0.59	29.61	29.08	-
	13.20	0.58	-	-	-
Deck 3	12.60	22.54	29.64	29.57	28.84
	11.95	5.04	-	-	-
-	11.70	-0.73	23.04	23.10	-
	11.45	-1.64	-	-	-
-	11.20	-1.40	20.68	20.79	-
	10.95	-0.47	-	-	-
-	10.70	0.88	18.80	18.94	-
	10.50	2.46	-	-	-
Deck 2	9.90	20.66	17.08	17.63	16.32
	9.25	3.13	-	-	-
-	9.00	-1.25	10.42	10.95	-
	8.75	-2.07	-	-	-
-	8.50	-1.09	8.04	8.57	-
	8.25	-0.47	-	-	-
-	8.00	0.84	6.13	6.66	-
	7.80	2.25	-	-	-
Deck 1	7.20	24.73	4.23	4.90	3.79
	6.63	10.50	-	-	-
-	6.45	6.42	-1.72	-1.25	-
	6.05	0.50	-	-	-
-	5.80	-0.08	-4.10	-3.71	-
	5.05	0.34	-	-	-
Main Deck	4.4	13.133	-9.10	-8.88	-9.21
Bottom	0	-53.14	-30.04	-30.5	-29.62

Table 14: Longitudinal Normal Stress Distribution at X = 49m

Deck/Position	Elevation, Z (m)	Normal Stress (MPa)			
		FE Analysis	NR 217	Proposal	Beam Theory
Sun Deck	15.30	34.02	39.80	37.21	41.37
	14.65	25.68	-	-	-
-	14.40	11.15	33.60	32.93	-
	14.10	-1.41	-	-	-
-	13.90	-2.53	31.38	30.79	-
-	13.40	-1.27	29.61	29.08	-
	13.20	2.21	-	-	-
Deck 3	12.60	24.36	29.64	29.57	28.84
	11.95	21.02	-	-	-
-	11.70	10.32	23.04	23.10	-
	11.45	-3.08	-	-	-
-	11.20	-2.55	20.68	20.79	-
	10.95	-1.21	-	-	-
-	10.70	2.16	18.80	18.94	-
	10.50	2.80	-	-	-
Deck 2	9.90	23.08	17.08	17.63	16.32
	9.25	20.00	-	-	-
-	9.00	9.04	10.42	10.95	-
	8.75	-2.76	-	-	-
-	8.50	-1.95	8.04	8.57	-
	8.25	-1.07	-	-	-
-	8.00	2.65	6.13	6.66	-
	7.80	2.49	-	-	-
Deck 1	7.20	23.81	4.23	4.90	3.79
	6.63	17.99	-	-	-
-	6.45	12.56	-1.72	-1.25	-
	6.05	2.01	-	-	-
-	5.80	1.20	-4.10	-3.71	-
	5.05	-1.06	-	-	-
Main Deck	4.4	10	-9.10	-8.88	-9.21
Bottom	0	-50.89	-30.04	-30.5	-29.62

Table 15: Longitudinal Normal Stress Distribution at X = 70m

Deck/Position	Elevation, Z (m)	Normal Stress (MPa)			
		FE Analysis	NR 217	Proposal	Beam Theory
Sun Deck	15.30	40.24	39.80	37.21	41.37
	14.65	28.05	-	-	-
-	14.40	9.21	33.60	32.93	-
	14.10	-2.09	-	-	-
-	13.90	-3.86	31.38	30.79	-
-	13.40	-1.94	29.61	29.08	-
	13.20	-2.51	-	-	-
Deck 3	12.6	15.68	29.64	29.57	28.84
	11.95	38.19	-	-	-
-	11.70	16.40	23.04	23.10	-
	11.45	3.30	-	-	-
-	11.20	-3.56	20.68	20.79	-
	10.95	-1.60	-	-	-
-	10.70	-2.57	18.80	18.94	-
	10.50	4.26	-	-	-
Deck 2	9.90	16.28	17.08	17.63	16.32
	9.25	42.84	-	-	-
-	9.00	19.09	10.42	10.95	-
	8.75	4.27	-	-	-
-	8.50	-3.47	8.04	8.57	-
	8.25	-1.71	-	-	-
-	8.00	-2.54	6.13	6.66	-
	7.80	3.55	-	-	-
Deck 1	7.20	11.43	4.23	4.90	3.79
	6.63	33.33	-	-	-
-	6.45	32.28	-1.72	-1.25	-
	6.05	6.74	-	-	-
-	5.80	4.83	-4.10	-3.71	-
	5.05	-2.38	-	-	-
Main Deck	4.4	26.586	-9.10	-8.88	-9.21
Bottom	0	-57.28	-30.04	-30.5	-29.62

Table 16: Longitudinal Normal Stress Distribution at X = 80.5m

Deck/Position	Elevation, Z (m)	Normal Stress (MPa)			
		FE Analysis	NR 217	Proposal	Beam Theory
Sun Deck	15.30	48.57	39.80	37.21	41.37
	14.65	31.62	-	-	-
-	14.40	15.09	33.60	32.93	-
	14.10	5.58	-	-	-
-	13.90	8.56	31.38	30.79	-
-	13.40	3.72	29.61	29.08	-
	13.20	2.92	-	-	-
Deck 3	12.60	21.76	29.64	29.57	28.84
	11.95	-21.83	-	-	-
-	11.70	-20.58	23.04	23.10	-
	11.45	10.38	-	-	-
-	11.20	8.05	20.68	20.79	-
	10.95	5.44	-	-	-
-	10.70	7.26	18.80	18.94	-
	10.50	2.59	-	-	-
Deck 2	9.90	19.32	17.08	17.63	16.32
	9.25	-22.62	-	-	-
-	9.00	-20.64	10.42	10.95	-
	8.75	11.50	-	-	-
-	8.50	6.80	8.04	8.57	-
	8.25	4.95	-	-	-
-	8.00	6.54	6.13	6.66	-
	7.80	-2.96	-	-	-
Deck 1	7.20	11.95	4.23	4.90	3.79
	6.63	17.43	-	-	-
	6.45	24.32	-1.72	-1.25	-
	6.05	12.78	-	-	-
-	5.80	10.32	-4.10	-3.71	-
	5.05	6.16	-	-	-
Main Deck	4.4	36.3775	-9.10	-8.88	-9.21
Bottom	0	-86.9471	-30.04	-30.5	-29.62

Table 17: Recommended Normal Stress Distribution at X = 49m

Deck/Position	Elevation, Z (m)	Normal Stress (MPa)			
		FE Analysis	NR 217	Proposal	Beam Theory
Sun Deck	15.30	34.02	39.80	37.21	41.37
	14.65	25.68	-	-	-
-	14.40	11.15	33.60	32.93	-
	14.10	-1.41	-	-	-
-	13.90	-2.53	31.38	30.79	-
-	13.40	-1.27	29.61	29.08	-
	13.35	2.21	-	-	-
Deck 3	12.60	24.36	53.48	50.89	28.84
	11.95	21.02	-	-	-
-	11.70	10.32	43.18	43.59	-
	11.45	-3.08	-	-	-
-	11.20	-2.55	39.50	39.94	-
	10.95	-1.21	-	-	-
-	10.70	2.16	36.55	37.02	-
	10.50	2.80	-	-	-
Deck 2	9.90	23.08	73.71	74.79	16.32
	9.25	20.00	-	-	-
-	9.00	9.04	55.32	56.35	-
	8.75	-2.76	-	-	-
-	8.50	-1.95	48.76	49.77	-
	8.25	-1.07	-	-	-
-	8.00	2.65	43.51	44.50	-
	7.80	2.49	-	-	-
Deck 1	7.20	23.81	113.60	113.60	3.79
	6.63	17.99	-	-	-
-	6.45	12.56	78.26	78.26	-
	6.05	2.01	-	-	-
-	5.80	1.20	64.12	64.12	-
	5.05	-1.06	-	-	-
Main Deck	4.4	10	-9.10	-8.88	-9.21
Bottom	0	-50.888	-30.04	-30.5	-29.62